Structure-property relationship of bimodal high density polyethylene: Effect on rheology

By

Hellen Lamola

Thesis presented in partial fulfilment of the degree of

Master of Science (Polymer Science)

at the

University of Stellenbosch

Supervisor: Prof. A.J. van Reenen

Co-supervisor: Prof. H. Pasch

December 2021

Declaration for thesis

By submitting this thesis electronically, I declare that the entirety of the work contained therein is my own, original work, that I am the sole author thereof (save to the extent explicitly otherwise stated), that reproduction and publication thereof by Stellenbosch University will not infringe any third-party rights and that I have not previously in its entirety or in part submitted it for obtaining any qualification.

Hellen Lamola December 2021

Abstract

Bimodal polyethylene is a version of HDPE that is tailor-made to possess better processability and mechanical strength. Polymerisation is carried out in a low-pressure dual reactor system in the presence of a catalyst. Hydrogen and ethylene are fed to the first reactor to produce a polyethylene homopolymer of very low molar mass. In the second reactor, comonomer of 1-alpha olefins is introduced to create short chain branching. A homogenous distribution of comonomer along the polyolefin chain is important in determining final resin performance.

The present work looks at three bHDPE resins with almost similar microstructural properties but different rheological behaviour during the film blowing process. A benchmark industrial resin (Reference) was compared to two similar resins (Resin 1 and Resin 2) where Resin 2 exhibited poor processability regarding bubble instability and melt strength.

In the first part of this work, bulk resins are analysed using various analytical techniques. Carbon-thirteen nuclear magnetic resonance (^{13}C NMR) was used to determine the type and quantity of the comonomer in all samples. Other techniques used included high-temperature size exclusion chromatography (HT-SEC), differential scanning calorimetry (DSC), crystallisation analysis fractionation (CRYSTAF), high-temperature interaction chromatography (HT-IC), high-temperature liquid chromatography (2D-LC), dynamic mechanical analysis (DMA) and tensile strength. Results showed that the Reference had a different comonomer to Resin 1 and Resin 2. Also, Resin 2 had a slightly higher comonomer content but overall, comonomer content was very low (<0.8 %) for all samples.

Fractionation was performed on a preparative scale and collected fractions were further analysed using ^{13}C NMR, HT-SEC, and DSC. Firstly, preparative temperature rising elution fractionation (pTREF) was performed followed by preparative molar mass fractionation (pMMF). Analyses of the fractions showed that the comonomer in Resin 2 was concentrated in certain fractions and not broadly distributed along the polyolefin chain. As a result, Resin 2 had certain fractions of significantly higher crystallinity to those of the Reference and Resin 1. It was also shown that Resin 2 had high molar mass in the lower TREF temperature fractions where it is expected to be of low molar mass. The Reference conversely had an even distribution of very low and very high molar mass chains as well as an evenly distributed comonomer throughout the polymer chains. Overall observed differences in chemical composition distribution (CCD) and molar mass distribution (MMD) do have an effect on the rheology and processability of bHDPE resins. More specifically, the narrow distribution of

comonomer in Resin 2 could justify the observed differences in rheological behaviour during processing.

Opsomming

Bimodale poliëtileen is 'n weergawe van HDPE wat pasgemaak is om beter verwerkbaarheid en meganiese sterkte te besit. Polimerisasie word uitgevoer in 'n laedruk dubbele reaktorsisteem in die teenwoordigheid van 'n katalisator. Waterstof en etileen word na die eerste reaktor gevoer wat 'n poliëtileen homopolimeer met 'n baie lae molêre massa lewer. In die tweede reaktor word komonomeer van 1-alfa-olefiene bygevoeg om kort ketting vertakkings vorm. 'n Homogene verspreiding van komonomeer in die poliolefin-ketting bepaal die finale produk prestasie.

Die huidige werk kyk na drie bHDPE produkte met byna soortgelyke mikrostruktuur-eienskappe, maar verskillende reologiese gedrag tydens die film blaas proses. 'n Standaard industriële hars (verwysing) is vergelyk met twee soortgelyke harse (hars 1 en hars 2), waar hars 2 swak verwerkbaarheid ten opsigte van film stabiliteit en smelt sterkte vertoon het.

In die eerste gedeelte van hierdie werk word grootmaat harse geanaliseer met behulp van verskillende analitiese tegnieke. Koolstof-dertien kernmagnetiese resonansie (^{13}C NMR) is gebruik om die tipe en hoeveelheid van die samekundige in alle monsters te bepaal. Ander tegnieke wat gebruik word, sluit in hoë-temperatuurgrootte-uitsluitingschromatografie (HT-SEC), differensiële skanderingskalorimetrie (DSC), kristallisasie-analise fraksionering (CRYSTAF), interaktiewe chromatografie met hoë temperatuur (HT-IC), vloeistofchromatografie met hoë temperatuur (2D-LC).), dinamiese meganiese analise (DMA) en treksterkte. Resultate het getoon dat die verwysing 'n ander comonomeer het as Resin 1 en Resin 2. Resin 2 het ook 'n effens hoër comonomer-inhoud, maar oor die algemeen was die comonomer-inhoud baie laag (<0,8%) vir alle monsters.

Fraksionering is op voorbereidende skaal uitgevoer en versamelde breuke is verder geanaliseer met behulp van ^{13}C NMR, HT-SEC en DSC. Eerstens is voorbereidende temperatuurstygende eluerings fraksionering (pTREF) uitgevoer, gevolg deur voorbereidende molêre massa fraksionering (pMMF). Analises van die breuke het getoon dat die komonomeer in Hars 2 in sekere fraksies gekonsentreer is en nie breed versprei is langs die poli-olefineketting nie. As gevolg hiervan het Hars 2 sekere fraksies met 'n beduidend hoër kristalliniteit as dié van die Verwysing en Hars 1. Daar is ook aangetoon dat Hars 2 'n hoë molêre massa in die laer TREF-temperatuurfraksies het, waar dit na verwagting 'n lae molêre massa het. Die verwysing het omgekeerd 'n eweredige verspreiding van baie lae en baie hoë molêre massakettings sowel as 'n eweredig verspreide komonomeer deur die polimeerkettings. Algehele waargenome verskille in chemiese samestellingsverspreiding

(CCD) en molêre massadistribusie (MMD) het 'n effek op die reologie en verwerkbaarheid van bHDPE-harse. Meer spesifiek, kan die smal verspreiding van komonomeer in Hars 2 die waargenome verskille in reologiese gedrag tydens verwerking regverdig.

Dedicated to:

My parents,

Mr. and Mrs Elias and Betty Semosa

I live to make you proud.

Table of Contents

Acknowledgements

First and foremost, I would like to thank God for granting me the strength and grace to carry on throughout this study.

I am most grateful to the following people:

Prof. Albert van Reenen and **Prof. Harald Pasch** for their guidance and unwavering support. Thank you for granting me an opportunity to be a part of your teams.

Dr. Anthony. Ndiripo for all his time, assistance with analytical instruments and results discussions. Your mentorship and the fruitful conversations we had were invaluable.

Dr. Nyambeni Luruli for his insightful advice.

Ms. S Mncwabe and **Ms. P Ndlovu** for their help in running DMA and tensile tests.

Dr. Jaco Brand and **Mrs. Elsa Malherbe** for their assistance with solution NMR analysis.

Dr. Jaco Smith and **Ms. Paula Nygard** for their help in acquiring the samples.

Dr. John Mellor and **Mr. Elias Thole** at Sasol PTSC for their support throughout the study.

Sasol for funding.

My colleagues at Sasol **AST** (more especially **Dixon Motaung**) and **ARST**.

My colleagues at Stellenbosch University **Dr. Sifiso Magagula**, **Dr. Paul Bungu** and **Ms Arina Wessels.**

My **family** for their unconditional love and support.

My **friends**, more especially **Hlengiwe Kleinbooi, Phodisho Thubakgale, Phindile Mahlangu, Lerato Moeti, Tshepiso Maja and Bathabile Ramalapa** for always listening and understanding.

Finally, my loving husband **Solomon Lamola** for always believing in me and pushing me to go further. Your support and sacrifices mean a great deal to me.

List of figures

List of tables

List of symbols

$-CH_2$	Methylene group
$-CH_3$	Methyl group
ΔH_m	Melting enthalpy
ΔH	Enthalpy
MM	Weight-average molar mass
T_c	Crystallisation temperature
T_m	Melting temperature
V_e	Elution volume
X_c	Crystallinity

List of abbreviations

2D-LC	2-dimensional liquid chromatography
^{13}C NMR	Carbon- thirteen nuclear magnetic resonance spectroscopy
bHDPE	Bimodal high density polyethylene
CC	Chemical composition
CCD	Chemical composition distribution
CEF	Crystallisation elution fractionation
CRYSTAF	Crystallisation analysis fractionation
DMA	Dynamic mechanical analyses
DSC	Differential scanning calorimetry
ELSD	Evaporative light scattering detector
HDPE	High density polyethylene
HT-2D-LC	High-temperature 2-dimensional liquid chromatography
HT-IC	High-temperature interaction chromatography
HT-SGIC	High-temperature solvent gradient interaction chromatography
HT- SEC	High-temperature size exclusion chromatography
HT-TGIC	High-temperature thermal gradient interaction chromatography
IR	Infrared
LDPE	Low density polyethylene
LLDPE	Linear low density polyethylene
MAO	Methylaluminoxane

MFI	Melt flow index
MM	Molar mass
MMD	Molar mass distribution
MMF	Molar mass fractionation
NMR	Nuclear magnetic resonance
PE	Polyethylene
RI	Refractive index
SCB	Short chain branching
SCBD	Short chain branching distribution
SGIC	Solvent gradient interaction chromatography
TCB	1,2,4-trichlorobenzene
TCE-d2	Deuterated 1,1,2,2- tetrachoroethane
TREF	Temperature rising elution fractionation
ZN	Ziegler- Natta

Chapter 1

Introduction

This chapter presents the purposes of the present study. The methods and approach used in the characterisation of bimodal molar mass distribution of high density polyethylene are highlighted and arranged into a list of specific goals. Finally, a layout of the thesis is given.

1.1 Background

Polyethylene (PE) is one of the highest volume commodity synthetic polyolefins after polypropylene (PP). The different classes of polyethylene include low density (LDPE), linear low density (LLDPE) and high density (HDPE) providing a wide range of plastic choices according to application. Some of the most common applications range from plastic packaging to building infrastructure and transport. Of growing interest is the bimodal molar mass distribution HDPE. The advantages of which include having a combination of low molar mass and high molar mass properties. Most notably, the result is a material with higher mechanical properties and better processability than unimodal HDPE.

Bimodal HDPE resins possess a unique combination of processability and good physical properties such as environmental stress crack resistance and impact strength.[1-5] For the blown film grades, the high impact strength is achieved even at very thin films.[6] These attributes are achieved through an in-reactor blending of low molar mass homopolymer and high molar mass copolymer making use of alpha olefins such as 1-butene and 1-hexene as the comonomer. Bimodal HDPE blends are obtained commercially by proprietary polymerisation in a cascade of reactors.[3,6]

The inclusion of comonomer in the higher molar mass regions creates short chain branches (SCB) to the otherwise very linear HDPE. These SCB act as tie molecules holding the linear chains together to prevent pull-out from crystallites thus, improving flexibility and mechanical properties of the polymer. The flexibility is attributed to the disruption of crystallinity by the SCB in the higher molar mass regions while the more linear, low molar mass regions provide good processability. [7]

Even between resins of similar weight average molar mass (MM), density and melt flow properties, each deviation in microstructural composition can alter specific properties of the polymer. Microstructure is described as molar mass, molar mass distribution (MMD), chemical composition (CC) and chemical composition distribution (CCD). In order to relate the microstructure to the final properties of bimodal HDPE, it becomes vital that the material be comprehensively analysed.

Many studies have employed the use of temperature rising elution fraction (TREF)[8-10], crystallisation analysis fractionation (CRYSTAF)[11-14] and more recently, crystallization elution fractionation (CEF)[15] as analytical techniques to fractionate semi-crystalline polyolefins according to their solubility-temperature relationship. None of these techniques, however, have been able to overcome the effects of co-crystallisation of bimodal HDPE. This was owed to the fact that co-crystallisation occurs between macromolecules of different molar mass although they have close to similar chemical compositions.[13,16] For this reason, high-temperature solvent gradient interaction chromatography (HT-SGIC) has been employed as a complementary tool to separate the bimodal HDPE polyolefins according to their chemical compositional heterogeneity.[15,17-19]

Better elucidation of the structural heterogeneities of semi-crystalline polymers is possible when preparative TREF (pTREF) fractions are analysed offline by other analytical techniques.[20-24] This way, fractions can be analysed independently and their contribution to the bulk polymer properties can be distinguished.

Over and above pTREF which fractionates according to crystallinity, we this work further fractionate the bimodal HDPE resins according to molar mass using preparative molar mass fractionation (pMMF). The expectation is that the higher molar mass chains of low dispersity will be the first fractions to precipitate out of solution followed by fractions of lower molar masses.[22,25,26] Through pMMF, fractions with narrow MMD but broad crystallinity are collected and are likewise, analysed individually.[10,27,28] Each of the collected fractions are to be analysed separately using various techniques.

In particular, high-temperature size exclusion chromatography (HT-SEC)[29] is used to analyse the MM and MMD. Melting and crystallisation properties of the bulk samples and fractions are determined using the differential scanning calorimetry (DSC)[29,30] and crystallisation analysis fractionation (CRYSTAF). Qualification and quantification of comonomer was determined by use of solution state carbon-thirteen nuclear magnetic spectroscopy (^{13}C NMR).[11,24,31]To the best of our knowledge, with the exception of Fan et.al.[4], multiple fractionation according to crystallinity and molar mass has not yet been performed on bimodal HDPE. Results obtained from this study should, therefore, be able to give new insight into the complete microstructure-property relationship of bimodal HDPE.

1.2 Research hypothesis

While bulk bimodal HDPE samples display similar characteristics (MM, rheological and thermal properties), they display major differences with regard to processing behaviour during blown film extrusion. This includes melt strength and bubble stability. The current work therefore seeks to prove that there are slight differences in the microstructure that contribute greatly to how the material behaves during processing. The following questions should then be addressed:

1. Are there similar amounts of the low molar mass and high molar mass components in all samples?
2. If so, how does comonomer distribution compare between all sample components?

1.3 Scope/ limitations

The current work is limited to analysis of film grade bimodal HDPE resins. Moreover, the samples are manufactured commercially and supplied as is, therefore, no changes can be made to how they are polymerised. Even more, polymerisation of such polymers is highly proprietary and as a result, the exact polymerisation conditions and catalyst packages are unknown.

1.4 Goal and objectives

The main goal of this study is to compare three bimodal high density polyethylene resins from different manufacturers. Two of the samples, “Resin1” and “Resin2” are produced in the same plant but are of different batches. Resin1 shows good rheological behaviour while Resin2 shows very poor rheological behaviour during processing. The third sample, “Reference” is an industrial benchmark resin made by a different manufacturer and possesses excellent rheological properties. Samples are produced using the same dual reactor, slurry phase polymerization technology with Ziegler-Natta catalysts. The main aim is to understand and relate the effect of the microstructure on the rheological properties. The effect of the amount and distribution of the short chain branches will be studied.

Specific objectives are to:

1. Fully analyse the bulk material using HT-SEC, DSC, CRYSTAF, ^{13}C NMR, HT-SGIC, HT-TGIC, HT-2D-LC, DMA and tensile testing.

2. Fractionate according to crystallinity using pTREF.

3. Fractionate according to molar mass using pMMF.

4. Characterize each fraction to investigate:

- Branching using ^{13}C NMR spectroscopy.
- Melting and crystallization behaviour using DSC.
- Molar mass and molar mass distribution using HT-SEC.
- Confirm the chemical composition distribution using HT-IC.
- Correlate the chemical composition distribution and molar mass distribution using HT-2D-LC.

1.5 Layout of the thesis

The thesis is divided into chapters as follows:

Chapter 1

This chapter introduces the work to be done and outlines its importance. Included is also a map of how the information is organised in the different chapters.

Chapter 2

This chapter briefly reviews the historical background of polyethylene with emphasis on bimodal HDPE, its polymerisation technology and catalysis. Furthermore, the different fractionation and analytical techniques to be employed are reviewed.

Chapter 3

The experimental procedures followed in this work are outlined in detail.

Chapter 4

Results of the three bulk bimodal HDPE resins are discussed in this chapter presenting the necessity for fractionation.

Chapter 5

This chapter discusses results of pTREF and analyses of the fractions. It also concludes on the contribution of each fractions' contribution on the final resin properties.

Chapter 6

Results of the pMMF are discussed in this chapter. Conclusions are drawn about the contributions of individual fractions on final resin properties.

Chapter 7

A summary of the research findings from Chapter 5 and Chapter 6 as well as recommendations for future work is presented in this chapter.

1.6 References

(1) Alt, F. P.; Böhm, L. L.; Enderle, H. F.; Berthold, J. *Macromol. Symp.* **2001**, *163*, 135–144.

(2) Sun, X.; Shen, H.; Xie, B.; Yang, W.; Yang, M. *Polymer* **2011**, *52*, 564–570.

(3) Frederick J.K, S. S. B.; *Process for the production of polyethylene with a broad and/or bimodal molecular weight distribution*, **1990**, United States Patents, US 4,918,038.

(4) Fan, Y.; Xue, Y.; Nie, W.; Xiangling, J.; Bo, S. *Polym. J.* **2009**, *41*, 622–628.

(5) Tian, Z.; Chen, K.-R.; Liu, B.-P.; Luo, N.; Du, W.-L.; Qian, F. *Chem. Eng. Sci.* **2015**, *130*, 41–55.

(6) Mack, M. P.; Meas Jr, J. H.; Nygard, P. L.; Wallace, L. R.; Garrison, P. J.; *Process for producing polyethylene film composition having broad molecular weight distribution and improved bubble stability*, **2000,** United States Patents, Houston, Tex, US 6,147,167.

(7) Hakim, S.; Moballegh, L., **2011**. In *Macromol. Symp.*; *302, 191*–197.

(8) Monrabal, B.; Del Hierro, P. *Anal. Bioanal.Chem.* **2011**, *399*, 1557–1561.

(9) Monrabal, B. *Encyclopedia of Analytical Chemistry: Applications, Theory and Instrumentation.* **2006**.

(10) Ndiripo, A.; Eselem Bungu, P. S.; Pasch, H. *Polym. Int.* **2019**, *68*, 206–217.

(11) Shan, C. L. P.; Soares, J. B.; Penlidis, A. *Polymer* **2002**, *43*, 7345–7365.

(12) Cheruthazhekatt, S.; Pasch, H. *Anal. Bioanal.Chem.* **2014**, *406*, 2999–3007.

(13) Anantawaraskul, S.; Soares, J. B.; Wood-Adams, P. M. *Macromol. Chem. Phys.* **2004**, *205*, 771–777.

(14) Bruaseth, I.; Soares, J. B.; Rytter, E. *Polymer* **2004**, *45*, 7853–7861.

(15) Cheruthazhekatt, S.; Mayo, N.; Monrabal, B.; Pasch, H. *Macromol. Chem. Phys.* **2013**, *214*, 2165–2171.

(16) Suriya, K.; Anantawaraskul, S.; Soares, J. B. P. *J. Polym. Sci. Polym. Phys.* **2011**, *49*, 678–684.

(17) Macko, T.; Brüll, R.; Alamo, R. G.; Stadler, F. J.; Losio, S. *Anal. Bioanal.Chem.* **2011**, *399*, 1547–1556.

(18) Macko, T.; Pasch, H. *Macromolecules* **2009**, *42*, 6063–6067.

(19) Prabhu, K.; Brüll, R.; Macko, T.; Remerie, K.; Tacx, J.; Garg, P.; Ginzburg, A. *J. Chromatogr. A* **2015**, *1419*, 67–80.

(20) Ndiripo, A. *Comparative study on the molecular structure of ethylene/1-octene, ethylene/1-heptene and ethylene/1-pentene copolymers using advanced analytical methods*. MSc thesis, Stellenbosch University: South Africa,**2015**.

(21) Sigwinta, M. *Ethylene-1-octene elastomers: Molecular structure characterization by advanced analytical methods*. MSc thesis, Cape Peninsula University of Technology: South Africa,**2019**.

(22) Bungu, P. S. E.; Pflug, K.; Pasch, H. *Polym. Chem.* **2018**, *9*, 3142–3157.

(23) Ndiripo, A.; Pasch, H. *Anal. Chim. Acta* **2018**, *1027*, 137–148.

(24) Assumption, H.; Vermeulen, J.; Jarrett, W. L.; Mathias, L. J.; van Reenen, A. *Polymer* **2006**, *47*, 67–74.

(25) Sigwinta, M.; Ndiripo, A.; Wewers, F.; Pasch, H. *Polym. Int.* **2020**, *69*, 291–300.

(26) Magagula, S. I.; Ndiripo, A.; van Reenen, A. J. *Polym. Deg. Stab.* **2020**, *171*, 109022.

(27) Eselem Bungu, P. S. *Development of a multiple fractionation protocol for the comprehensive analysis of low density polyethylene*. PhD dissertation, Stellenbosch University: South Africa,**2018**.

(28) Krumme, A.; Basiura, M.; Pijpers, T.; Vanden Poel, G.; Heinz, L. C.; Bruell, R.; BF Mathot, V. *Mater. Sci.* **2011**, *17*, 260–265.

(29) Shanks, R.; Amarasinghe, G. *J. Therm. Anal. Calorim.* **2000**, *59*, 471-482.

(30) Seger, M. R.; Maciel, G. E. *Anal. Chem.* **2004**, *76*, 5734–5747.

Chapter 2

Literature Review

This chapter gives a background into the history of polyolefins and reviews some of the analytical and preparative fractionation methods used to comprehensively analyse the complex microstructure of the bimodal high density polyethylene.

2.1. 1ntroduction

Polyolefins are the biggest commodity plastics by volume with uses ranging from shopping bags to shampoo bottles and underground water pipes. The most commonly used polyolefins are polyethylene and polypropylene. Different ranges of polyethylene include low density polyethylene (LDPE), linear low density polyethylene (LLDPE) and high density polyethylene (HDPE) to be discussed further in section 2.2.

History of polyolefins

Von Pechmann in his report (1898) states that he discovered a white substance while dissolving diazomethane in ether. He called this polymethylene.[1]

LDPE was first discovered accidentally in March 1933 by scientists Eric Fawcett and Reginald Gibson working at Imperial Chemical Industries Limited. The chemists in an attempt to produce a ketone, reacted ethylene and benzaldehyde at 1500 atm but found a white waxy polymer lining the reaction vessel instead.[2] Resulting from a leak in the reaction vessel, oxygen entered the experiment and acted as a catalyst for the radical polymerisation of ethylene. Unfortunately, further attempts to reproduce the experiment were unsuccessful as either the reaction would simply not proceed or, would end up in an explosion. This was seemingly due to incorrect amounts of oxygen taking part in the reaction. Ultimately, for safety reasons following the explosions, Fawcett and Gibson were banned from conducting the experiment for another two years.

Eventually, upon resuming the experiment, they were finally successful from addition of the correct amount of cold ethane to the reaction. It was in December 1935, when they managed to produce 8 g of polymer and from then on until 1939, work was done to develop commercial manufacturing. Following that, Dupont also, between 1939 and 1945 succeeded in their first commercial manufacture of free radical polymerisation of polyethylene. Their product had an approximate density and alkyl substituents per 1000 carbon atoms of 0.955 g/cm^3 and 0.80 respectively.[3]

In the 1950s, polymerisation of a more crystalline, more linear polyethylene was realised when J.P. Hogan and R.L Banks working at Phillips Petroleum discovered transition metal catalysts. They used this catalyst system (Phillips catalysts) which consisted of a chromium oxide supported on silica alumina to synthesise propylene and later, copolymers of ethylene and alpha olefins.

Still in the early 1950s, Karl Ziegler also discovered a range of transition metal catalysts that could produce a more linear polyethylene. His catalyst system however consisted of combinations of both zirconium or titanium salts and aluminium co-catalysts. The work he carried out with this catalyst system yielded polyethylene of high molar masses.[4,5] Subsequent to that, Giulio Natta after certain pre-conditioning and preparation of these heterogeneous catalysts, used them to synthesise a highly crystalline isotactic polypropylene. It was this work by Ziegler and Natta that got them awarded the 1963 Nobel peace prize for the now famous Ziegler-Natta catalysts.[4,6]

Full on commercial production by various organisations including DuPont and the Union Carbide Corp. was realised in the 1970s. Using the Unipol gas phase technology, they added alpha olefins to ethylene polymerisation yielding a wide range of linear low density polyethylene (LLDPE).[3]

Still in the mid to late 1970s, Kaminsky and Sinn reported yet another range of catalysts. These were unique in that they were single site catalysts and of much higher activity in the polymerisation of ethylene. These soluble transition metal catalysts consisted of a combination of a metallocene complex as pro-catalyst and methylaluminoxane (MAO) as co-catalyst.[6,7]

2.2 Catalyst chemistry of polyolefins

Catalysts are an essential part of the olefin polymerisation process. Together with other polymerisation conditions like temperature and pressure, they determine the reaction rates and kinetics, as well the yield and properties of the resultant polymer. Furthermore, they speed up the polymerisation reaction by lowering the required activation energy. The benefit of lowered activation energy allows for the reaction to proceed using lower pressures and temperatures than those employed in catalyst free polymerisation reactions.[8,9]

The most commonly used catalysts for the polymerisation of olefins include the Zieglar-Natta, Chromium (Phillips) and Metallocene catalysts. Catalyst choice is dependent on the required end properties of the polymer. Some of these properties include physical properties and chemical composition like branching type and stereoregularity.

2.2.1 Ziegler- Natta catalysts

Ziegler-Natta catalysts were first discovered accidentally in the 1950s by Ziegler and his team. The discovery was that nickel had the ability to act as a catalyst during the reactions between ethylene aluminium alkyls. On further enquiries, they found that it was the group IV – VII transition metals that could be active as polymerisation catalysts. Most importantly, it was titanium in combination with the aluminium alkyls.[10] Following this discovery, Natta used these catalysts to produce isotactic polypropylene.[11]

Ziegler-Natta catalysts can be homogeneous (vanadium based, metallocene) or heterogeneous (catalyst is in a different phase from medium of reaction) with the latter being the most commonly used in the polymerisation of polyolefins. Typically, a heterogeneous Ziegler-Natta catalyst will be made up of a titanium halide ($TiCl_4$) as a catalyst, a trialkyl aluminium compound (AlR_3) as a co- catalyst and, a magnesium dichloride (MgCl2) as support. From the first discovery of this type of catalyst, modifications up to the 5th generation have been made in an attempt to improve yield and selectivity. The modifications saw yield improve from about 0.2 $kg_{polymer}/g_{catalyst}$ to about 30 $kg_{polymer}/g_{catalyst}$ while selectivity improved with about 10 % isotactic index over the generations.[9]

In the early 1960s, the 1st generation used a metallic aluminium in the reduction of titanium tetrachloride (TiCl4). This yielded trichloride aluminium ($AlCl_3$) dispersed in a titanium trichloride matrix ($TiCl_3/3AlCl_3$) and was of poor activity. The yield was a maximum of 1.5 kg/g. Later on, in the early 1970s, a 2nd generation was born which employed an ether as a complexing agent. This was used in the preparation of catalytically active complexes based on $TiCl_3$. The activity was however still quite low with a yield maximum of 5 kg/g. Moreover, the catalyst residue had to be deactivated using TiO_2. Following that in the late 1970s, several manufactures used activated, anhydrous $MgCl_2$ as support combined with $TiCl_4$ and AlR_3 as co-catalyst. This was deemed the 3rd generation and the catalyst activity was increased, achieving a yield maximum of 25 kg/g. Adding to that, the high reactivity of the catalyst meant that the costly step of residual catalyst removal at the end of the reaction was no longer necessary. Apparently, along with each generation modification came a significant reduction in catalyst residue.[9]

Further modifications in the 1990s yielded the 4th generation which was based on aluminium-oxane activated metallocene complexes. Lastly, the 5th generation was based on 1.3-diethers, and succinates as donors. The catalyst activity approached 100 kg/g and the polymer produced was in pellet form. This eliminated the need for further extrusion and pelletizing.[8]

The insertion or coordination polymerisation of all Ziegler-Natta catalysts follow the Cosee and Arlman pathway as depicted in Figure 2.1 below. Cosee and Arlman in contrast to the earlier beliefs by Ziegler and Natta reported that the polymerisation follows a non-metallic as opposed to a bimetallic mechanism and occurs at the transition metal-carbon bond.[12]

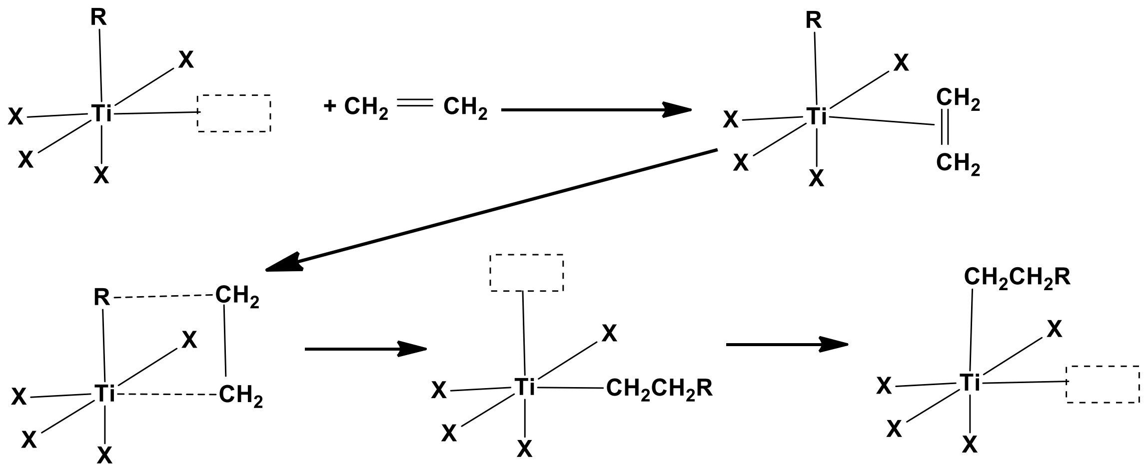

Figure 2.1 Cosee and Arlman mechanism: X are ligands and R is the growing polymer chain.[13]

The heterogeneous nature of the Ziegler-Natta catalysts produces polymers with a broad distribution of molar mass and short chain branch content resulting from the multiple active sites with different rates of activity. Work done by McKenna e.al[14] showed some advantages of such a broad distribution on the mechanical properties and rheological behaviour during processing. This makes the catalyst a favourable choice for the polymerization of bimodal HDPE resins.

2.2.2 Metallocene catalysts

Metallocene (m) catalysts were first discovered by Breslow and Newburg[15] in 1958. Initially, they had poor reactivity for ethylene and even worse, could not polymerise propylene all together. Fortunately, Reichert and Meyer were later successful in their attempts to improve the poor reactivity.[16] This led to the development of methylaluminoxane (MAO) as a co-catalyst to the metallocene with very high activity in the polymerisation of olefins.[17] The nature of the catalyst is such that organometallic compounds with group 4 transition metal (Ti,Zr,Hf,V) centres are sandwiched between aromatic ligands. The ligands are joined together by a silyl bridge $(CH_3)_2Si$. The most commonly used ligands include dicyclopentadienyl, indenyl or fluoroenyl groups.[18] Examples of these are given Figure 2.2.

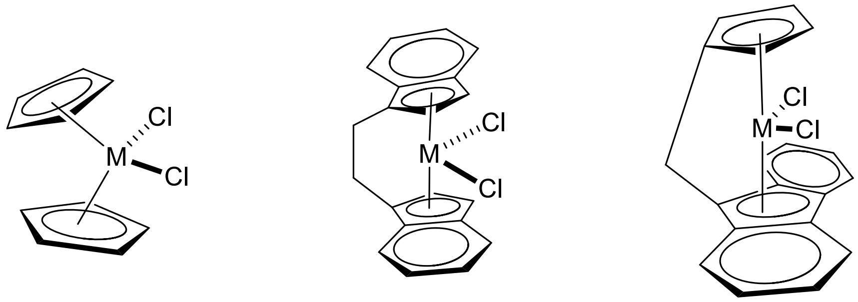

Figure 2.2 Examples of the metallocene catalysts.[19]

Unlike their heterogeneous counterparts, metallocenes are single site catalysts which allow excellent control over the polymer microstructural properties including tacticity, molar mass (MM) and molar mass distribution (MMD) through controlled comonomer content distribution. Furthermore, not only did the m-catalysts introduce different property combinations but also, the use of "novel" comonomers such as styrene, norbonene, and carbon monoxide".[9] However, with all the great features of the m-catalysts, they are expensive owing to the high costs of the MAO, therefore, their use is limited. To combat this, MAO-free systems have been developed.[10,20]

Some of the early users of the m-catalysts for bimodal HDPE production include Borealis, Exxon, Dow, Mitsui, and Lyondellbasell in their slurry phase processes. To date, many other producers have adopted similar technologies to produce polyolefins with improved properties like high mechanical and rheological properties.

2.2.3 Phillips catalysts

Phillips catalysts were first discovered in 1951 by Hogan and Banks.[21] In their synthesis, a silica is impregnated with CrO_3 before being calcined at high temperatures (200 – 900 ºC). The calcination causes the Cr species to link to the silica. The catalytically active sites are generated before polymerization through mixing together chromium oxide and silicon oxide.[22,23] For this reason, a co-catalyst is not required.

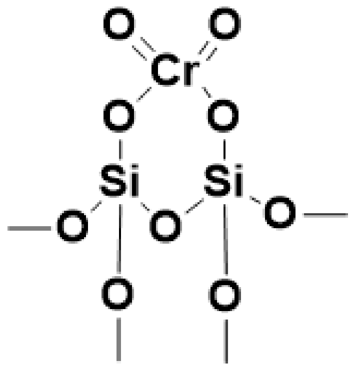

Figure 2.3 Chromium catalyst structure.

Although the Phillips catalysts have a seemingly lower reactivity with regard to alpha olefin incorporation, they do however result in a very broad MMD HDPE resin.[24] The MMD is even broader than those produced with Ziegler-Natta and metallocene catalysts. The most commonly employed technologies for the Phillips catalysts include the gas and slurry phase for the polymerisation of PE.[24]

2.3. Classes of polyethylene

Differences in the listed ranges of polyethylene are as a result of their structures, mainly branching type, content and distribution. Molecular structure also determines the end use properties of the different polymers. In other instances, different polymers are blended together to optimise properties.

2.3.1 Low density polyethylene (LDPE)

LDPE is produced by a high pressure high temperature free radical polymerisation technology in tubular or autoclave reactors. The polymer is characterised by a high concentration of long and short side branches which give it its flexibility and great optical properties. The high branching content results in low density (0.91 - 0.925 g/cm^{-3}) polymer and subsequent low crystallinity. This type of polyethylene finds its use in flexible packaging applications. The high level of entanglements hinders ease of processing in the molten state, and the low densities render polymers with lower mechanical properties but exceptional optical properties.

2.3.2 Linear low density polyethylene (LLDPE)

LLDPE on the other hand is produced by a friendlier low pressure low temperature technology using either a slurry, solution or gas phase polymerisation technology. Polymerisation is carried out in the presence of a catalyst usually, heterogeneous Ziegler-Natta or a single site type of catalysts and, an alpha olefin usually 1-butene, 1-hexene or 1-octene. The lower specification densities of LLDPE are slightly higher than those of LDPE (0.919 – 0.925 g/cm^3) due to the reduced amount of branching. This polymer is also characterised by an almost linear structure comprising short chain branches. LLDPE is more crystalline than its LDPE counterpart and has higher tensile and impact strengths but reduced optical and processing properties. Applications include blown and shrink films as well as extrusion coatings.

2.3.3 High density polyethylene (HDPE)

HDPE which can be unimodal, bimodal or multimodal is more linear in its structure, more crystalline and much stiffer than both its low and linear low counterparts. This is owed to the much less short chain branches. Its polymerisation is much like that of the LLDPE in that it uses low pressure, low temperature processes in the presence of catalysts and, in the case of bimodal HDPE, comonomer of alpha olefins too. Polymerisation is carried out in the presence of Ziegler-Natta or chromium (Phillips) catalysts using the slurry, solution or gas phase technologies. In the case of bimodal HDPE, either a combination of reactors is used in series or a single reactor is used with two single-site tailor made catalysts to produce a bimodal molar mass resin.

2.3.4 Bimodal HDPE (bHDPE)

Bimodal HDPE is a blend of low molar mass (LMM) and high molar mass (HMM) components and their different functions. The blends are produced using low pressure polymerisation processes like the slurry loop, Continuous Stirred Tank Reactors (CSTR) Ziegler slurry and gas phase in the presence of either Ziegler-Natta or chromium ("Phillips") catalysts.[25-28] The production involves cascade reactors in series. The first reactor produces the LMM homopolymer by addition of ethylene monomer and hydrogen. The hydrogen acts as chain terminators ensuring a very low molar mass homopolymer. The product from the first reactor and the hydrogen is removed and placed in the second reactor. In the second reactor, comonomer, usually 1-butene, 1-hexene or 1-octene is introduced to produce a HMM product with short chain branches (SCB).[29] In instances where the HMM component is produced in the first reactor, the process is termed reversed phase.[29] Production of bimodal MMD polyethylene using a single reactor with a dual catalyst system has also been reported in literature.[30,31] A schematic diagram of the low pressure slurry process is depicted in Figure 2.4.

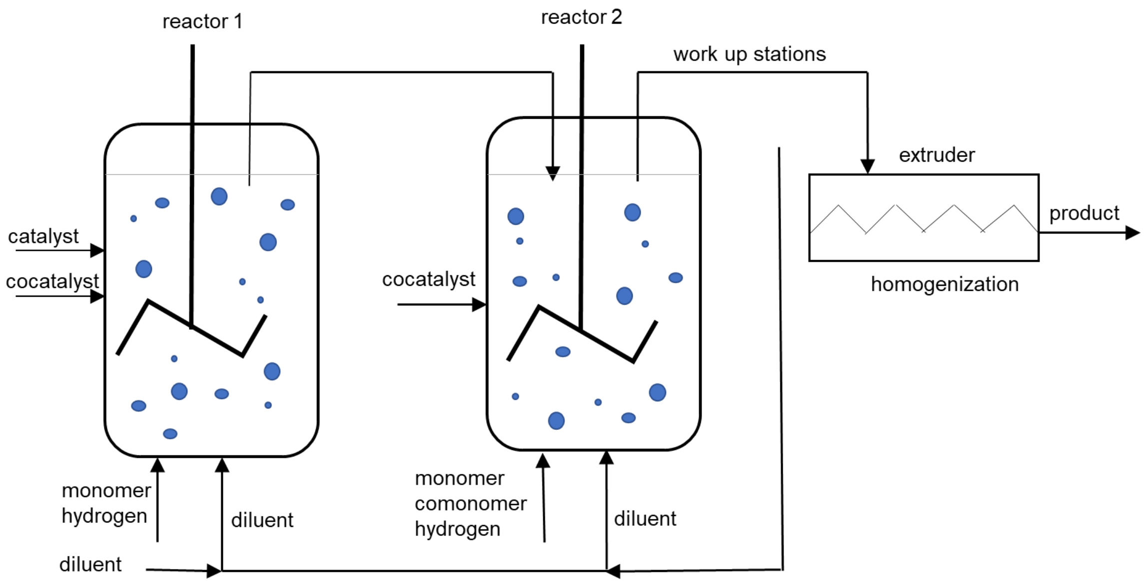

Figure 2.4 Schematic diagram of a low-pressure slurry process.[29]

Fan et.al[25] concluded that the SCB give bimodal HDPE its high mechanical properties such as good environmental stress crack resistance (ESCR), resistance to rapid crack propagation (RCP) and stiffness. The LMM components however contribute to improved rheological/ processing properties. This combination of properties renders bimodal HDPE popular for use in pipe manufacturing and heavy-duty plastic films which can perform even at very thin gauges. The structure-property relationship of bimodal polyethylene is given in Figure 2.5.

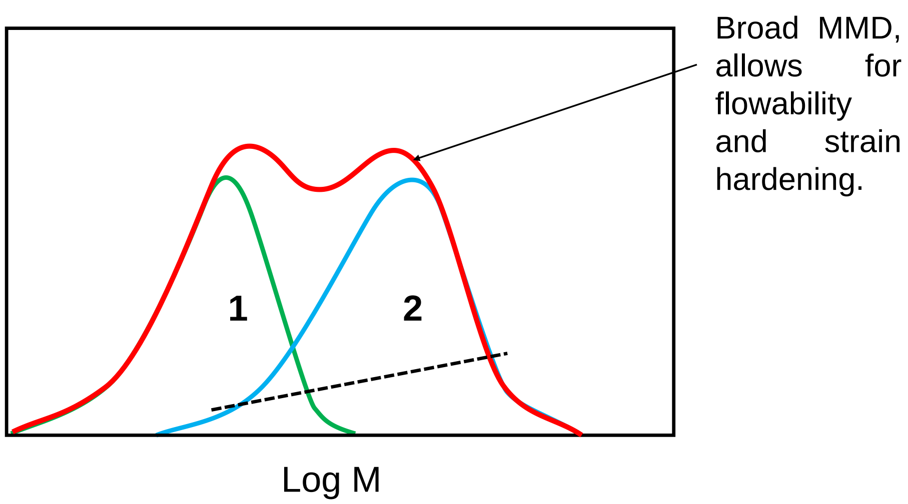

Figure 2.5 Structure-property relationship of bimodal polyethylene. A low molar mass polyethylene homopolymer component (1) has high crystallinity and allows for processability and stiffness of the final product. A second component (2) is very high molar mass copolymer with low crystallinity and allows for high impact strength and stress crack resistance.[29]

2.4. Characterization techniques of polyolefins

Each of the analytical techniques employed in this study highlight different aspects of the complex microstructural properties of polyolefins. It is also demonstrated how a single technique cannot fully characterize the microstructure of polyolefins. The preparative techniques herein also demonstrate the quality of information that can be obtained by fractionating polyolefins according to the different microstructural properties (CCD and MMD). Further analysis of the fractions demonstrate the importance of each fraction's contribution to the bulk properties of bHDPE. Coupling of certain techniques also proves that meaningful correlation between the different aspects of the microstructure can be achieved.

2.4.1. Spectroscopic techniques

Solution Carbon-thirteen nuclear magnetic resonance spectroscopy

Solution ^{13}C magnetic resonance spectroscopy (^{13}C NMR) is sensitive to microstructural differences in polymers. As such, it was used to determine the comonomer and comonomer content of the bulk bHDPE resins and their fractions. Polymer molecules in solution are exposed to an external magnetic field and an electromagnetic radiation is applied. This causes the nucleus which behaves like a magnetic bar to be aligned and the energy required to bring the various nuclei into resonance to be measured. The energies required to bring each nuclei into resonance is represented by peaks/signals on the spectrum.[23]

Tetramethylsilane (TMS) is considered to have a chemical shift of 0 ppm and is usually used as an internal reference when reporting NMR signals. From these signals, it is possible to predict the chemical structure of the sample. Integration of the areas under the peak signals allow the quantification of the comonomer and short chain branching using Equation 3.1 as described in the experimental section.

NMR has proven very useful in identifying and quantifying the different chemical compositions of complex polymers when coupled to separation techniques including SGIC, GPC and two dimensional liquid chromatography.[32-36] Uncoupled, it has also been used extensively in the analysis of ethylene 1-olefin copolymers.[37-41]

2.4.2. Crystallization-based techniques

Differential scanning calorimetry (DSC)

This technique was developed by Watson and O'Neil in the early 1960s for the determination of thermal properties like melting, crystallisation and mesomorphic temperatures. A picture of the furnace set-up is depicted in Figure 2.6. Other properties like physical and chemical transitions like the glass transition temperature are determinable by DSC.[42,43]. These changes are observed as changes in enthalpy, entropy, heat capacity or latent heat.[44] Later, improvements to the technique with regards to speed and significantly reduced sample sizes were realised with the invention of high performance DSC (HPer DSC) and flash DSC.[45] HPer DSC has been used extensively in the analyses of complex polyolefin microstructures.[46-50]

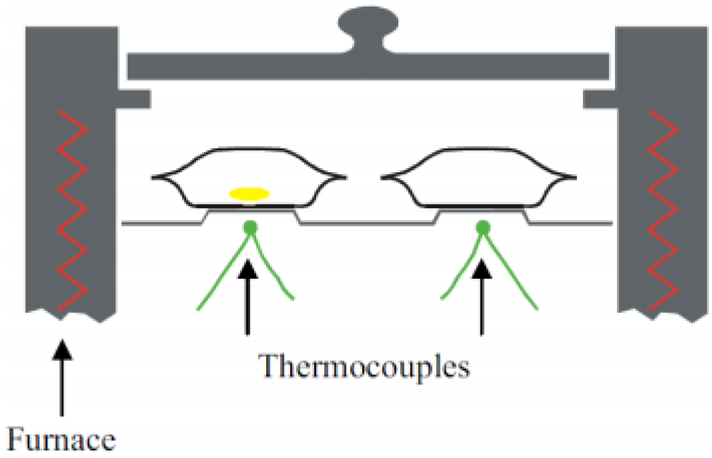

Figure 2.6 DSC furnace with a polymer sample and a reference pan.[44]

More recently, DSC has proven to be a useful tool in the characterization of chemical composition distribution and short chain branch distributions.[51-55] Additionally, it has been used to study the isothermal and non-isothermal crystallisation kinetics of bHDPE to simulate the cooling that occurs during film blowing.[56,57]

Crystallisation analysis fractionation (Crsytaf)

The crystallization analysis fractionation technique was developed in 1991 by Benjamin Monrabal.[58] The technique separates polymer chains according to crystallinity in a similar way to TREF. Analysis involves firstly dissolving polymer in a good solvent like 1,2,4-trichlorobenzene (TCB) at 160 ºC under continuous stirring (200 rpm). Secondly, the solution temperature is stabilized at 100 ºC before being cooled down at very slow rates (0.1 – 0.2 ºC) to ambient temperatures. As a result, polymer molecules crystallize out of solution as temperature is decreased. This causes a change in the concentration of the solution. The change is captured by a concentration detector operating at 150 ºC and results of the solution concentration are reported as a function of temperature.

The advantage of CRYSTAF over TREF is quicker analysis times. This is because CRYSTAF eliminates the elution step that is in TREF by collecting data during crystallization.[59] Also, the instrument is equipped with five stainless steel reactors enabling simultaneous analysis of up to five samples. The main disadvantage of CRYSTAF is the effect of co-crystallization.[60] For this reason, samples are analyzed at a very low concentration (0.1 to 1.0 mg/mL) and the crystallization rate is kept very low.

Polymers with high crystallinity (containing low amount of comonomer and branching) crystallize out of solution first while the least crystalline polymers only crystallize out of solution at lower temperatures. Calibration of the instrument is obtained with use of narrow CCD polyolefins. CRYSTAF has been used extensively in the analysis of the complex microstructural properties of polyolefins.[61-65]

2.4.3. Chromatographic techniques

High-temperature size exclusion chromatography (HT-SEC)

Ideally, size exclusion chromatography (SEC) separates polymer chains according to their size or hydrodynamic volume in solution. This gives information on molar mass averages, distributions and dispersity.[66] Thermodynamically good solvents like TCB and ODCB are used as a mobile phase to carry dissolved polymer analyte into the column. Once in the column, separation is driven by interaction of the analyte with porous gels used as column packing. Unlike the smaller molecules which have more pore volume accessible to them, bigger molecules have less and are therefore eluted first from the column. The amount of analyte in the column is continuously monitored by a detector.

The detector(s) employed produce a signal based on the concentration and/or molar mass of the polymer in the detector cell as a function of elution volume. The most conventional detectors used are concentration detectors namely refractive index (RI) and infrared (IR). Once calibration of the column is successful, the concentration profile is converted to a MMD as a function of elution volume.[67] The detectors are capable of correlating molecular size to molar mass but are incapable of the effective measurement of complex polymers. Complex polymers that include a distribution of composition or long chain branching require that the concentration detector be coupled to a molar mass sensitive detector. This is because their molecular size is not only dependant on concentration but also on molar mass.[68-70]

The most popular of molar mass sensitive detectors include the light scattering (LS) and viscometer (Vis). They can accurately measure molecular size and branching irrespective of elution volume. This overcomes the challenge of co-elution by chemically different species of similar hydrodynamic volume.[71-73] More recently, triple detection SEC using a combination of three different detectors namely, an online concentration, light scattering and viscometer

(SEC-IR-LS-Vis) has proven even more effective at detecting the presence of long and short chain branching of complex polymers.[74,75]

While coupling of SEC to other techniques like FTIR and NMR enables effective analysis of SCB, coupling with other separation techniques gives even more detailed information about the polymer architecture.[70,76-78] More specifically, SEC has been used successfully in the fractionation of bHDPE in the evaluation of its short chain branch distribution.[50]

High-temperature solvent gradient interaction chromatography (HT-SGIC)

HT-SGIC is an excellent adsorption-desorption technique used to separate polymers according to their chemical composition and tacticity. Separation is driven by enthalpic (ΔH) interactions between the analyte and the stationary phase. Until the inception of HT-SGIC, the most utilised separation methods according to chemical composition included crystallisation-based techniques like TREF, CRYSTAF and CEF. One of the biggest challenges with the crystallisation based techniques however, was their inability of separate non crystalline chains which HT-SGIC overcomes. During a HT-SGIC experiment, an analyte is injected into a stationary phase column, is adsorbed onto the column with the aid of a poor solvent (1-decanol) and, is captured by a detector when it is finally desorbed and eluted from the column with the aid of a good solvent. The experiment runs at a temperature above 160 ^{o}C above the polyolefin melting point to allow complete dissolution and resolution.

The best column for the adsorption of linear polyethylene was found to be packed with a porous graphite carbon invented by Knox et.al[79] namely Hypercarb®. The Hypercarb is ideal because of its strong adsorptive forces upon interaction with polyolefin molecules. This results in separation according to chemical composition rather than crystallisation.[80] Although normally 100 mm are used, longer columns have been related to better polyolefin separation efficiency.[81] Before the discovery of the Hypercarb®, zeolite was initially employed by Macko and Pasch[82-85] in earlier experiments to separate polyolefins. Later, Heinz and Pasch[86] used silica and successfully separated blends of polyethylene and polypropylene using a solvent gradient of EGMBE – TCB. For the system using the Hypercarb®, a linear solvent gradient system is used.

A solvent gradient mixture consists of 1-decanol as a poor, non-polar solvent and polar TCB as the mobile phase. Careful consideration is made when choosing the solvent mixture including. To name but a few, the ability to withstand high operating temperatures, the ability to efficiently dissolve all polymer components and, the ability to promote good adsorption to prevent immediate elution of the polymer. In addition, Ndiripo et.al[81] reported that better separation is achieved with an increasing carbon chain length of the adsorption promoting solvent. Firstly, 1-decanol dissolves the polymer by weakening it's inter- and intra- molecular interactions. Once dissolved, the analyte is carried into the column where it is adsorbed. Secondly, polar solvent TCB is gradually introduced to elute the analyte fractions from the column where they are then captured by a detector.

Detection of the eluted fractions is limited to using an evaporative light scattering detector (ELSD). This is mainly because using other detectors like infrared is impossible for non-transparent adsorption promoting solvents like 1-decanol. The type of detector settings however, differ for the different solvent systems and analyte types.

During elution, the longer methylene chains remain attached to the PGC stationary phase for longer because of the strong interactions with the van der Waals forces. This causes them to be eluted last. In contrast, the shorter methylene sequences resulting from the presence of short chain branches are eluted first. This is in agreement with the report by Macko et al[87] stating that "elution volume is indirectly related to the concentration of branches". The same elution patterns have been observed in other studies involving bHDPE and ethylene/ alpha olefin copolymers.[28,81,88]

High-temperature two-dimensional liquid chromatography (HT-2D-LC)

HT-2D-LC involves coupling HT-SGIC in the first dimension to HT-SEC in the second dimension. On-line coupling of the two techniques is achieved by way of an eight-port valve with matching sample loops. Each of the dimensions employ the same separation procedures as described in the respective sections above but polymer fractions are automatically transferred from the first dimension into the second using a valve. Successful transfer depends on careful selection of sample flow rates and sampling times in each dimension.

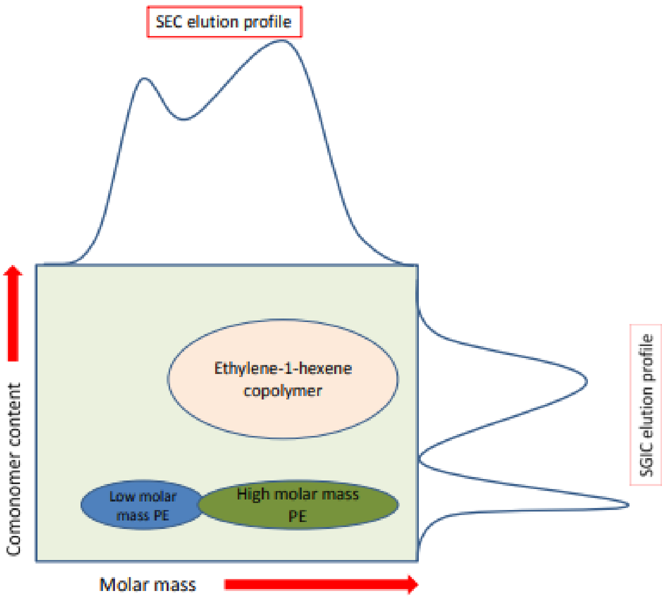

Figure 2. 7 Schematic diagram depicting the complexity in the microstructure of bimodal HDPE obtained via 2D-LC.[80]

Polyolefins comprise of complex microstructures that include both chemical composition and molar mass being most important. Comprehensive analyses through cross fractionation is therefore imperative for complete elucidation of the properties. Figure 2.8 shows a correlation of CCD and MMD of bHDPE. Two dimensional liquid chromatography separates copolymer according CCD in the 1st dimension and the separate fractions are in the second dimension analysed for MMD. Although the two techniques can be done off-line, [89,90]coupling online offers benefits such as eliminating possible contamination and sample recrystallization The technique has proven to be very successful in the correlating of CCD and MMD.[91-95]

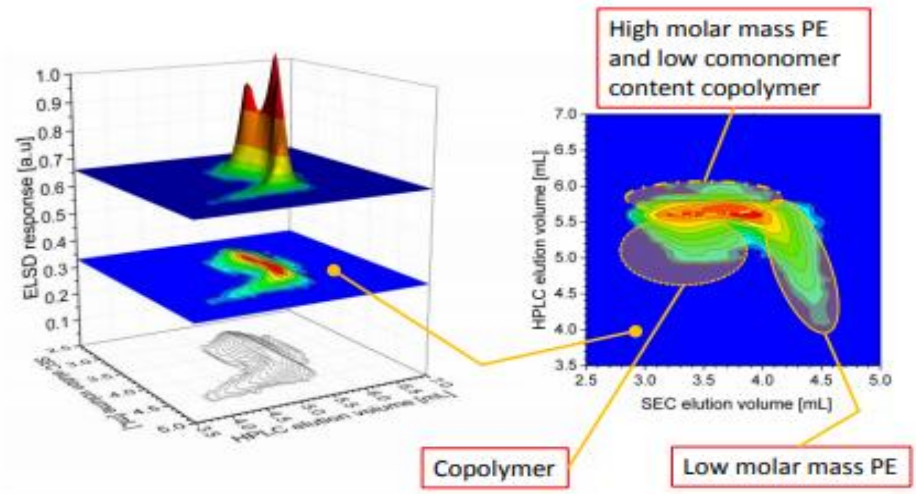

Figure 2.8 Correlation of CCD and MMD of bimodal HDPE.[80]

2.4.4. Preparative fractionation

Preparative temperature rising elution fractionation and preparative molar mass fractionation (pTREF and pMMF)

Preparative TREF is a separation technique used in separating semi crystalline polyolefins according to differences in chain crystallinity or solubility and, the temperature at which chains dissolve. Preparative MMF on the other hand uses a solvent/non-solvent mixture to separate polyolefin chains according to narrow molar mass dispersity irrespective of having broad comonomer content distribution.[96] A combination of these techniques enables better understanding of the complex polymer microstructure including the presence and distribution of short chain branches. Preparative TREF has especially been proven successful in separating polymer blends and copolymers.[97]

TREF involves two stages wherein the first step, polymer is dissolved in a high-temperature solvent like xylene. The hot solution is then transferred to a glass reactor with an inert support. The support can be in the form of sea sand particles, glass beads or silica gel. The temperature of the glass reactor is then reduced from about 130 ºC to ambient temperature at a very slow cooling rate of about 1 ºC/ hour. Successful separation and crystallisation of different chains is dependent on the slow cooling rate being low enough. The most crystalline chains precipitate out of solution first and crystallise around the inert support while the least crystalline chains remain in solution as the temperature is decreased. Finally, the non-crystalline chains remain in solution even at ambient temperatures.

In the second step, dissolution involves first packing a column with the crystallised polymer layers and running a gradually heated solvent through the column in order to dissolve the crystallised layers. As the dissolution temperature is gradually increased, the least crystalline fractions elute first while the most crystalline elutes latest at the highest dissolution temperatures. In pTREF the dissolved layers are collected and analysed further with various analytical techniques.

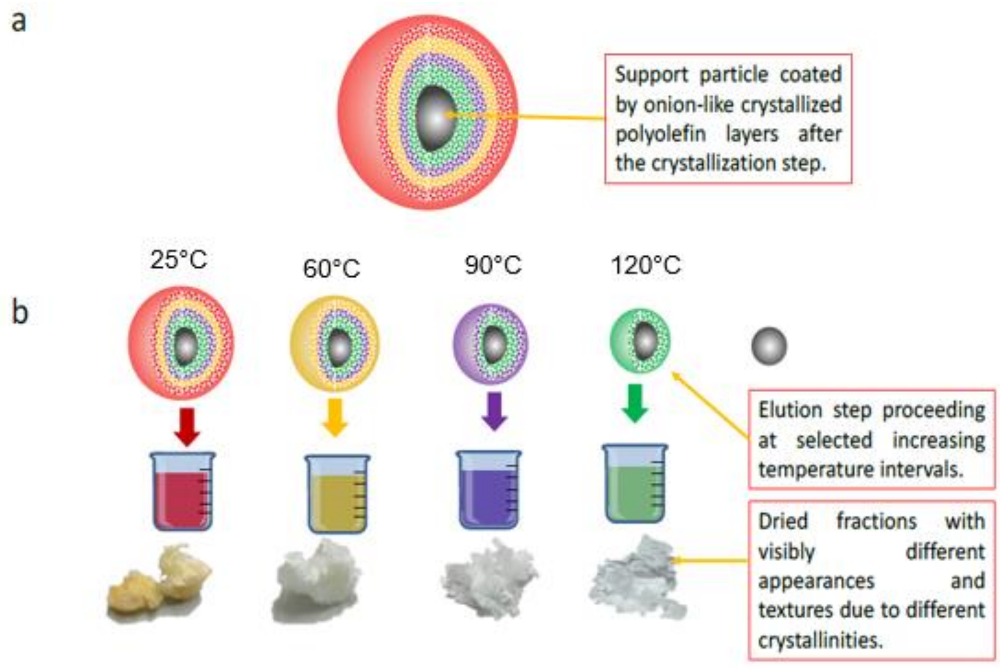

Figure 2.9 Schematic representation of the collected fractions from pTREF showing (a) the crystallisation and (b) elution step.[80]

Shirayama[98] and colleagues were the first people to use the technique and they observed a distribution of short chain branches over various molar masses of polyethylene. Some of the earliest uses of the technique were reported in the 1950s by Desreux and Spiegels[99] for work done to separate fractions of polyethylene. To this day, the shortcomings of TREF still persist regarding long cycle times, requirement of large volumes of solvent, general labour intensity, inability to separate non crystalline material, and co-crystallisation effects.

The co-crystallisation effect for bHDPE is a bigger challenge than it is for other polyolefins of longer chain branches. This is because crystallinity temperatures of the very short chain branches are usually closely related to that of the homopolymer. This negatively affects efficient compositional separation of the different chains.[100,101] Successful pTREF separations however, have been achieved in studies to investigate the chemical heterogeneities in bHDPE.[27,80] Results were in agreement with those of fractionation of other polyolefin blends stating that, chain separation is according to crystallisability and comonomer content.[46,47,102-107] The most crystalline, least branched chains eluted at the highest temperatures while the most branched chains eluted at lower elution temperatures as TREF has been designed to perform.[108-110]

Despite the challenge of chemical composition influences as a result of chain solubility on the fractionation process, pMMF has recently been used successfully in the fractionation of various polyolefins.[103,104,111-113] To the best of our knowledge, no pMMF has yet been carried out on any bHDPE resins. Krumme et.al[50] however fractionated bHDPE according to molar mass successfully using analytical size exclusion chromatography.

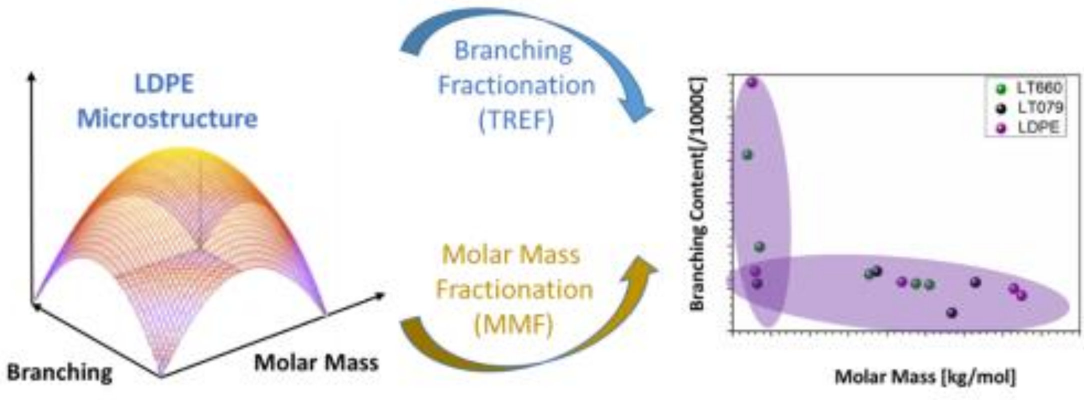

Figure 2.10 A diagram showing the multiple preparative fractionation concept on LDPE.[114]

2.4.5 Mechanical analysis

Dynamic mechanical analysis (DMA)

DMA is a technique that measures a material's response (strain) to an applied oscillating force (stress). Measurements can provide information on various mechanical properties at different temperatures, times or frequency.[115] This helps in predicting the material's behaviour in response to various processing temperatures. The most important mechanical properties obtainable from DMA include storage modulus, loss modulus and tan delta. The stiffness (loss) modulus in DMA experiments is given by the slope of the stress-strain curve. It provides information on a material's ability to either store or dissipate energy. The ratio of which is given as the material's damping ability (tan delta).

Tensile strength and Young's modulus

Tensile strength is a mechanical property that measures a material's response to a uniaxial pulling force on a tensiometer instrument. Test specimens (normally dumbbell shaped) of a fixed cross sectional area are pre-conditioned to specified temperature and humidity for up to 48 hrs before testing. The deformation rate of applied force is specific to specimen dimensions and polymer type. Typical rates or speed of testing range between 1 and 500 mm/min and refer to the motion of the grips. Usually, multiple repeats between three and ten are performed on each sample and the average of which is reported.[117]

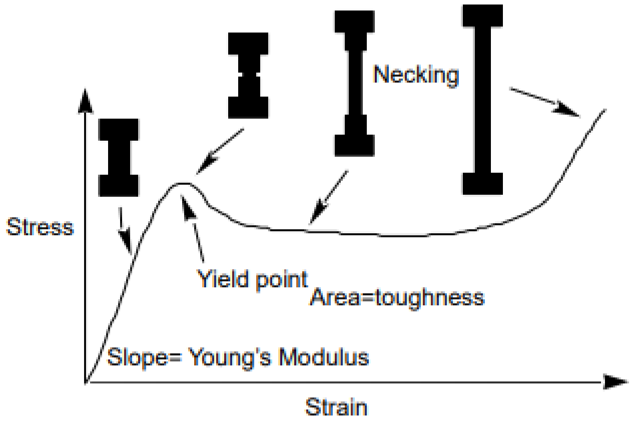

Figure 2.11 Stress-strain curve showing deformation of a semi-crystalline polymer material.

Many semi-crystalline polyolefin specimen deformations follow the trend displayed in Figure 2.11. On application of stress (pulling force), the sample extends until it reaches breaking point at maximum strain. The area under the stress strain curve gives the material's toughness. The initial slope in the stress-strain curve before the material yields is referred to as Young's modulus or elastic modulus. This region obeys Hooke's law and refers to the stiffness of a material. The exact measure of Young's modulus is calculated as per Equation 2.1.

$$E = \frac{\frac{F}{A}}{\frac{\Delta L.}{L}}$$

Equation 2.1 Young's modulus

Where:

E = Young's modulus (Pa)

F = Force (N)

L = Original length (m)

A = Area (m^2)

ΔL = Change in length (m)

The stress-strain behaviour of a polymeric material depends on various parameters such as molecular characteristics, microstructure, strain-rate and temperature.[118-120] A higher –

comonomer content in polyolefins tends to lower the stiffness of the material in comparison to the more crystalline materials.[120-121]

2.5 References

(1) Von Pechmann, H.; Frobenius, L. *Ges* **1898**, *31*, 2643.

(2) Peacock, A. *Handbook of Polyethylene: Structures: Properties, and Applications*; CRC Press: New York, **2000**, p 1–24.

(3) Mark, H. F.; Kroschwitz, J. I. *Encyclopedia of Polymer Science and Engineering*; John Wiley and Sons,: New York, **1985**, p 383 - 436.

(4) Kaminsky, W.; Böhm, L. *Polyolefins: 50 Years After Ziegler and Natta*; Springer, **2013**.

(5) Ziegler K, Gellert H, *Polymerization of ethylene*,**1955**, United States Patents, Germany, US 2699457A.

(6) Krentsel, B.; Kissin, Y.; Kleiner, V.; Stotskaya, L. *Hanser* **1997**, 243–335.

(7) Malpass, D. B. *Introduction to Industrial Polyethylene: Properties, Catalysts, and Processes*; John Wiley & Sons: New Jersey, ***2010***.

(8) Shamiri, A.; Chakrabarti, M. H.; Jahan, S.; Hussain, M. A.; Kaminsky, W.; Aravind, P. V.; Yehye, W. A. *Materials* **2014**, *7*, 5069–5108.

(9) Vasile, C. *Handbook of polyolefins*, Second ed.; CRC Press, **2000**.

(10) Albizzati, E.; Galimberti, M. *Catal.* **1998**, *41*, 415–421.

(11) Natta, G. *J. Polym. Sci.* **1959**, *34*, 21–48.

(12) Chikkali, S. H. *Resonance* **2017**, *22*, 1039–1060.

(13) Böhm, L. L. *Angew. Chem. Int.* **2003**, *42*, 5010–5030.

(14) McKenna, T. F.; Di Martino, A.; Weickert, G.; Soares, J. B. *Macromol. React. Eng.* **2010**, *4*, 40–64.

(15) Breslow, D. *J. Am. Chem. Soc* **1957**, *79*, 5072.

(16) Bochmann, M. *J. Chem. Soc., Dalton Transactions* **1996**, 255–270.

(17) Sinn, H.; Kaminsky, W. In *Ziegler-Natta catalysis*; Elsevier, **1980**, p 99–149.

(18) Alt, H. G.; Köppl, A. *Chem. Rev.* **2000**, *100*, 1205–1221.

(19) Kaminsky, W.; Laban, A. *Appl. Catal., A* **2001**, *222*, 47–61.

(20) Harrison, D.; Coulter, I. M.; Wang, S.; Nistala, S.; Kuntz, B. A.; Pigeon, M.; Tian, J.; Collins, S. *J. Mol. Catal. A: Chem.* **1998**, *128*, 65–77.

(21) Kissin, Y. *Stud. Surf. Sci. Catal.* **2007**, *173*, 1–34.

(22) Spalding, M. A.; Chatterjee, A. *Handbook of industrial polyethylene and technology: Definitive guide to manufacturing, properties, processing, applications and markets set*; John Wiley & Sons, **2017**.

(23) Rodriguez, F.; Cohen, C.; Ober, C. K.; Archer, L. *Principles of polymer systems*; CRC Press: United States of America, **2014**.

(24) McDaniel, M. P. *Adv. Catal.* **2010**, *53*, 123–606.

(25) Fan, Y.; Xue, Y.; Nie, W.; Xiangling, J.; Bo, S. *Polym. J.* **2009**, *41*, 622–628.

(26) Sun, X.; Shen, H.; Xie, B.; Yang, W.; Yang, M. *Polymer* **2011**, *52*, 564–570.

(27) Ginzburg, A.; Macko, T.; Dolle, V.; Brüll, R. *J. Appl. Polym. Sci.* **2013**, *129*, 1897–1906.

(28) Prabhu, K.; Brüll, R.; Macko, T.; Remerie, K.; Tacx, J.; Garg, P.; Ginzburg, A. *J. Chromatogr. A* **2015**, *1419*, 67–80.

(29) Alt, F. P.; Böhm, L. L.; Enderle, H. F.; Berthold, J. *Macromol. Symp.* **2001**, *163*, 135–144.

(30) Tian, Z.; Chen, K.-R.; Liu, B.-P.; Luo, N.; Du, W.-L.; Qian, F. *Chem. Eng. Sci.* **2015**, *130*, 41–55.

(31) Chatzidoukas, C.; Kanellopoulos, V.; Kiparissides, C. *Macromol. Theor. Simul.* **2007**, *16*, 755-769.

(32) Hiller, W.; Pasch, H.; Macko, T.; Hofmann, M.; Ganz, J.; Spraul, M.; Braumann, U.; Streck, R.; Mason, J.; van Damme, F. *J. Magn. Reson.* **2006**, *183*, 290–302.

(33) Hiller, W.; Hehn, M.; Sinha, P.; Raust, J.-A.; Pasch, H. *Macromolecules* **2012**, *45*, 7740–7748.

(34) Hehn, M.; Maiko, K.; Pasch, H.; Hiller, W. *Macromolecules* **2013**, *46*, 7678–7686.

(35) Hiller, W.; Sinha, P.; Hehn, M.; Pasch, H. *Prog. Polym. Sci.* **2014**, *39*, 979–1016.

(36) Hiller, W.; Hehn, M.; Hofe, T.; Oleschko, K. *Anal. Chem.* **2010**, *82*, 8244–8250.

(37) Assumption, H.; Vermeulen, J.; Jarrett, W. L.; Mathias, L. J.; van Reenen, A. *Polymer* **2006**, *47*, 67–74.

(38) Seger, M. R.; Maciel, G. E. *Anal. Chem.* **2004**, *76*, 5734–5747.

(39) Luruli, N.; Heinz, L. C.; Grumel, V.; Brüll, R.; Pasch, H.; Raubenheimer, H. G. *Polymer* **2006**, *47*, 56–66.

(40) Su, Z.; Zhao, Y.; Xu, Y.; Zhang, X.; Zhu, S.; Wang, D.; Han, C. C.; Xu, D. *Polymer* **2004**, *45*, 3577–3581.

(41) Galland, G. B.; de Souza, R. F.; Mauler, R. S.; Nunes, F. F. *Macromolecules* **1999**, *32*, 1620–1625.

(42) Watson, E. S.; O'Neill, M. J.; Justin, J.; Brenner, N. *Anal. Chem.* **1964**, *36*, 1233–1238.

(43) O'neill, M. *Anal. Chem.* **1964**, *36*, 1238–1245.

(44) Schick, C. *Anal. Bioanal. Chem.* **2009**, *395*, 1589.

(45) Vanden Poel, G.; Mathot, V. B. F. *Thermochim. Acta* **2007**, *461*, 107–121.

(46) Cheruthazhekatt, S.; Pijpers, T. F. J.; Harding, G. W.; Mathot, V. B. F.; Pasch, H. *Macromolecules* **2012**, *45*, 5866–5880.

(47) Cheruthazhekatt, S.; Pijpers, T. F. J.; Harding, G. W.; Mathot, V. B. F.; Pasch, H. *Macromolecules* **2012**, *45*, 2025–2034.

(48) Cheruthazhekatt, S.; Pijpers, T. F. J.; Mathot, V. B. F.; Pasch, H. *Anal. Bioanal.Chem.* **2013**, *405*, 8995–9007.

(49) Cheruthazhekatt, S.; Pijpers, T. F. J.; Mathot, V. B. F.; Pasch, H. *Macromol. Symp.* **2013**, *330*, 22–29.

(50) Krumme, A.; Basiura, M.; Pijpers, T.; Vanden Poel, G.; Heinz, L. C.; Bruell, R.; BF Mathot, V. *Mater. Sci.* **2011**, *17*, 260–265.

(51) Liu, T.; Harrison, I. *Thermochim. Acta.* **1994**, *233*, 167–171.

(52) Shanks, R.; Amarasinghe, G. *J. Therm. Anal. Calorim.* **2000**, *59*, 471-482.

(53) Starck, P. *Polym. Int.* **1996**, *40*, 111–122.

(54) Gabriel, C.; Lilge, D. *Polymer* **2001**, *42*, 297–303.

(55) Razavi-Nouri, M. *Polym. Test.* **2006**, *25*, 1052–1058.

(56) Treviño-Quintanilla, C. D.; Krishnamoorti, R.; Bonilla-Ríos, J. *J. Polym. Sci. Polym. Phys.* **2016**, *54*, 2425–2431.

(57) Treviño-Quintanilla, C. D.; Krishnamoorti, R.; Bonilla-Ríos, J. *J. Polym. Sci. Polym. Phys.* **2017**, *55*, 1822–1827.

(58) Monrabal, B. *J. Appl. Polym. Sci.* **1994**, *52*, 491–499.

(59) Anantawaraskul, S.; Soares, J. B. P.; Wood-Adams, P. M. *J. Polym. Sci., Part B: Polym. Phys.* **2003**, *41*, 1762–1778.

(60) Pasch, H.; Malik, M. I. *Advanced separation techniques for polyolefins*; Springer: Switzerland, **2014**.

(61) Brüll, R.; Grumel, V.; Pasch, H.; Raubenheimer, H. G.; Sanderson, R.; Wahner, U. M. In *Macromol. Symp.*; Wiley Online Library, **2002**, pp 81–92.

(62) Pasch, H.; Brüll, R.; Wahner, U.; Monrabal, B. *Macromol. Mater. Eng.* **2000**, *279*, 46–51.

(63) Kissin, Y. V.; Fruitwala, H. A. *J. Appl. Polym. Sci.* **2007**, *106*, 3872–3883.

(64) Cheruthazhekatt, S.; Mayo, N.; Monrabal, B.; Pasch, H. *Macromol. Chem. Phys.* **2013**, *214*, 2165–2171.

(65) Anantawaraskul, S.; Soares, J. B.; Wood-Adams, P. M.; Monrabal, B. *Polymer* **2003**, *44*, 2393–2401.

(66) Pasch, H.; Malik, M. I. *Advanced separation techniques for polyolefins*; Springer, **2014**.

(67) Dawkins, J.; Maddock, J. *Eur. Polym. J.* **1971**, *7*, 1537–1548.

(68) Kostanski, L. K.; Keller, D. M.; Hamielec, A. E. *J. Biochem. Biophys.* **2004**, *58*, 159–186.

(69) Beer, F.; Capaccio, G.; Rose, L. *J. Appl. Polym. Sci.* **2001**, *80*, 2815-2822.

(70) DesLauriers, P. J.; Rohlfing, D. C.; Hsieh, E. T. *Polymer* **2002**, *43*, 159–170.

(71) Podzimek, S. In *Light Scattering, Size Exclusion Chromatography and Asymmetric Flow Field Flow Fractionation: Powerful Tools for the Characterization of Polymers, Proteins and Nanoparticles*; John Wiley & Sons: New Jersey, **2011**, pp 99–206.

(72) Wyatt, P. J. *Instrum Sci. Technol.* **1997**, *25*, 1–18.

(73) Wyatt, P. J. *Anal. Chim. Acta* **1993**, *272*, 1–40.

(74) Jackson, C.; Chen, Y. J.; Mays, J. W. *J. Appl. Polym. Sci.* **1996**, *61*, 865–874.

(75) Gaborieau, M.; Gilbert, R. G.; Gray-Weale, A.; Hernandez, J. M.; Castignolles, P. *Macromol. Theory. Simul.* **2007**, *16*, 13-28.

(76) Luruli, N. *New synthetic and characterization strategies for polyolefins*. PhD dissertation, Stellenbosch University: South Africa, **2007**.

(77) Wang, W. J.; Kolodka, E.; Zhu, S.; Hamielec, A. E.; Kostanski, L. K. *Macromol. Chem. Phys.* **1999**, *200*, 2146–2151.

(78) Pasch, H. In *Macromol. Symp.,* ***2002***; 178, 25-38.

(79) Knox, J. H.; Kaur, B.; Millward, G. R. *J. Chromatogr. A* **1986**, *352*, 3–25.

(80) Ndiripo, A. *High temperature multidimensional chromatography of complex and functionalized polyolefins* PhD dissertation, Stellenbosch University: South Africa, **2018**.

(81) Ndiripo, A.; Albrecht, A.; Pasch, H. *RSC Advances* **2020**, *10*, 17942-17950.

(82) Macko, T.; Pasch, H.; Denayer, J. F. *J. Chromatogr. A* **2003**, *1002*, 55–62.

(83) Macko, T.; Pasch, H.; Denayer, J. F. *J. Sep. Sci.* **2005**, *28*, 59–64.

(84) Macko, T.; Brüll, R.; Zhu, Y.; Wang, Y. *J. Sep. Sci.* **2010**, *33*, 3446–3454.

(85) Macko, T.; Pasch, H.; Brüll, R. *J. Chromatogr. A* **2006**, *1115*, 81–87.

(86) Heinz, L.-C.; Pasch, H. *Polymer* **2005**, *46*, 12040–12045.

(87) Macko, T.; Brüll, R.; Alamo, R. G.; Stadler, F. J.; Losio, S. *Anal. Bioanal.Chem.* **2011**, *399*, 1547–1556.

(88) Chitta, R.; Macko, T.; Brüll, R.; Boisson, C.; Cossoul, E.; Boyron, O. *Macromol. Chem. Phys.* **2015**, *216*, 721–732.

(89) Glöckner, G. In *Gradient HPLC of Copolymers and Chromatographic Cross-Fractionation*; Springer, **1991**, pp 148–174.

(90) Gerber, J.; Radke, W. *Polymer* **2005**, *46*, 9224–9229.

(91) Ginzburg, A.; Macko, T.; Malz, F.; Schroers, M.; Troetsch-Schaller, I.; Strittmatter, J.; Brull, R. *J. Chromatogr. A* **2013**, *1285*, 40–47.

(92) Ginzburg, A.; Macko, T.; Dolle, V.; Brüll, R. *Eur. Polym. J.* **2011**, *47*, 319–329.

(93) Cheruthazhekatt, S.; Harding, G. W.; Pasch, H. *J. Chromatogr. A* **2013**, *1286*, 69–82.

(94) Cheruthazhekatt, S.; Pasch, H. *Macromol. Symp.* **2014**, *337*, 51–57.

(95) Ginzburg, A.; Macko, T.; Dolle, V.; Brüll, R. *J. Chromatogr. A* **2010**, *1217*, 6867–6874.

(96) Jørgensen, J. K.; Larsen, A.; Helland, I. *e-Polymers* **2010**, *10*, 1596–1612.

(97) Kaminsky, W. *Macromol. Chem. Phys.* **2008**, *209*, 459–466.

(98) Shirayama, K.; Okada, T.; Kita, S. I. *J. Polym. Sci., Part A: Polym. Chem.* **1965**, *3*, 907–916.

(99) Desreux, V.; Spiegels, M. *Bull. Soc. Chim. Belg* **1950**, *59*, 476.

(100) Suriya, K.; Anantawaraskul, S.; Soares, J. B. P. *J. Polym. Sci. Polym. Phys.* **2011**, *49*, 678–684.

(101) Anantawaraskul, S.; Soares, J. B.; Wood-Adams, P. M. *Macromol. Chem. Phys.* **2004**, *205*, 771–777.

(102) Knooren, J., *Recent developments in polyolefin fractionations, MSc thesis, Universiteit van Amsterdam: Amsterdam, **2013.*** .

(103) Eselem Bungu, P.; Pasch, H. *Polym. Chem.* **2017**, *31*, 4565–4575.

(104) Ndiripo, A.; Eselem Bungu, P. S.; Pasch, H. *Polym. Int.* **2019**, *68*, 206–217.

(105) Ndiripo, A. *Comparative study on the molecular structure of ethylene/1-octene, ethylene/1-heptene and ethylene/1-pentene copolymers using advanced analytical methods*. MSc thesis, Stellenbosch University: South Africa, **2015**.

(106) Keulder, L. *The effect of molecular composition on the properties of linear low density polyethylene*. MSc thesis, University of Stellenbosch: South Africa,**2008**.

(107) Mncwabe, S.; Luruli, N.; Marantos, E.; Nhlapo, P.; Botha, L. *Macromol. Symp.* **2012**, *313-314*, 33–42.

(108) Wild, L.; Glöckner, G. In *Separation Techniques Thermodynamics Liquid Crystal Polymers*; Springer, **1991**, pp 1–47.

(109) Soares, J. B. P.; Hamielec, A. E. *Polymer* **1995**, *36*, 1639–1654.

(110) Monrabal, B. *Encyclopedia of Analytical Chemistry: Applications, Theory and Instrumentation.* **2006**.

(111) Magagula, S. I.; Ndiripo, A.; van Reenen, A. J. *Polym. Degrad. Stab.* **2020**, *171*, 109022.

(112) Sigwinta, M.; Ndiripo, A.; Wewers, F.; Pasch, H. *Polym. Int.* **2020**, *69*, 291–300.

(113) Bungu, P. S. E.; Pflug, K.; Pasch, H. *Polym. Chem.* **2018**, *9*, 3142–3157.

(114) Eselem Bungu, P. S. *Development of a multiple fractionation protocol for the comprehensive analysis of low density polyethylene*. PhD dissertation, Stellenbosch University: South Africa,**2018**.

(115) Menard, K. *Dynamic mechanical analysis: a practical introduction* **1999**, *2*, p 3–10.

(116) Starck, P. *Eur. Polym. J.* **1997**, *33*, 339–348.

(117) Stuart, B. H. *Polymer analysis*; John Wiley & Sons, **2008**; Vol. 30, p 209–235.

(118) Swallowe, G. M. *Mechanical Properties and Testing of Polymers: an A–Z reference*; Springer Science & Business Media, **1999**; Vol. 3, p 242–247.

(119) Mark, J. E. *Physical properties of polymers handbook*; Springer, **2007**; Vol. 1076, p 430–411.

(120) Gupta, P.; Wilkes, G. L.; Sukhadia, A. M.; Krishnaswamy, R. K.; Lamborn, M. J.; Wharry, S. M.; Tso, C. C.; DesLauriers, P. J.; Mansfield, T.; Beyer, F. L. *Polymer* **2005**, *46*, 8819–8837.

(121) Adisson, E.; Ribeiro, M.; Deffieux, A.; Fontanille, M. *Polymer* **1992**, *33*, 4337–4342.

(122) Shahid, S.; Gukhool, W.; *Experimental testing and material modeling of anisotropy in injection moulded polymer materials*, MSc thesis, Blekinge Institute of technology: Sweden, **2020**.

Chapter 3

Experimental design

This chapter describes the materials and experimental methods used in characterizing three bimodal high density polyethylene samples (bHDPEs). All resins were polymerised in a slurry phase using dual reactors in series to create resins with a broad molar mass distribution. Characterization was carried out on bulk resins and on fractions obtained from pTREF and pMMF to gain complete understanding of the complex microstructure of the bHDPE resins.[1-4]

3.1 Material and reagents

Three Ziegler-Natta polymerised bimodal high-density polyethylene (bHDPE) resins were sampled in the present work. Resin 1 and Resin 2 were obtained from one manufacturer, Ineos[5] however, they are from different batches. Both samples contained 1-butene as comonomer. The Reference was produced by Lyondelbasell[6] and contained 1-butene as comonomer.

High purity (≥99 %) 1,2,4-trichlorobenzene (TCB), 1-decanol (≥99 %), 1,2-dichlorobenzene (ODCB) (>99 %), xylene (>99 %) and sea sand were obtained from Sigma-Aldrich South Africa. 1,1,2,2-tetrachloroethane (>99.5 %)) was obtained from Merck® South Africa. All reagents were used as received.

3.2 Chromatographic techniques

3.2.1 High-temperature size exclusion chromatography (HT-SEC)

Molar mass and molar mass distribution of the bHDPE samples were measured using a PL220 high temperature chromatograph (Church Stretton, UK). The instrument is equipped with an infrared (IR) detector. Tests were carried out at 150 ºC and flow rate of 1 mL min^{-1} using three PLgel Olexis columns with internal diameter 300 mm × 7.5 mm and a PLgel Olexis guard column with internal diameter 50 mm x 7.5 mm (Agilent Technologies, UK). Approximately 4 mg of polymer were dissolved in 2 mL of 1,2,4-trichlorobenzene (TCB) with 0.025 % BHT as stabiliser for 1-2 hrs prior to 0.2 mL being injected. 2,6-d-tert-butyl-4-methylphenol (BHT, 0,0125 %) with TCB was used as the mobile phase. Instrument calibration was performed using linear polystyrene (PS) standards of narrow molar mass distribution (MMD). All reported molar mass values are PS equivalents.

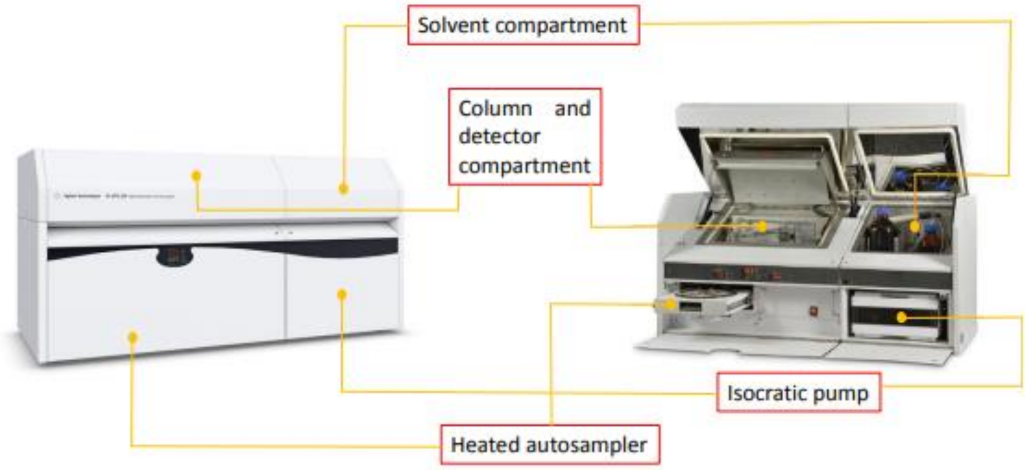

Figure 3.1 Diagram of the HT-SEC/GPC instrument used in determining molar masses.[4]

3.2.2 High-temperature solvent gradient interaction chromatography (HT-SGIC)

Separations of polymer chains according to ethylene sequence length were achieved using a high-pressure binary gradient pump (Agilent, Waldbronn, Germany). A schematic of the gradient profile is shown in Figure 3.2. A porous graphitic carbon column (Hypercarb®, Thermo Scientific, Dreieich, Germany) with an internal diameter of 100 mm x 4.6 mm was used. The column was packed with porous graphite particles of diameter 5 µm and pore size of 250 Å. The gradient time from 1-decanol to TCB was 30min. The concentration of each sample was 1 mg mL-1 and the injection volume 50 µL. The evaporative light scattering detector was used at an evaporative temperature of 270 °C, gas flow rate of 1.5 SLM and a nebulizer temperature of 160 °C.

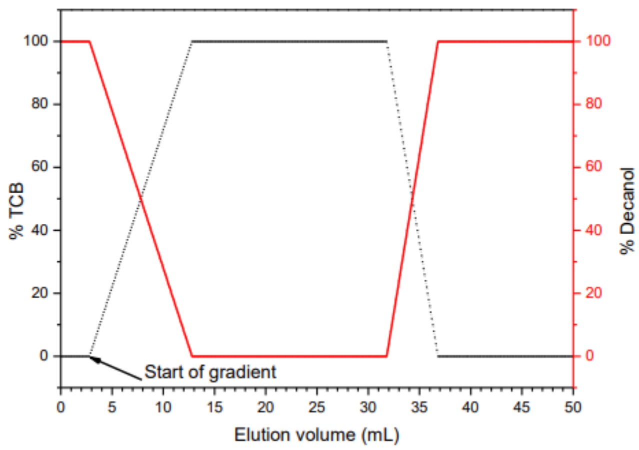

Figure 3.2 HT-SGIC solvent gradient profile.

3.2.3 High-temperature two- dimensional liquid chromatography (HT-2D-LC)

HT-SGIC and HT-SEC were coupled using an electronically controlled eight-port valve system (VICI Valco instruments, Houston, Texas) having two 100 μL sample loops. In the first dimension (HT-SGIC), a 200 μL sample loop with flow rate was 0.05 mL min^{-1} was used to inject each sample with the same gradient as explained in Section 3.2.2. In the second dimension (HT-SEC), A PL Rapide H (Polymer Laboratories, Church Stretton, UK.) 100mm × 10 mm internal diameter column with a 10 μm particle diameter was used at 140 °C. ODCB as the mobile phase was used at a flow rate of 3.25 mL min^{-1}. The following parameters were used for the evaporative light scattering detector: gas flow rate of 1.5 SLM, 140 °C nebulizer temperature, and an evaporative temperature of 230 °C.

3.2.4 High-temperature thermal gradient interaction chromatography (HT-TGIC)

Chains were separated on a 100 × 4.6 mm Hypercarb® column as stationary phase and ODCB (1,2-dichlorobenzene) as the mobile phase. Flow rates of 0.02 mL/min and 0.5 mL/min were used during the cooling and elution stages respectively. Elution volumes were corrected to start at 0 mL, excluding the cooling stage volume. Linear temperature gradients of 10 ºC and 4 ºC for cooling and heating respectively were applied. An infrared detector was used for detection.

3.3 Crystallisation based techniques

3.3.1 Differential scanning calorimetry (DSC)

The melting and crystallization properties of the bimodal HDPE resins were determined using a DSC TA Q20 instrument. A nitrogen atmosphere was maintained at a purge gas flow rate of 50 mL min^{-1} throughout the measurement. Three cycles were performed with the first (first heating) used to erase the samples thermal histories. Quantitative and qualitative results were obtained from the second and third cycles (first cooling and second heating respectively). Temperature was kept constant for 2 min at the end of each cycle. Approximately 4 mg of each sample was used with heating and cooling rates of 10 °C min^{-1}. The applied analysis temperature range was 10 to 200 °C for all samples. Instrument calibration with an indium metal standard was performed according to standard procedures. The samples were contained in aluminium pans with flat lids. An empty aluminium pan and lid were used as reference.

3.3.2 Crystallisation analysis fractionation (CRYSTAF)

A CRYSTAF instrument 200 Polymer Char S.A (Valentia, Spain) was used to analyse the crystallisation from solution of the bHDPE samples. Each sample of approximately 20 mg was dissolved at 160 °C using 35 mL of TCB in five stainless steel reactors simultaneously. Complete dissolution in approximately 150 min was achieved under continuous stirring. The reactor temperature was then reduced to 100 °C and held constant for 60 min. Thereafter, the temperature was reduced slowly at a rate of 0.1 °C min^{-1} to allow for crystallisation with minimum co-crystallisation effects.[8] During the crystallisation stage, solution concentration was measured as a function of temperature and the results were recorded using an infrared detector.

3.4 Spectroscopic techniques

3.4.1 Solution carbon-thirteen nuclear magnetic resonance (^{13}C NMR)

Solution ^{13}C NMR analysis of the bulk bHDPE resins and its fractions was conducted using a 600 MHz Varian Unity Inova NMR spectrometer at a 150 MHz resonance frequency. 1.5 mL of deuterated 1,1,2,2-tetrachloroethane (TCE-d2) was used to completely dissolve approximately 60 mg of each sample. The TCE-d2 was also used as an internal reference (74.3 ppm) and analysis was performed at 120 °C.

Comonomer content in mol % was determined by integrating the area under the peaks associated with branching and backbone carbons as per equation 3.1 below.

$$Comonomer\ content\ (Mol\%) = \frac{2\int Branched\ Carbons}{\Sigma\int Backbone\ Carbons} X\ 100$$

Equation 3.1 Comonomer content

3.5 Preparative fractionation techniques

3.5.1 Preparative temperature rising elution fractionation (pTREF)

An in-house built instrument was used for the preparative TREF experiment. For the first (crystallisation) step, approximately 3 g of polymer was dissolved in 300 mL of xylene. Dissolution was carried out at 130 ºC and stabilized with 2wt % of Irganox 1010 (Ciba Specialty Chemicals, Switzerland). Once the samples were completely dissolved, the reactor was quickly placed in a preheated (130 ºC) oil bath. Preheated sea sand used as crystallisation support was then added to the reactor. The oil bath with a reactor and sea sand were cooled down slowly at a rate of 1 ºC/hr to allow for controlled crystallisation of the polymer from solution.

In the second (elution) step, polymer coated sea sand was transferred into a stainless-steel column. The column was placed into a modified gas chromatography oven as shown in Figure 3.5. Column temperature was gradually increased, and xylene was used as an eluent to elute different fractions out of the column. The fractions were collected sequentially at temperatures of 25, 40, 60, 80, 90, 100, 110 and 120 ºC. Collected fractions were each dried in a rotary evaporator and then precipitated in 200 mL acetone. The precipitate was dried under vacuum at 55 ºC, and collected fractions were weighed.

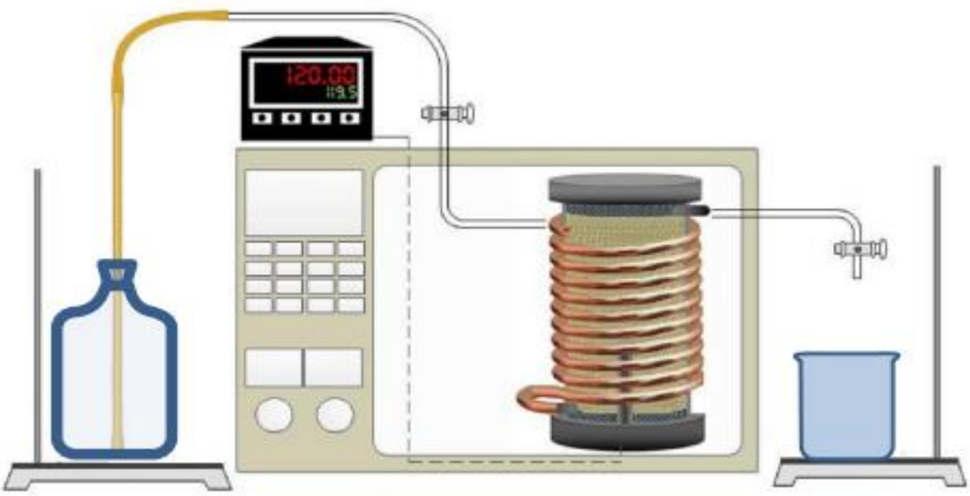

Figure 3.3 Elution step during the pTREF experiment.[9]

3.5.2 Preparative molar mass fractionation (pMMF)

Molar mass fractions were obtained by dissolving approximately 3 g of bHDPE in 500 mL ODCB (solvent) for 2 hrs at 140 °C. A 2.0 wt. % Irganox 1010 (Ciba Specialty Chemicals, Switzerland) was added as stabilizer. Dissolution was carried out in a glass column with an oil inlet and outlet connecting the column to an external oil circulator as shown in Figure 3.6. The solution temperature was reduced and maintained at 120 ºC and then left to settle for 6 hrs.

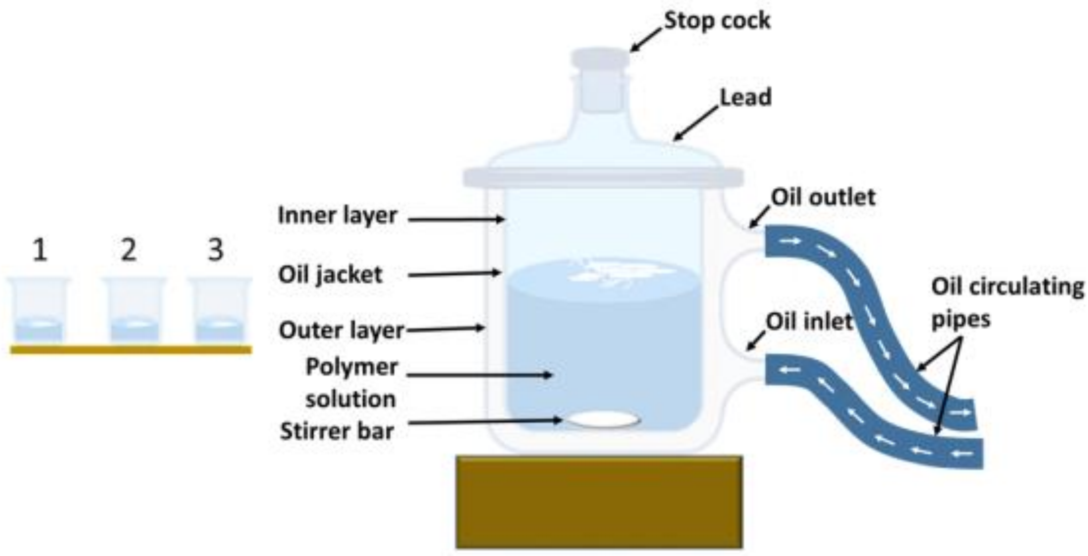

Figure 3.4 Diagram showing the setup of a pMMF experiment.[10]

Thereafter, 290 mL 2-ethoxy ethanol (non-solvent) was slowly added to the polymer solution under continuous stirring until the appearance of a first stable cloud (first fraction). The following fractions were collected by sequentially adding non-solvent in volumes of 20, 40, 60 mL to obtain fractions 2, 3 and 4 respectively. The last, soluble fraction 5 was obtained by washing the remaining solution with acetone. The collected precipitates (fractions) were collected using a suction device, washed in acetone, filtered and dried to a constant weight under vacuum.

3.6 Mechanical analysis techniques

3.6.1 Dynamic mechanical analysis (DMA)

The dynamic mechanical measurements were performed on 3 mm thick compression moulded rectangular specimens. Experimental conditions on the DMA instrument were set to a constant frequency of 10 Hz, amplitude of 20 µm, data sampling interval of 2 s/pt and a temperature range between -145 and 100 ºC at a heating rate of 3 ºC/minute. A single cantilever clamp with a clamping force of 5 N was used. The test was conducted under cryogenic conditions.

3.6.2 Tensile strength and Young's modulus

Test specimens were injection moulded on a Thermo Scientific Haake machine. The melt was maintained between 200 °C and 250 °C while the mould was kept at 60 °C for all samples.

The injection force was set according to the samples melt flow index. Samples were rapidly cooled immediately after completion of the injection cycle. Test specimens of 5.2 mm thickness, 1.6 mm width and 42 mm gauge length were tested in accordance with ASTM D 638 M.

Tensile properties of the injection-moulded test specimens were determined according to ASTM D 638 M on a Lloyd Instruments LRX tensile tester. All samples were 5.2 mm thick, 1.6 mm wide and had a 42 mm gauge length. Testing was conducted under a cross head speed of 50 mm/min.

3.6 References

(1) Bungu, E. *Development of a multiple fractionation protocol for the comprehensive analysis of low density polyethylene*. PhD dissertation, Stellenbosch University: South Africa,**2018**.

(2) Ndiripo, A.; Eselem Bungu, P. S.; Pasch, H. *Polym. Int.* **2019**, *68*, 206–217.

(3) Magagula, S. I.; Ndiripo, A.; van Reenen, A. J. *Polym. Degrad. Stab.* **2020**, *171*, 109022.

(4) Ndiripo, A. *High temperature multidimensional chromatography of complex and functionalized polyolefins*. PhD dissertation, Stellenbosch University: South Africa,**2018**.

(5) Amos, J.; Chai, C. K.; Dheur, L. M. G.; *Bimodal polyethylene film*, **2011**, United States Patents, US7897710B2.

(6) Mack, M. P.; Meas Jr, J. H.; Nygard, P. L.; Wallace, L. R.; Garrison, P. J.; *Process for producing polyethylene film composition having broad molecular weight distribution and improved bubble stability*, **2000,** United States Patents, Houston, Tex, US 6,147,167.

(7) Pasch, H.; Trathnigg, B. *Multidimensional HPLC of Polymers*; Springer: Berlin, **2013**.

(8) Pasch, H.; Brüll, R.; Wahner, U.; Monrabal, B. *Macromol. Mater. Eng.* **2000**, *279*, 46–51.

(9) Spalding, M. A.; Chatterjee, A. *Handbook of industrial polyethylene and technology: Definitive guide to manufacturing, properties, processing, applications and markets set*; John Wiley & Sons, **2017**.

(10) Sigwinta, M. *Ethylene-1-octene elastomers: Molecular structure characterization by advanced analytical methods*. MSc thesis, Cape Peninsula University of Technology: South Africa,**2019**.

Chapter 4

Bimodal high-density polyethylene (bHDPE) bulk sample analyses

This chapter focuses on employing various techniques to analyse the three bulk bHDPE resins. An industrial benchmarking grade referred to as Reference and two molecularly similar but rheologically different developmental resins Resin 1 (good) and Resin 2 (bad). The aim is to identify any differences in the microstructure that could be causing the observed differences in rheological properties during the extrusion film blowing process. Investigated bulk properties include firstly the qualification and quantification of comonomer using ^{13}C NMR. Secondly, molar mass distribution and chemical composition in melt and in solution using DSC and CRYSTAF respectively. Additionally, complementary liquid chromatographic techniques are applied to determine chemical composition without the challenges of co-crystallisation and co-elution. Lastly, mechanical properties are investigated.

4.1 Introduction

The bimodal HDPE resins are produced in a slurry loop dual reactor system wherein one reactor produces a linear, low molar mass polyethylene. To the second reactor, comonomer is introduced to create a short chain branched, high molar mass copolymer using in this case, heterogeneous Ziegler-Natta type catalysts.[1-3] Molar mass distribution (MMD) and chemical composition distribution (CCD) play a vital role in the determination of final PE resin behaviour in the molten state including processability and melt strength. This necessitates thorough analyses of all three samples by various techniques.

4.2 Bulk bHDPE analysis

Molar mass distribution (MMD) as a result of comonomer was established using HT-SEC. Profiles given in Figure.4.1 show the bimodal nature of the MMD for all samples. The Reference sample appears to have a more pronounced peak in the lower molar mass region (from the reactor fed with hydrogen) than Resin 1 and Resin 2. This could be indicative of much lower molar masses of very narrow distribution. Preparative fractionation could be useful in studying the different segments of the polyolefin chain. A summary of the molecular properties is found in Table 4.1. Overall results obtained for the bulk samples however do not show significant differences in the amount and distribution of comonomer. A more sensitive technique to chemical composition is Carbon-thirteen NMR.

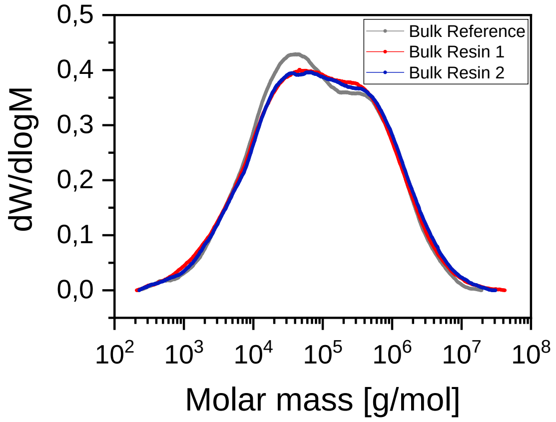

Figure 4.1 Molar mass distribution curves of the bulk samples obtained from HT-SEC using an RI. detector.

Table 4.1 A summary of the molar mass properties, comonomer content, melt flow index, melting and crystallization temperatures as well as calculated crystallinity for the bHDPE bulk samples.

Sample	M_w [a] (kg/mol.)	Đ [a]	[C] [b] mol.%	MFI (g/10min)
Reference	974.0	44.9	0.55	0.285
Resin 1	735.0	41.9	0.68	0.326
Resin 2	1017.0	54.9	0.77	0.319

[a] Determined by HT-SEC, [b] Determined by Solution ^{13}C NMR spectra.

Solution ^{13}C NMR was used to determine the type and average comonomer content as described in Section 3.3.1 of Chapter 3. The peaks in Figure 4.2 were assigned according to Randall[4] and indicate that the Reference sample has 1-butene as the comonomer. The branching and methyl peaks are at 39.7 ppm and 11.1 ppm respectively. The same peak assignment method alludes to Resin 1 and Resin 2 having 1-hexene as the comonomer. The branching and methyl peaks of both Resin 1 and Resin 2 are at 38.1 ppm and 14.1 ppm respectively. This difference in comonomer is expected to yield differences in processability.

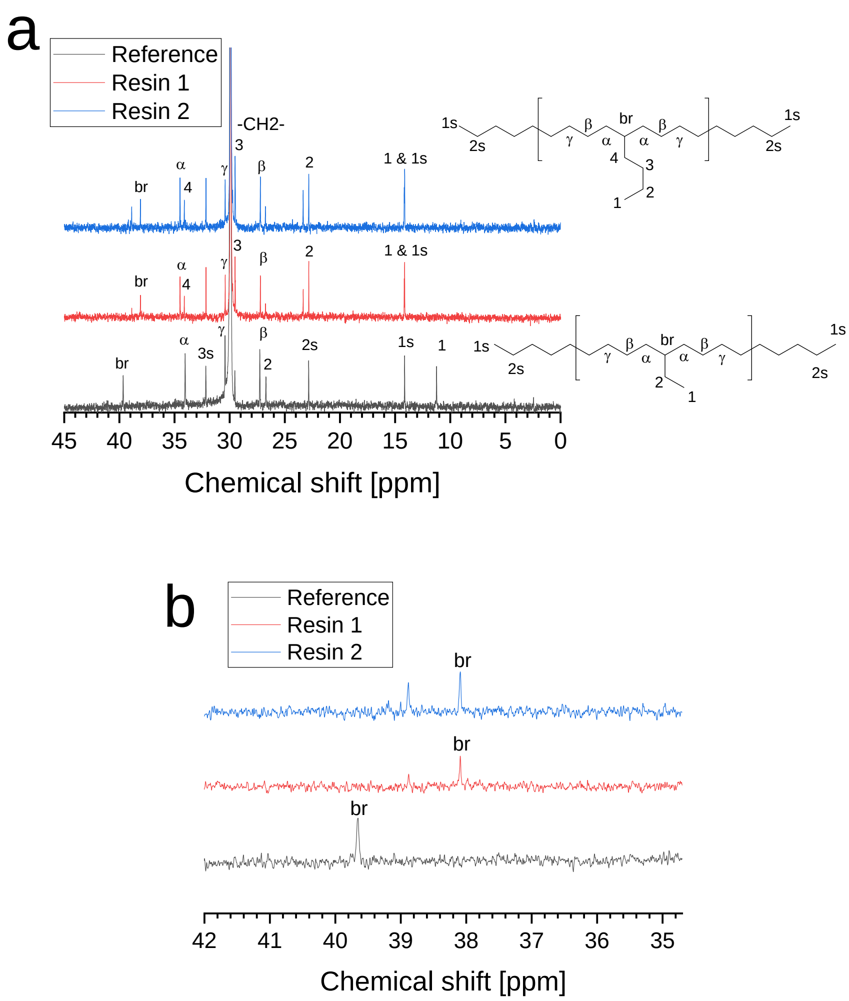

Figure 4.2 Solution Carbon-thirteen NMR spectrum of the bHDPE resins showing (a) Reference with comonomer 1-butene, Resin 1 and Resin 2 with comonomer 1-hexene and (b) zoomed in branching peak region of all resins.

Comonomer content values listed in Table 4.1 were obtained by integration of the branch and backbone peaks and inserting the peak area values into Equation 3.1. (Chapter 3). These show that Resin 1 and Resin 2 are of the same comonomer type, although Resin 2 has a slightly higher percentage of comonomer at 0.77 mol.%. This is higher than Resin 1 at 0.68 mol. % and the Reference at 0.55 mol. %.

It is interesting to note that for Resin 1 and Resin 2, there is a peak appearing at 38.9 ppm just after the branching peak at 38.1 ppm. The peak height is more pronounced for Resin 2 than it is for Resin 1 and though speculative, it paves a way for further investigation. It is further speculated that the origin of these peaks in the electron deficient range on NMR could be due to high concentration of poorly dispersed comonomer resulting in branches that are next to one another. Comonomer should ideally be evenly distributed along the polymer chain to avoid phase separation of the two very different chains in the molten state.

Observed differences in comonomer content across the molar mass distribution are confirmed with the use of an IR detector in HT-SEC as shown in Figure 4.3. Results express the amount of comonomer as CH_3/CH_2 and agree with the calculated CC from ^{13}C NMR that shows the lowest CC for the Reference and highest for Resin 2. It is also worth noting that the Reference and Resin 1 show a decrease in CC in the highest molar mass region while resin 2 shows an increase.

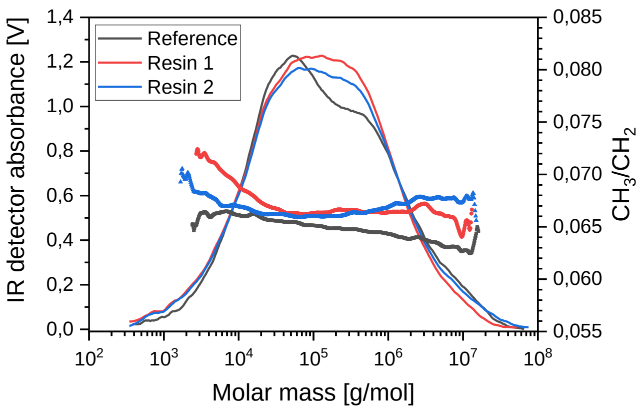

Figure 4.3 Molar mass distribution curves of the bulk bHDPE samples showing comonomer content per ethylene backbone expressed as CH_3/CH_2.

Further attempts to identify any microstructural differences between the three samples are made regarding the melting and crystallization behaviour. The effects of branching and/or comonomer distribution are studied first by DSC, and then by CRYSTAF. The two techniques are closely related although, DSC measures chain crystallisation in melt while CRYSTAF measures it in solution.

DSC procedure described (Section 3.3.1) is used to compare the melting and crystallisation behaviour of the three samples. The second melting and first crystallisation behaviour of a polymer have a direct impact on the way in which the polymer behaves during processing i.e. during extrusion and thereafter during the cooling stage.

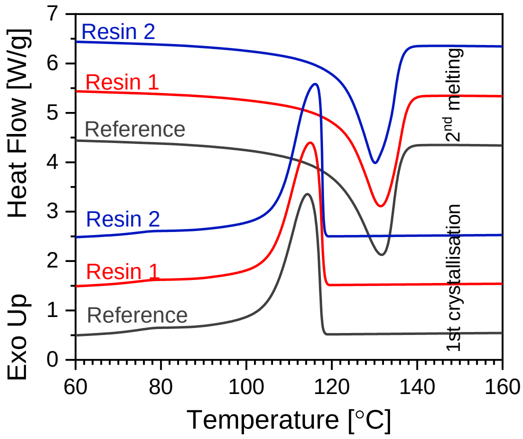

Figure 4.4 DSC thermograms of the second melting endotherms and first crystallisation exotherms of the three bHDPE samples.

Melting endotherms presented in Figure 4.4 show no significant differences in peak temperatures between the three samples but, a slightly broader peak for the Reference sample. Interestingly though, the crystallisation endotherms show secondary peaks that appear at approximately 80 ºC. These indicate a secondary component with chains of lower crystallinity in all samples which could be attributed to the short chain branched copolymer.

Table 4.2 A summary of the melting and crystallisation properties of the bHDPE samples.

Sample identification	[C][a] mol.%	T_m(ºC)[b]	T_c(ºC)[b]	X_c(%)[b, c]
Reference	0.55	131.8	114.3	64.2
Resin 1	0.68	131.5	115.0	59.5
Resin 2	0.77	130.2	116.1	58.2

[a] Determined by Solution Carbon-thirteen NMR spectra, [b] Determined by DSC

[c] $X_c = (\Delta H_m / \Delta H_m^{\circ} \times 100\ \%)$, $\Delta H_m^{\circ} = 293$ J/g[5]

Peak crystallisation temperatures in Table 4.2 and Figure 4.5(b) show a higher T_c for Resin 2 than expected for a sample with lower T_m. It is speculated that Resin 2 could possibly contain chains of high crystallinity. Isolating certain regions through the preparative temperature rising elution fractionation technique could better serve to pre concentrate the different chains and individually assess their effect. Overall, the three samples appear to be similar in the molten state with no major differences detected. This is expected when analysing bulk samples, moreover, those with very low comonomer contents. Peak crystallisation behaviour of the PE chains can, however, also be analysed in a solution of dilute TCB using CRYSTAF where differences are expected to be more visible than in DSC.

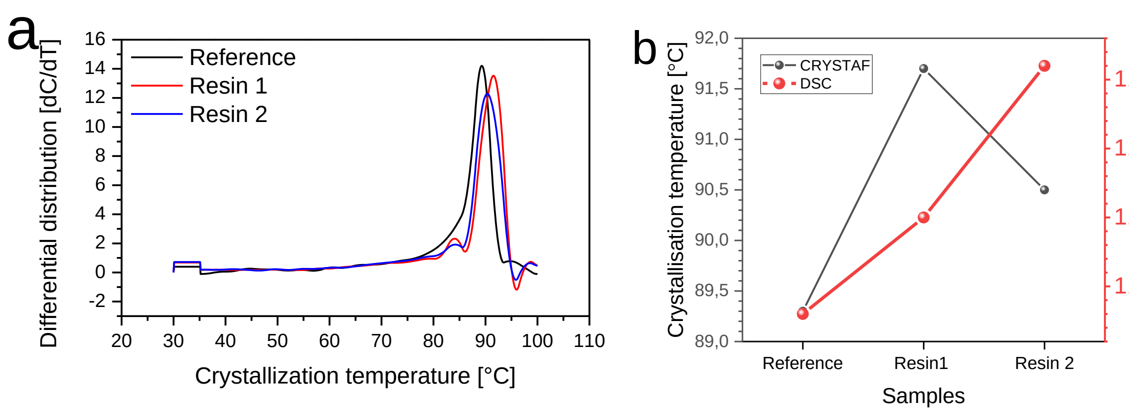

Figure 4.5 (a) Differential CRYSTAF curves of the three bulk bHDPE samples and (b) a comparison of peak crystallisation temperatures obtained from DSC and CRYSTAF.

CRYSTAF curves shown in Figure 4.5 (a) show three fractions for the Resin 1 and Resin 2. The first, non-crystallisable fraction around 30 ºC is assigned to soluble material of either high comonomer content and/or very low MM species. The second is a much smaller fraction just before the main peak at a crystallisation temperature of approximately 84 ºC that can be assigned to semi-crystalline material. Lastly, the third is the main crystallisation peak around 90 °C. The high crystallisation temperatures between 80 and 90 ºC confirm highly linear polyethylene chains.[6-9] Furthermore, there is an agreement between DSC and CRYSTAF results on the presence of a smaller component of lower crystallisation temperature that the main component in all samples. These crystallisation-based techniques are however, not as sensitive as interaction chromatographic techniques.

Interaction chromatography uses different modes of separation to crystallisation-based techniques as explained in Section 3.2. Results show that samples are indeed quite similar regarding close proximity of comonomer.HT-SGIC chromatograms in Figure 4.6 show that for each bHDPE sample, there are three distinct peaks consisting of one main component and two others that are not very well resolved. Peak 1, Peak 2 and Peak 3 represent low MM PE, high MM copolymer and high MM PE chains respectively.

The lower elution volume (V_e) peaks indicate chains of lower crystallinity and higher comonomer content. Conversely, the later eluting peaks at higher V_e indicate linear and less comonomer chains thus, higher crystallinity.[11-13] Linear PE 73K standard elutes with a narrow peak at the highest V_e as is expected. This elution volume corresponds to Peak 3 of the bHDPE samples. However, an overlap of the PE 73K with Peak 2 of the bHDPE samples is observed. This indicates that there are some chains of high crystallinity in the component represented by Peak 2. Figure 4.6 (b) shows differences in each of the three peaks.

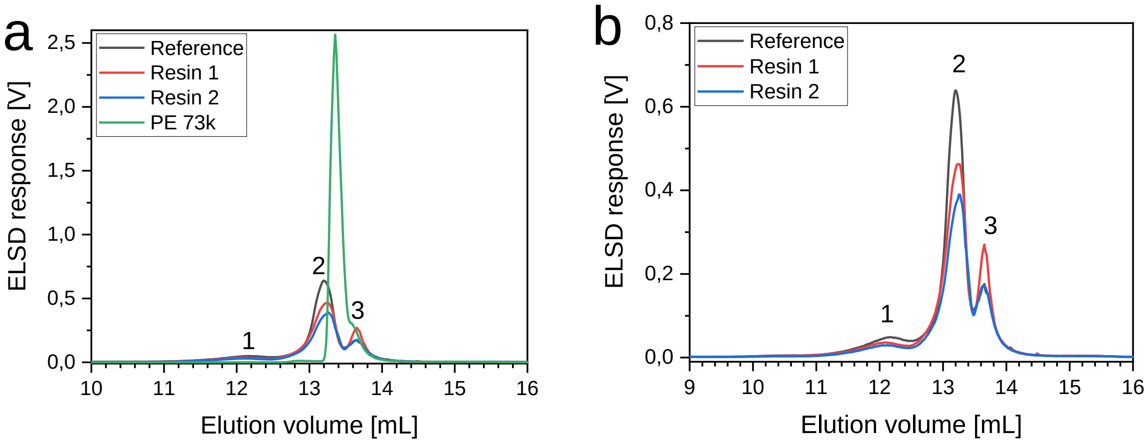

Figure 4.6 (a) Chromatograms showing elution volumes of the bulk bHDPE samples and a polyethylene standard PE 73k (b) zoomed in peak area showing differences in peak intensities for each sample.

It is notable that the poor processing Resin 2 has less of the linear material corresponding to Peak 3 than that of Resin 1. As shown before (Figure 2.5), the linear material in bHDPE is responsible for ease of processing by acting as a lubricant for the otherwise hard to process HDPE. In an attempt to relate the different chemical composition fractions (SGIC peaks) to molar mass, 2D-LC is performed.

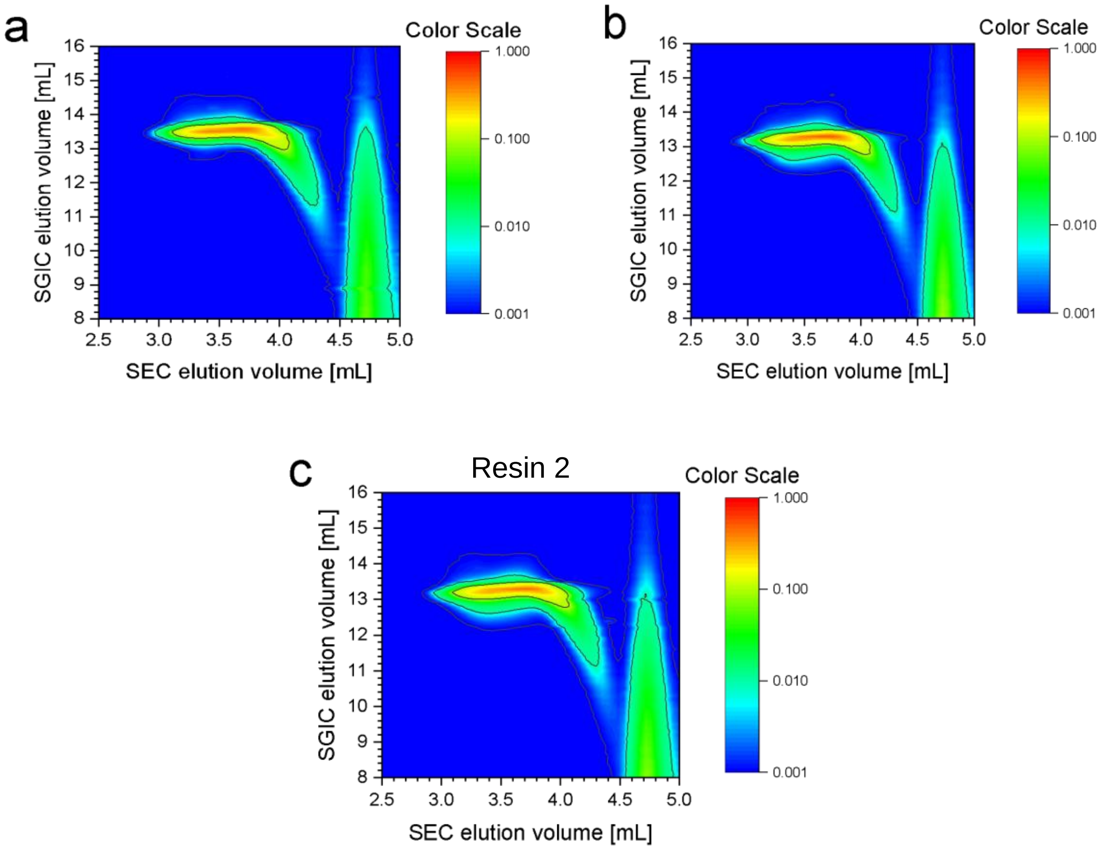

Figure 4.7 HT-2D-LC counter plots of the bHDPE samples, 1st dimension HT-SGIC on a Hypercarb column, 2nd dimension HT-SEC on a PLgel Olexis column for (a) Reference, (b) Resin 1 and (c) Resin 2.

Profiles of the 2-D curves in Figure 4.7 are very similar for the three bulk samples. Firstly, at low SGIC V_e below 13 mL, chains corresponding to low MM with V_e above 4.0 mL in the second dimension are eluted. Conversely, the higher SGIC V_e profiles above 13 mL relate to the low MM chains eluting at SEC V_e below 4.0 mL. Figure 4.8 clearly shows the broad second dimension profile that firstly confirms a broadly distributed chemical composition of the bHDPE samples. This is also in agreement with the very high polydispersity observed in HT-SEC. Moreover, these broad extended profiles also indicate that in the first dimension SGIC, there is a co-elution of the low and high MM components.[11] Further investigation of the CC heterogeneities are carried out using thermal gradient interaction chromatography.

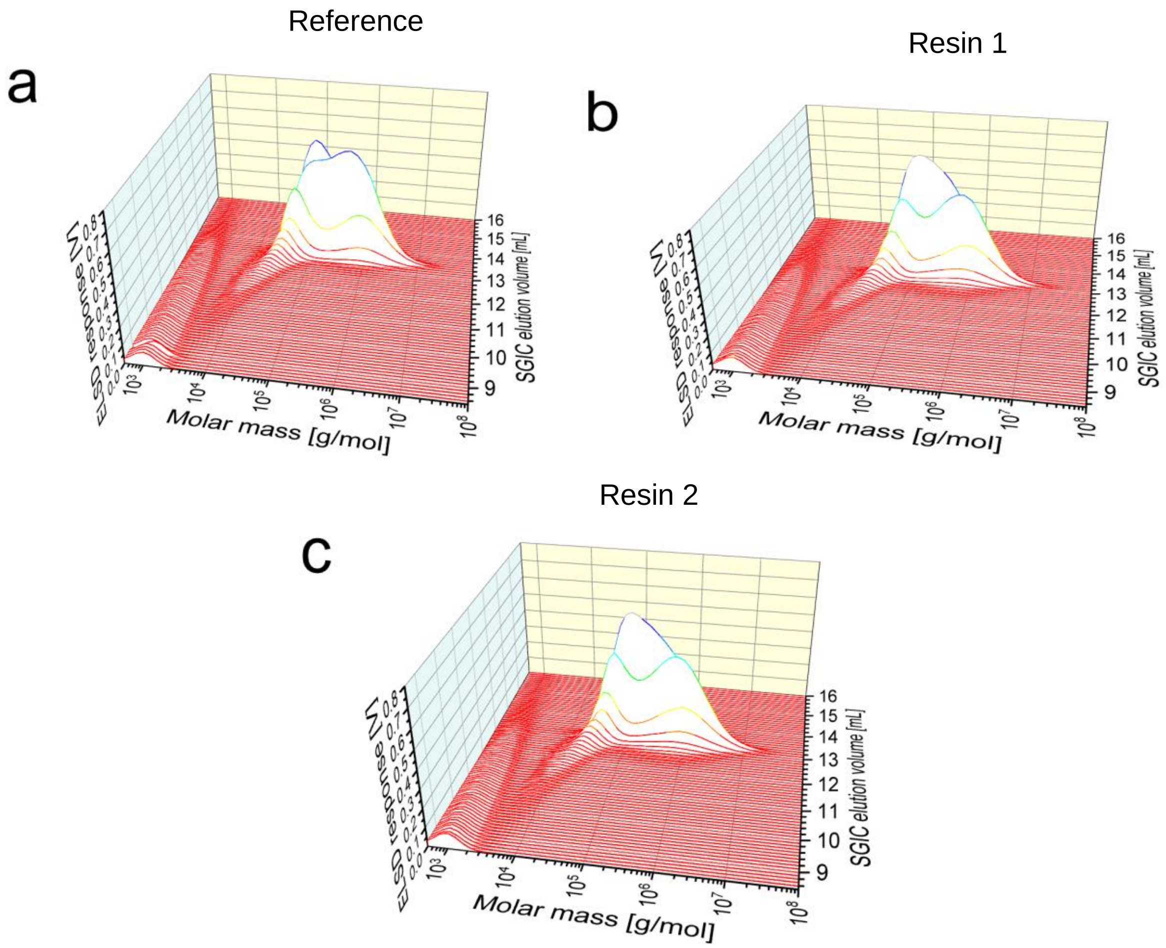

Figure 4.8 3D contour plots generated from HT-2D-LC analysis of the three bHDPE samples showing molar mass distribution as a function of SGIC elution volume for (a) Reference, (b)Resin 1 and (c) Resin 2.

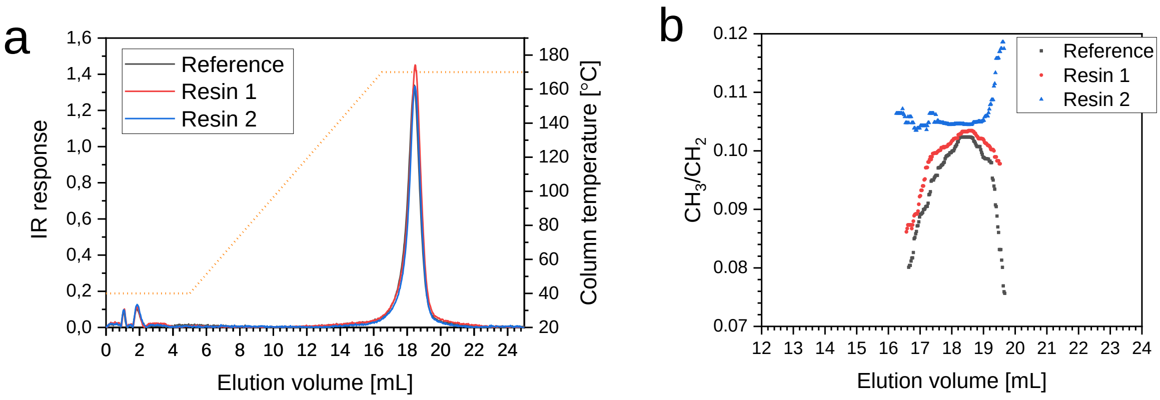

Figure 4.9 TGIC separations of the bulk bHDPE samples on a PGC column showing (a) the temperature gradient profile and (b) the methyl content per ethylene backbone as a function of elution volume.

Temperature gradient interaction chromatography based on a porous graphite column in Figure 4.9(a) shows a single main peak for all samples at a V_e of approximately 18 mL. This indicates that at a bulk level, samples have a close chemical composition distribution hence they elute in a similar way. Despite the observed close CCD for these samples, Figure 4.9(b) shows and agrees that Resin 2 has a slightly higher comonomer content (CH_3/CH_2) than those of Resin1 and the Reference. This result agrees with the higher calculated comonomer content from ^{13}C NMR and HT-SEC-IR.

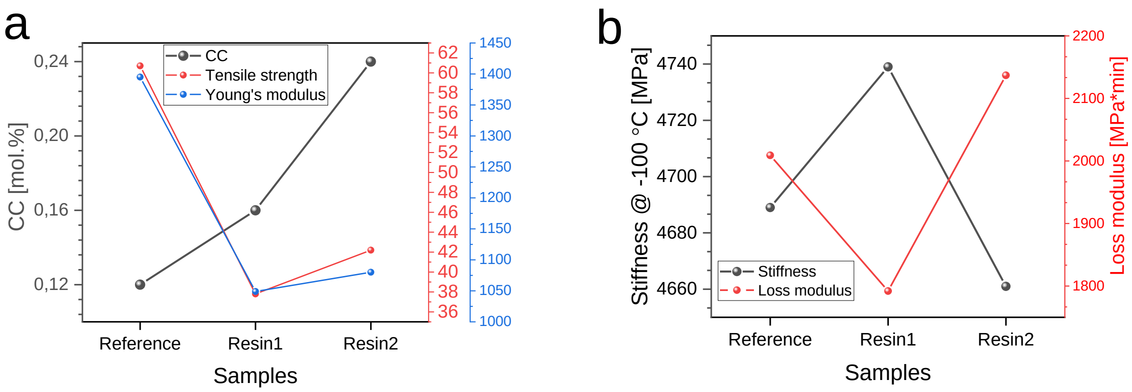

Figure 4.10 Plots comparing (a) tensile properties of the bHDPE samples and (b) stiffness and loss modulus as measured by DMA.

Figure 4.10(a) shows a considerably higher tensile strength and Young's modulus for the Reference sample. Both properties relate to the ease with which chains straighten out and re-orientate when an external force is applied. The more amorphous materials of the same comonomer are expected to possess higher tensile strength and thus higher Young's modulus.[14]

Table 4.3 A summary of the tensile properties and DMA of the bulk bHDPE samples.

Sample identification	Tensile strength (MPa)	Young's modulus (MPa)	[C][b] mol.%	Stiffness at (-) 100 ºC	Loss modulus (MPa*min)
Reference	60.7	1395	0.55	4689	2009
Resin 1	37.8	1049	0.68	4739	1792
Resin 2	42.4	1080	0.77	4661	2137

Resin 2 displays higher tensile strength and Young's modulus than Resin 1. Furthermore, a higher loss modulus is also observed for Resin 2 than those of Resin 1. These results suggest that Resin 2 is more branched than Resin 1 in agreement with ^{13}C NMR results that show a higher comonomer content for Resin 2.

4.3 Conclusions

BHDPE samples namely Resin 1 and Resin 2 of different developmental batches exhibit different rheological behaviour during processing although they have similar targeted microstructures. The two are being investigated and compared to a benchmark resin Reference for any differences in chemical composition leading to the observed differences in processability.

Solution Carbon-thirteen NMR showed that the Reference had 1-butene as comonomer while Resin 1 and Resin 2 had 1-hexene as comonomer. Resin 1 and Resin 2 are suspected of having different levels of poorly distributed of comonomer as seen in NMR peaks. The difficult to process Resin 2 was also found to possess a higher comonomer content which was confirmed by the various techniques. It is expected that bulk analysis on bHDPE with such low comonomer contents will not yield much information on the structural differences. For this reason, it is important to perform fractionation on the samples to isolate different regions of the polymer chain and study their compositions separately.

4.5 References

(1) Alt, F. P.; Böhm, L. L.; Enderle, H. F.; Berthold, J. *Macromol. Symp.* **2001**, *163*, 135–144.

(2) Tian, Z.; Chen, K.-R.; Liu, B.-P.; Luo, N.; Du, W.-L.; Qian, F. *Chem. Eng. Sci.* **2015**, *130*, 41–55.

(3) Sun, X.; Shen, H.; Xie, B.; Yang, W.; Yang, M. *Polymer* **2011**, *52*, 564–570.

(4) Randall, J. C. *J. Polym. Sci., Part B: Polym. Phys.* **1973**, *11*, 275–287.

(5) Mirabella, F. M.; Bafna, A. *J. Polym. Sci., Part B: Polym. Phys.* **2002**, *40*, 1637–1643.

(6) Eselem Bungu, P.; Pasch, H. *Polym. Chem.* **2017**, *31*, 4565–4575.

(7) Bungu, P. E.; Pasch, H. *Polym. Chem.* **2018**, *9*, 1116–1131.

(8) Ndiripo, A.; Eselem Bungu, P. S.; Pasch, H. *Polym. Int.* **2019**, *68*, 206–217.

(9) Monrabal, B.; Sancho-Tello, J.; Mayo, N.; Romero, L. *Macromol. Symp.* **2007**, *257*, 71–79.

(10) Ndiripo, A. *High temperature multidimensional chromatography of complex and functionalized polyolefins* PhD dissertation, Stellenbosch University: South Africa, **2018**.

(11) Prabhu, K.; Brüll, R.; Macko, T.; Remerie, K.; Tacx, J.; Garg, P.; Ginzburg, A. *J. Chromatogr. A* **2015**, *1419*, 67–80.

(12) Chitta, R.; Macko, T.; Brüll, R.; Boisson, C.; Cossoul, E.; Boyron, O. *Macromol. Chem. Phys.* **2015**, *216*, 721–732.

(13) Arndt, J.-H.; Brüll, R.; Macko, T.; Garg, P.; Tacx, J. *Polymer* **2018**, *156*, 214–221.

(14) Huff, T.; Bushman, C.; Cavender, J. *J. Appl. Polym. Sci.* **1964**, *8*, 825–837.

.

Chapter 5

Preparative temperature rising elution fractionation (pTREF) of bimodal HDPE and analyses of pTREF fractions

5.1 Introduction

HDPE is made up of many chains of different lengths with branches positioned along the backbone. The heterogeneities in the distribution of the SCB as a result of incorporated comonomer 1-butene for Reference and 1-hexene for Resin 1 and Resin 2 determine the final microstructure and, consequently, the properties of the polymer.[1,2] The previous chapter showed that very little information on differences in microstructure is obtainable from bulk analysis. For this reason, samples are fractionated, in this case according to segments of similar crystallisability using pTREF in order to assess the contribution of each fraction to the overall properties of the polymer.

TREF has been proven to be successful in separating different microstructures within crystalline and semi crystalline chains. It is important to note, however, that fractionation by crystallisability in order to study the branching distribution is limited in that, during cooling from solution, co-crystallisation of chains with different microstructures could occur.[3] It is expected that pTREF separates bHDPE into linear, low MM, copolymer and high MM chains eluting at different TREF temperatures.

In this chapter, the three bHDPE samples are fractionated according to chain crystallisability using pTREF and each fraction is analysed using advanced analytical techniques to provide a comprehensive understanding of the molecular heterogeneities in comparison to the bulk samples.[4-8]

5.2 Fractionation of bulk samples

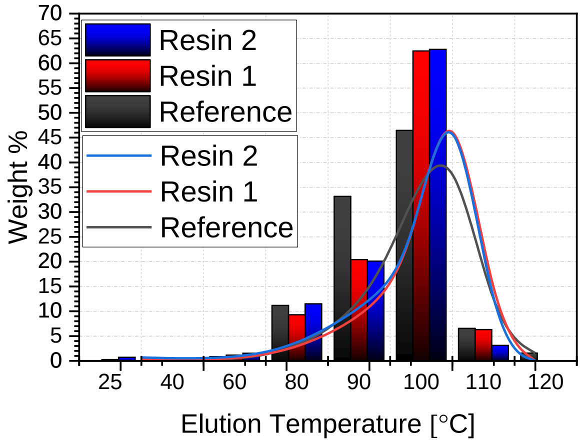

Figure 5.1 Plot showing the weight % of material recovered at each pTREF temperature and the fractions distribution curves for the bHDPE samples.

Table 5.1 Elution data of the bHDPE pTREF fractions.

	Reference		*Resin 1*		*Resin 2*	
Fraction (ºC)	W_i (g)	W_i (%)	W_i (g)	W_i (%)	W_i (g)	W_i (%)
25	0.016	0,18	0,008	0,25	0,021	0,67
40	0,004	0,12	0,004	0,14	0,009	0,30
60	0,024	0,80	0,033	1.10	0,045	1,47
80	0,325	10,7	0,266	8,82	0,342	11,1
90	0,965	31,7	0,584	19,4	0,597	19,4
100	1,352	44,4	1,788	59,4	1,867	60,6
110	0,190	6,25	0,180	5,98	0,092	3.00
120	0,046	1,50	-	-	-	-
Recovery (%)	95.7		95.1		97.1	

-No fraction collected

The benchmarking Reference, the good processing Resin 1 and bad processing Resin 2 samples were fractionated at temperatures between 25 ºC and 120 ºC. The Reference was the only sample to have material elute at 120 ºC with chains of much higher molar mass than Resin 1 and Resin 2. At lower temperatures, soluble and semi-crystalline chains are eluted while the most crystalline, least branched chains are eluted at higher temperatures.

The distribution of fractions is broader for the Reference than that of Resin 1 and Resin 2 which are much narrower at 100 ºC where most of their material are eluted. The trend however, is similar for all samples as marked by an increase in the amount of material collected between 60 and 100 ºC, followed by a decrease at 110 ºC. At lower temperatures

25 – 60 ºC the Reference has the lowest amount of material but, was the only sample to also elute any fraction at the highest temperature 120 ºC. This indicates that the Reference is made up of more crystalline material and less of the soluble material (25 ºC fraction) than Resin 1 and Resin 2. According to literature, the crystalline parts of a bimodal HDPE contribute to good processing properties while the SCB parts contribute to excellent mechanical properties.[6,9]

Resin 1 and Resin 2 show a similar trend at 60 - 100 ºC with a continuous increase in the amount of fraction collected and a decrease thereafter at 110 ºC which is also the last collectable fraction for both. At 60 and 80 ºC however, Resin 2 has a higher amount compared to Resin 1. Furthermore, a notable difference is observed at 110 ºC where Resin 2 has less material compared to Resin 1. For all samples, the largest amount of fractions (>75 %) were collected between 90 ºC and 100 ºC. In this region also, distribution of material was broader for the Reference sample.

TREF results show that the distribution of material by wt% is not dependant on the overal comonomer content. That is to say, although the Reference has the lowest bulk comonomer content (0.55 mol%), it has the highest wt% at 90 °C and the lowest at 100 °C compared to Resin 1 and Resin 2 with higher bulk comonomer content (0.68 and 0.77 mol% respectively).

5.3 pTREF fraction analysis

5.3.1 Solution carbon-thirteen NMR analysis

Chemical composition was established by integrating spectra of ^{13}C NMR. Peak integrals were used in equation 3.1, of Chapter 3 to obtain comonomer contents listed in Table 5.2. The normalised spectral signals in Figure 5.2 shows a branching peak at 40 ppm for the Reference and branching at 38 ppm for Resin 1 and Resin 2. These differences indicate incorporation of different comonomer, 1-butene and 1-hexene respectively.

All samples appear to have the highest concentration of comonomer in the 80 ºC fraction with Resin 2 having a significantly higher amount. Branching in Resin 2 also appears to be poorly distributed with a high concentration in fractions 80 and 90 ºC and very little in the other fractions as presented also in Table 5.2. Inconsistancies in comonomer content at given TREF temperatures are observed. This indicates crystallinity differences in fractions of similar TREF temperatures. It is plausible that over and above comonomer content, crystallisation is also affected by the distribution of these comonomer (block vs random sequence distribution) and molar mass.

The peak appearing after the branching peak of Resin 1 and Resin 2 is also seen to originate from the 80 ºC fraction of Resin 2 but, is spread out between fractions 90 and 100 ºC of Resin 1. This is the peak which was speculated to result from poorly dispersed comonomer in the previous chapter and appears to be much more abundant in the bulk of poorly processing Resin 2.

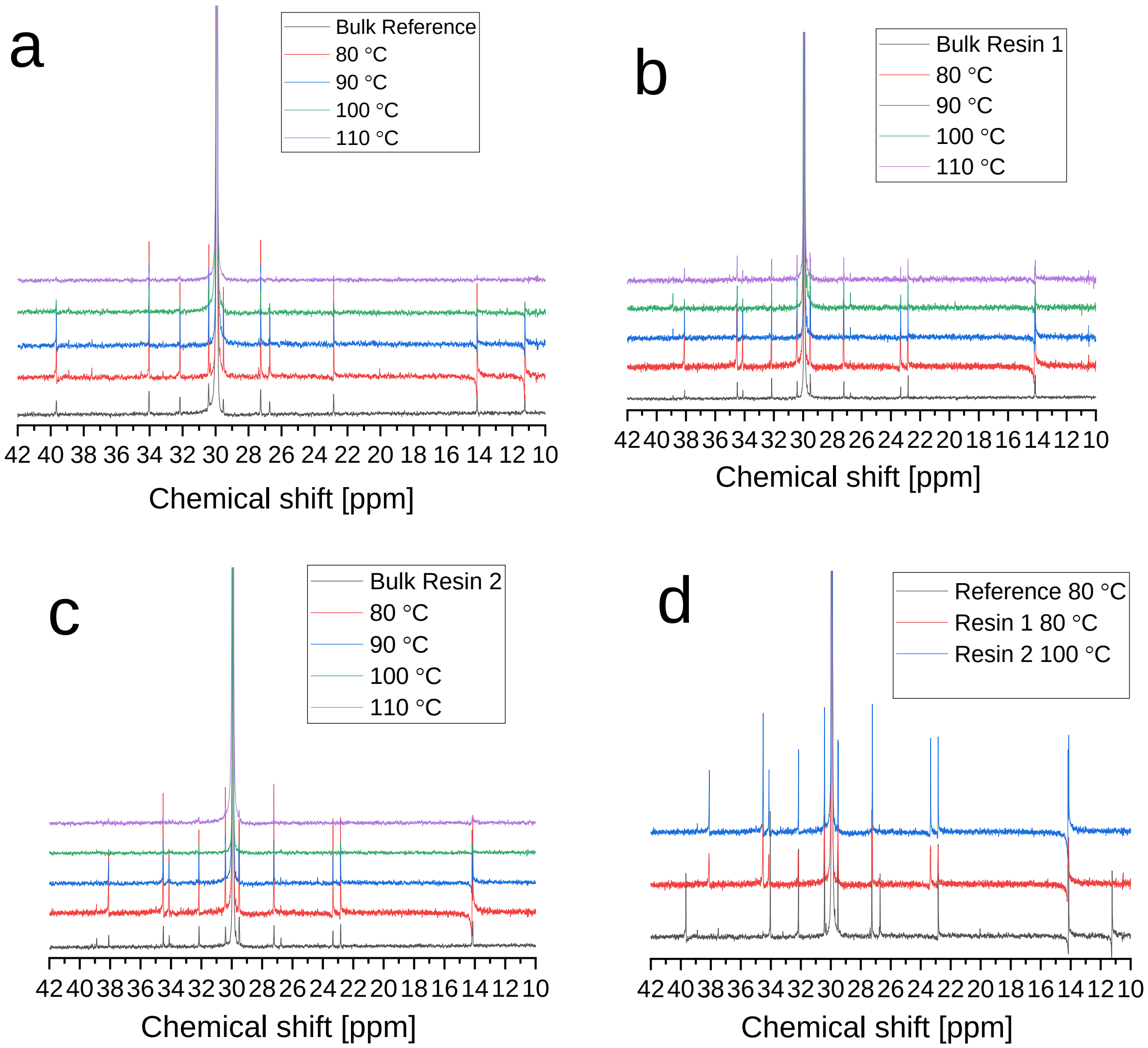

Figure 5.2 Solution ^{13}C NMR spectrum of bHDPE pTREF fractions (a) Reference with 1-butene comonomer, (b) Resin 1 with 1-hexene and (c) Resin 2 with 1-hexene comonomer and (d) overlay of the 80 ºC fractions.

5.3.2 Molar mass (MM) and molar mass distribution (MMD)

Table 5.2 Summary of molar mass data and comonomer content of pTREF fractions as determined by HT-SEC and ^{13}C NMR spectroscopy.

Sample	Fractions (ºC)	[C][a] mol %	Đ[b]	MM[b] (kg/mol)	M_n[b] (kg/mol)	M_p[b]
Reference	25	-	2.2	2.8	1.3	1.3
	60	-	3.8	12.0	3.1	4.7

	80	1.15	44.3	477	10.8	8.7
	90	0.63	30.2	1022	33.9	27.0
	100	0.30	16.2	1226	75.7	106
	110	0.00	19.3	1235	63.9	94.4
	120	-	23.2	1264	54.5	89.0
	Bulk	0.55	44.9	974	21.6	57.7
Resin 1	25	-	12.6	17.9	1.4	1.1
	60	-	45.0	156	3.5	2.2
	80	1.63	46.7	477	10.2	7.2
	90	0.73	31.4	679	21.6	16.2
	100	0.40	19.0	814	43.0	65.6
	110	0.30	21.6	905	41.9	88.7
	Bulk	0.68	41.9	735	17.6	356
Resin 2	25	-	19.5	32.4	1.7	1.3
	60	-	58.2	232	4.0	2.4
	80	1.71	49.3	567	11.5	7.7
	90	0.55	35.7	802	22.5	15.1
	100	0.00	20.6	990	48.1	64.4
	110	0.00	-	-	-	-
	Bulk	0.77	54.9	1017	18.5	407

[a] Determined by Solution ^{13}C NMR spectra, [b] Determined by HT-SEC

-Not enough material for testing

The Reference fractions between 25 and 60 ºC have much lower MM and narrower molar mass distributions in comparison to Resin 1 and Resin 2. This supports the observed pronounced low molar mass peak for the bulk Reference sample. Furthermore, at 60 ºC, the Reference is bimodal in the low mass segments indicating the presence of more than one component. The Reference also has high molar mass chains from 90 ºC with much higher weight and number average molar masses than those of Resin 1 and Resin 2 at the same TREF temperatures as seen in Table 5.2. This results in the overall higher averages observed for the bulk resin.

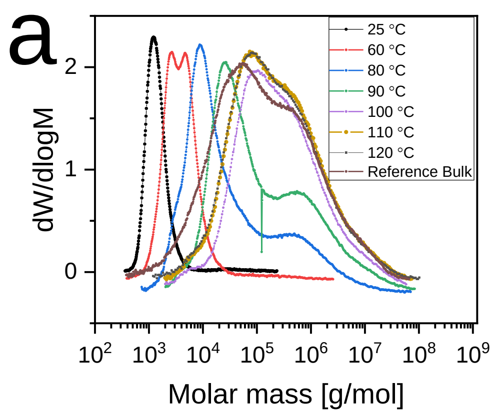

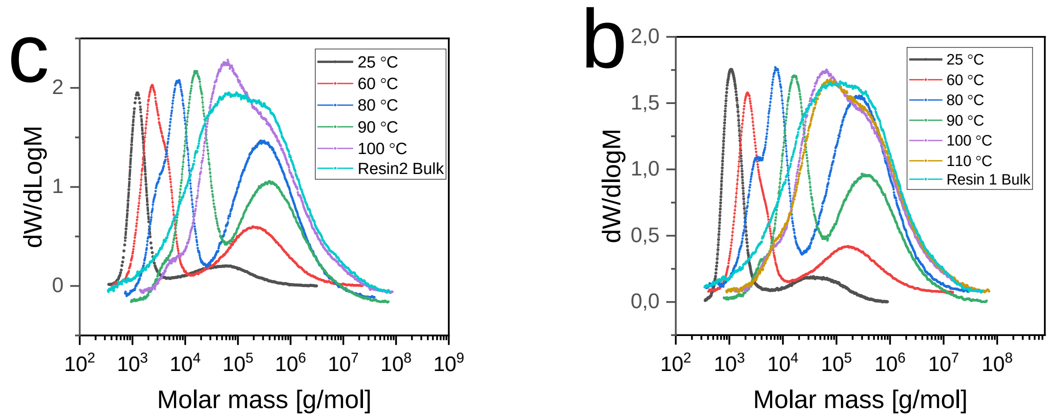

Figure 5.3 Molar mass distribution curves of bHDPE samples and their pTREF fractions.

The fact that the molar masses of the fractions and their MMD are within the range of the bulk samples shows successful fractionation. As shown in Table 5.2, there is a trend of an increase in MM with an increase in the pTREF temperature in agreement with literature.[7,10-13] Distribution curves in Figure 5.3 show that at 25 ºC, the Reference has a bimodal tail at the higher MM while Resin 1 and Resin 2 show a clearly defined bimodal distribution at this fraction.

For TREF fractions below 60 ºC, soluble material of very low MM is expected. This expectation is not met for Resin 2 which shows much higher MM at fraction 60 ºC. Fractions 80 and 90 ºC of the Reference show broader bimodal distributions whereas Resin 1 and Resin 2 have narrower distributions of the low and the high MM segments.

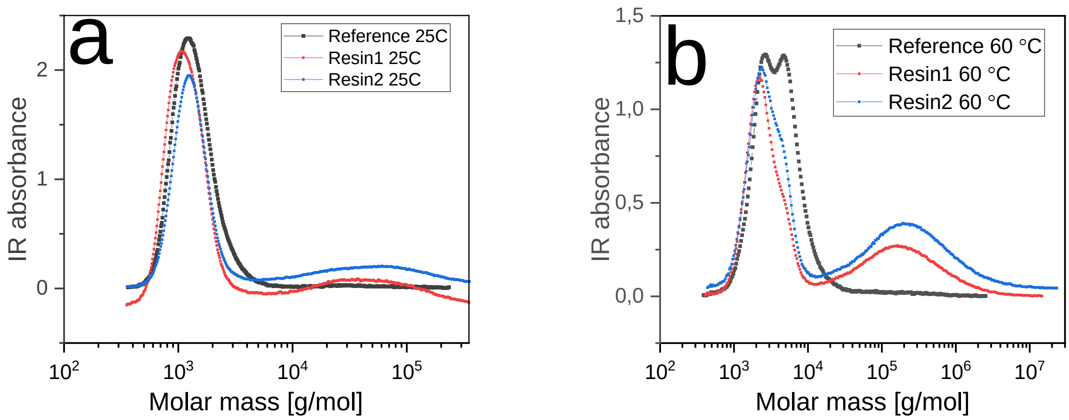

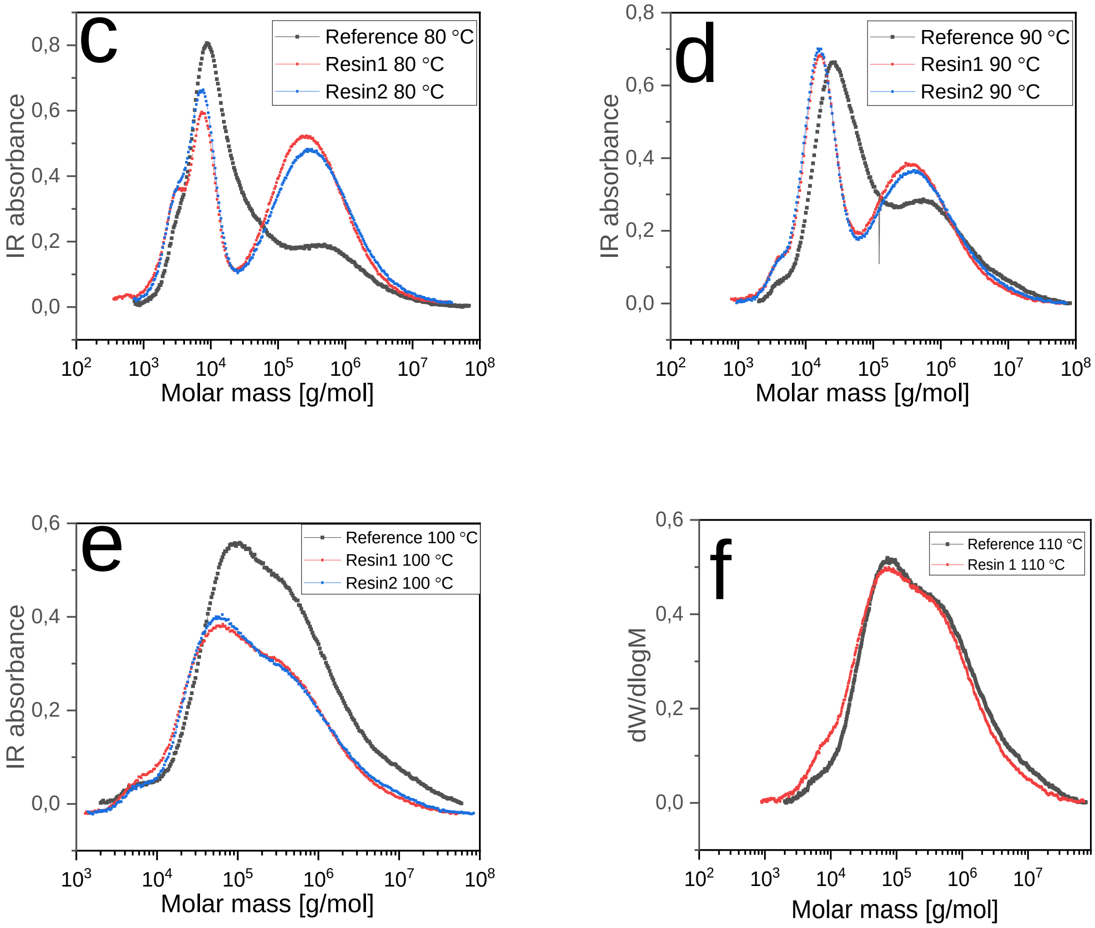

Figure 5.4 Comparison of molar mass distributions of similar TREF fractions of the bHDPE samples.

Overlays of the fractions in Figure 5.4 show clearly that the major differences between Resin 1 and Resin 2 are seen first at the 25 ºC fraction. This is where Resin 2 has more of the higher MM species and a subsequent higher MM than Resin 2 as shown also in Table 5.2. Also, at 25 and 60 ºC Resin 2 appears to have a much higher MM and molar mass dispersity than that of Resin 1. This, along with the high dispersity suggests that the chains could possibly have a high content of SCB. For Resin 1 and Resin 2 at 80 and 90 ºC, there is a clear definition between the two low and high MM species. For the Reference however, there is a merge between the low and high MM species at these fractions. There, the distribution of the bimodal curves is broader.

According to work done by Yu and Wilkes, [14] the more evenly distributed the branches along the chain, the better the processing and melt strength of the polymer. No notable differences in MMD are observed between the highest TREF temperature fractions 100 ºC and 110 ºC. Also interesting to note, Figure 5.4 shows that at every fractionation temperature, there is some form of bi- and even multimodality in the distributions. This shows that even the low molar mass linear chains possibly co- elute.

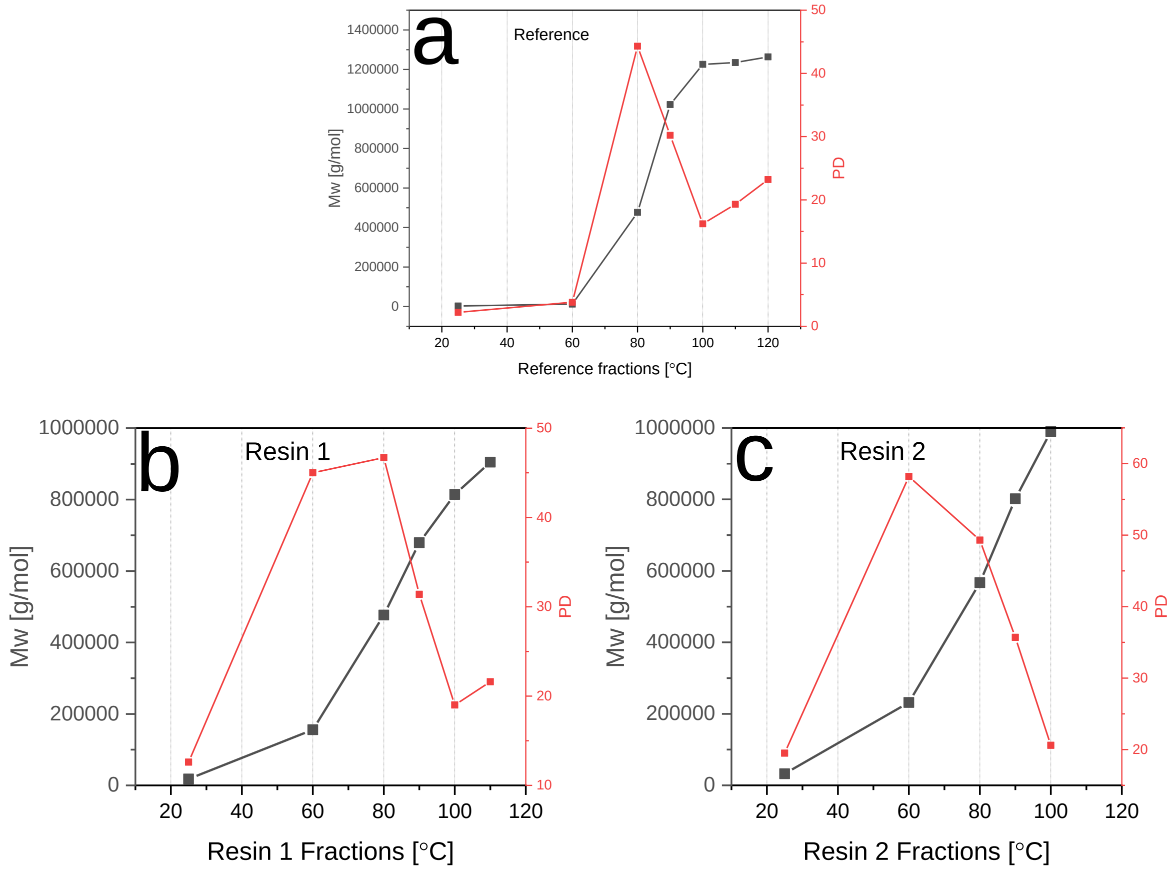

Figure 5.5 Distribution patterns of molar mass and molar mass dispersity for the pTREF fractions of the bHDPE samples.

5.3.3 DSC analysis

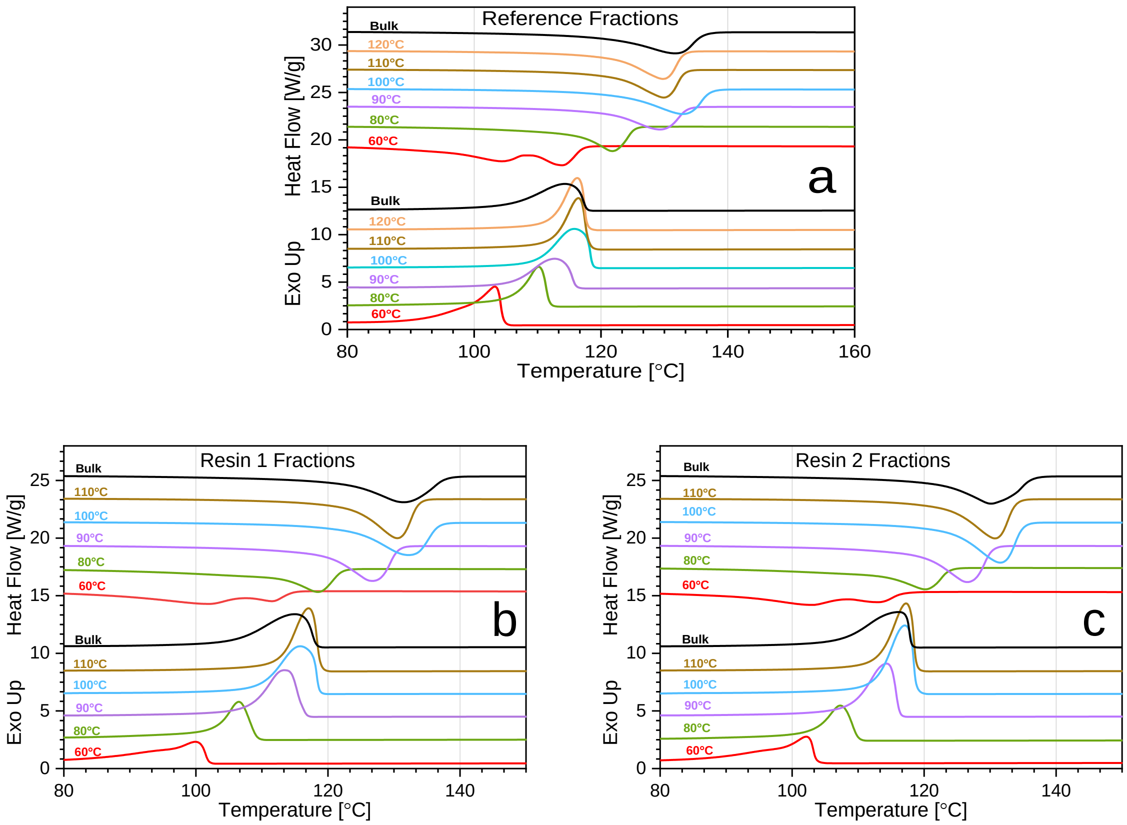

Figure 5.6 DSC second melting endotherms and first crystallisation exotherms of the pTREF fractions and their bulk samples.

The crystallisation exotherms and melting endotherms of the three samples as per Figure 5.6 show a shift in peak temperatures towards the lower temperatures as the fraction TREF temperature is decreased.[16] However, the increase in peak temperatures T_m and T_c with increase in pTREF fraction temperature is not identified. At higher fraction temperatures, the peak T_m and T_c level off because it has been reported that at high molar mass, there is no more dependence of the chains crystallisation on chain length, since parts of the chains crystallise apart from each other.[3] This shows clearly the contribution of each fraction on the bulk peak temperatures. At lower elution temperatures, peaks are broader, indicating a broader distribution of molecular chains, followed by a narrowing of peaks at the highest elution temperatures. This agrees with the MMD data in Table 5.1 that shows broader dispersity between 60 and 90 ºC followed by narrower dispersity at 100 and 110 ºC. Furthermore, a clearly bimodal distribution is observed at the melting endotherms of all the 60 ºC fractions.

Table 5.3 Summary of pTREF fractions' melting and crystallisation properties.

Sample	Fractions (ºC)	T_m (ºC)[a]	T_c (ºC)[a]	X_c (%)[a,b]
Reference	60	104.5, 113.3	103.3	60.2
	80	121.8	110.2	42.4
	90	129.3	112.8	52.1
	100	132.9	114.7	59.8
	110	129.9	116.5	52.8
	120	129.8	116.3	53.3
Resin 1	60	101.9, 111.5	93.5, 99.9	46.3
	80	118.5	106.5	43.8
	90	126.7	113.5	56.0
	100	132.1	115.8	60.3
	110	130.5	117.1	60.4
Resin 2	60	103.0, 113.0	97.1, 102.3	45.4
	80	120.2	107.3	31.5
	90	126.5	114.3	56.0
	100	131.5	117.1	63.4
	110	130.8	117.3	57.6

[a] Determined by DSC , [b] $X_c = (\Delta H_m / \Delta H_m^{e} \times 100\%)$, $\Delta H_m^{e} = 293$ J/g[15]

The summary of thermal properties in Table 5.3 highlights the bimodality of the 60 ºC fractions for all samples. While most of the fractions showed similar melting and crystallisation trends, a much higher X_c was observed for the Reference at 60 ºC in comparison to Resin 1 and Resin 2. This behaviour is also supported by the extremely low Đ in Table 5.2 indicating very narrow MMD and thus higher crystallinity. The X_c at the 80 ºC fraction of Resin 2 is however, significantly lower. This indicates a higher incorporation of short chain branches disrupting crystallinity.[3,5,17,18] The aforementioned differences in X_c between the samples are in agreement with the high comonomer content obtained via ^{13}C NMR spectroscopy as plotted in Figure 5.8(b). Fraction crystallinity were determined by dividing the heat of fusion ΔH_m obtained in DSC by the constant heat of fusion of a 100 % crystalline polyethylene ΔH_m^{e}. This method was proven adequate in the determination of polyethylene-α-olefin copolymers crystallinity in the work carried out by Mirabella et al[15] when they compared the crystallinity from DSC and X-ray diffraction (XRD).

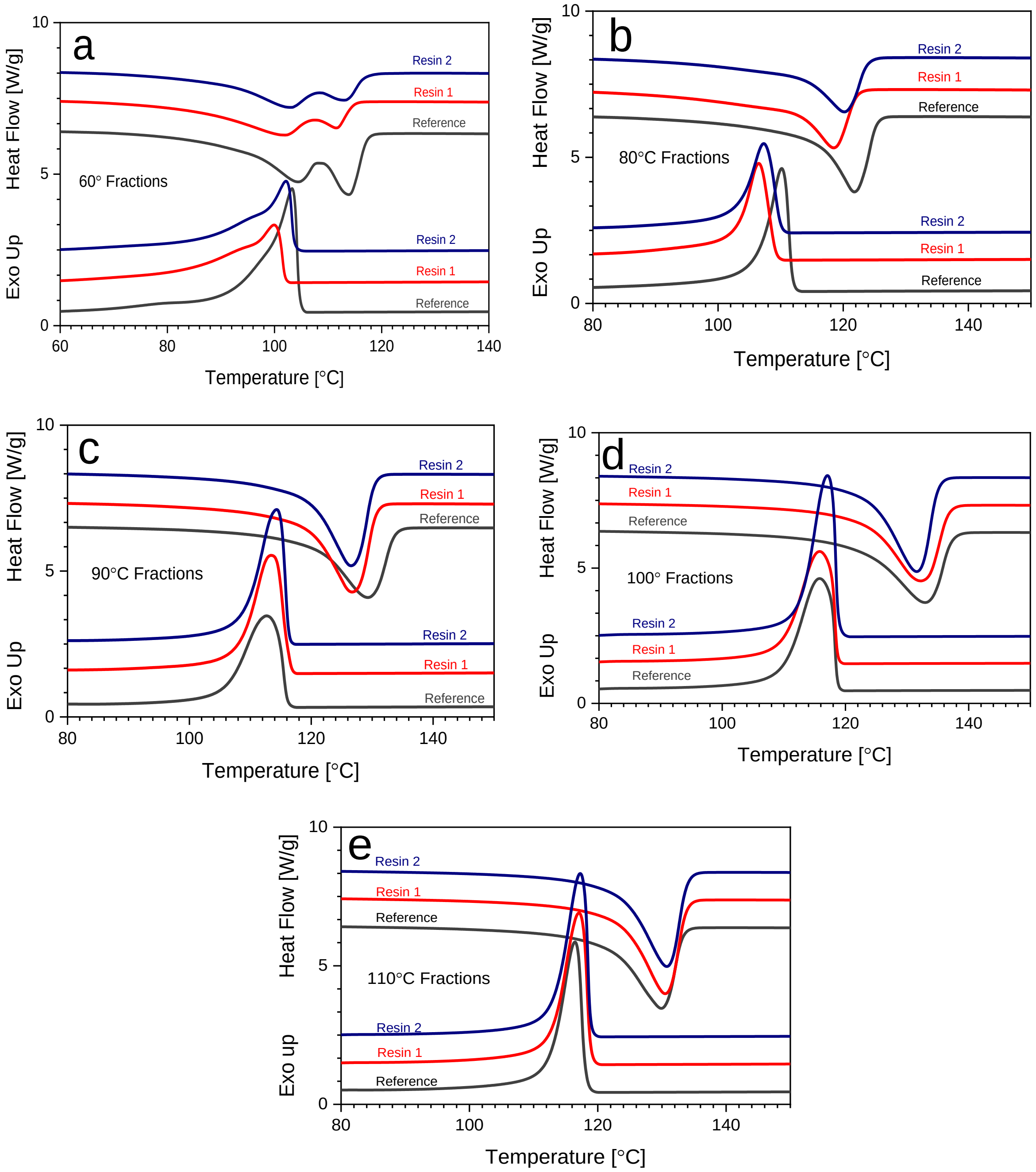

Figure 5.7 Comparison of the DSC second melting endotherms and first crystallisation exotherms for the pTREF fractions.

The Reference sample displays much narrower melting and crystallisation peaks than Resin 1 and Resin 2 at the 60 ºC fraction. At the 80 ºC fraction, Resin 1 has a slightly lower melting and subsequent crystallisation temperature than Resin 2 and the Reference.

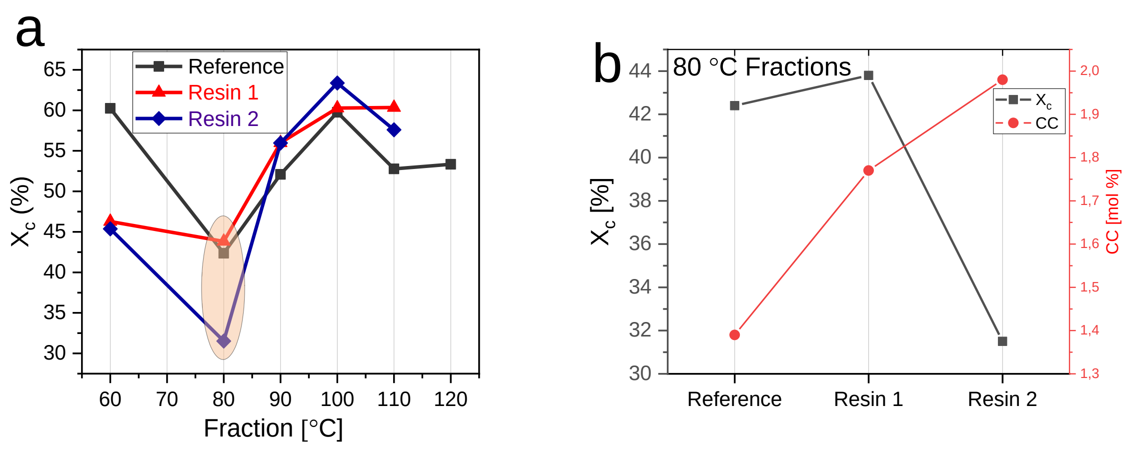

Figure 5.8 Plot of (a) the percentage crystallinity vs. TREF fraction temperatures for all samples. The circled area represents the fraction wherein X_c. is vastly different between Resin 1 and Resin 2. (b) Plot of percentage crystallinity as a function of comonomer content obtained via solution ^{13}C NMR.

5.4 Conclusions

High crystallinity in the low temperature regions of the bimodal polymer chains constitute better processing properties.[6,9,17,19,20] Resin 2 however does not have this high crystallinity because at fraction 60 ºC, chains are already high MM indicating a possibility of branching where chains are expected to be linear and soluble.

According to DSC results however, the main differences between Resin 1 and Resin 2 are observed at 80 ºC where Resin 2 displays a much lower percentage crystallinity confirming a high concentration of comonomer at the fraction. Although the comonomer is concentrated at this fraction, dispersity is similar to that of Resin 1 which has a lower comonomer content. This indicates a poor distribution of comonomer.

5.5 Reference

(1) Pasch, H. *Polym. Adv. Technol.* **2015**, *26*, 771–784.

(2) Soares, J. B.; Kim, J. D.; Rempel, G. L. *Ind. Eng. Chem. Res.* **1997**, *36*, 1144–1150.

(3) Krumme, A.; Basiura, M.; Pijpers, T.; Vanden Poel, G.; Heinz, L. C.; Bruell, R.; BF Mathot, V. *Mater. Sci.* **2011**, *17*, 260–265.

(4) Eselem Bungu, P.; Pasch, H. *Polym. Chem.* **2017**, *31*, 4565–4575.

(5) Ndiripo, A.; Eselem Bungu, P. S.; Pasch, H. *Polym. Int.* **2019**, *68*, 206-217.

(6) Fan, Y.; Xue, Y.; Nie, W.; Xiangling, J.; Bo, S. *Polym. J.* **2009**, *41*, 622–628.

(7) Ginzburg, A.; Macko, T.; Dolle, V.; Brüll, R. *J. Appl. Polym. Sci.* **2013**, *129*, 1897–1906.

(8) Knooren, J., *Recent developments in polyolefin fractionations,* MSc thesis, Universiteit van Amsterdam: Amsterdam*, **2013.*** .

(9) Shan, C. L. P.; Soares, J. B.; Penlidis, A. *Polymer* **2003**, *44*, 177-185.

(10) Assumption, H.; Vermeulen, J.; Jarrett, W. L.; Mathias, L. J.; van Reenen, A. *Polymer* **2006**, *47*, 67–74.

(11) Keulder, L. *The effect of molecular composition on the properties of linear low density polyethylene*. MSc thesis, University of Stellenbosch: South Africa,**2008**.

(12) Ndiripo, A. *High temperature multidimensional chromatography of complex and functionalized polyolefins* PhD dissertation, Stellenbosch University: South Africa, **2018**.

(13) Ortin, A.; Monrabal, B.; Sancho-Tello, J. *Macromol. Symp.* **2007**, *257*, 13–28.

(14) Yu, T. H.; Wilkes, G. L. *Journal of Rheology* **1996**, *40*, 1079-1093.

(15) Mirabella, F. M.; Bafna, A. *J. Polym. Sci., Part B: Polym. Phys.* **2002**, *40*, 1637–1643.

(16) Luruli, N. *New synthetic and characterization strategies for polyolefins*. PhD dissertation, Stellenbosch University: South Africa, **2007**.

(17) Shan, C. L. P.; Soares, J. B.; Penlidis, A. *Polymer* **2002**, *43*, 7345-7365.

(18) Chitta, R.; Macko, T.; Brüll, R.; Boisson, C.; Cossoul, E.; Boyron, O. *Macromol. Chem. Phys.* **2015**, *216*, 721–732.

(19) Kim, Y.; Chung, C.; Lai, S.; Hyun, K. *Journal of applied polymer science* **1996**, *59*, 125-137.

(20) Sun, X.; Shen, H.; Xie, B.; Yang, W.; Yang, M. *Polymer* **2011**, *52*, 564–570.

Chapter 6

Preparative molar mass fraction (pMMF) of bimodal HDPE and analyses of pMMF fractions

6.1 Introduction

Three bimodal HDPE (bHDPE) samples synthesised with 1-butene and 1-hexene are being compared for microstructural differences resulting in differences in their rheological behaviour during film extrusion. A benchmark industrial resin (referred to as Reference) is a 1-butene copolymer produced by a different manufacturer and hence, has optimal rheological performance. Developmental resins referred to as Resin 1 and Resin 2 are 1-hexene bHDPE of the same grade, produced in the same plant but possess different rheological properties as seen in the film extrusion process. Resin 1 has good processability while Resin 2 experiences low melt strength and bubble instabilities rendering it difficult to blow a film. The advantage of bimodal HDPE is its combination of melt strength and good processability owing to short chain branches. The distribution of the SCB determines its rheological properties as a result of the combination of its chemical composition and molar mass distributions.

Understanding the complex molecular makeup of bHDPE often with very low comonomer contents requires cross relation of CCD and MMD. While 1-alkene copolymerised bHDPE have been fractionated extensively according to chemical composition using TREF in the past, very little fractionation according to MM has been studied thus far.[1-4] This chapter aims to fractionate the three bHDPE resins according to differences in MM according to their solubility in a solvent/ non-solvent system using pMMF. The fractions collected in milligram amounts are further analysed using various analytical techniques and compared to the fractions of pTREF as per previous chapter were suitable.

6.2 Fractionation of bulk samples

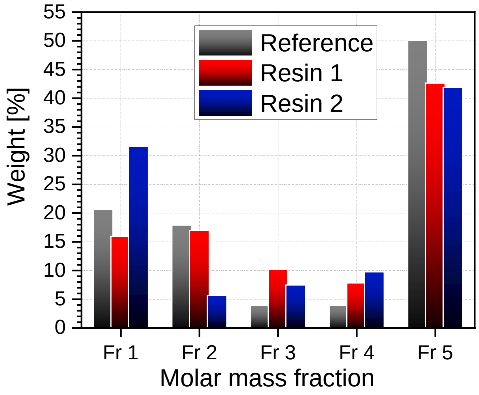

Figure 6.1 Plot showing recovered fractions of material at different solvent/ non-solvent ratios of the bHDPE samples.

Table 6.1 Elution data of the bHDPE pMMF fractions.

	Reference		*Resin 1*		*Resin 2*	
Fraction number	W_i (g)	W_i (%)	W_i (g)	W_i (%)	W_i (g)	W_i (%)
Fr 1	0.62	20.6	0.48	16.0	0.95	31.7
Fr 2	0.54	17.9	0.56	17.0	0.17	5.61
Fr 3	0.12	3.96	0.34	10.1	0.22	7.47
Fr 4	0.12	3.96	0.26	7.82	0.29	9.76
Fr 5	1.50	50.0	1.25	42.6	1.26	41.9
Recovery (%)	96.5		96.1		96.1	

-No fraction collected

Fractions were collected according to procedure detailed in Chapter 3. The high recoveries indicate successful and reliable fractionation. While the lower fraction numbers relate to high MM chains, the higher fraction numbers indicate chains of lower MM. The Reference and Resin 1 elute with a similar pattern at Fraction 1 and Fraction 2. Conversely, the bad processing Resin 2 elutes a much higher amount of material at Fraction 1 and a much lower amount at Fraction 2 in comparison. This is to say that between Fraction 1 and Fraction 2, Resin 2 elutes more material compared to Resin 1. Furthermore, the distribution of material is narrow with Fraction 1 having over 31%. Again, at the low MM Fraction 4, Resin 2 has more material eluting compared to Resin 1. Also, the high amount of the soluble fraction for the Reference increases melt miscibility between the high MM and low MM chains resulting in high melt strength.[5] Solution Carbon-thirteen NMR spectroscopy is employed to investigate comonomer content distribution.

6.3 pMMF fraction analysis

6.3.1 Solution carbon-thirteen NMR analysis

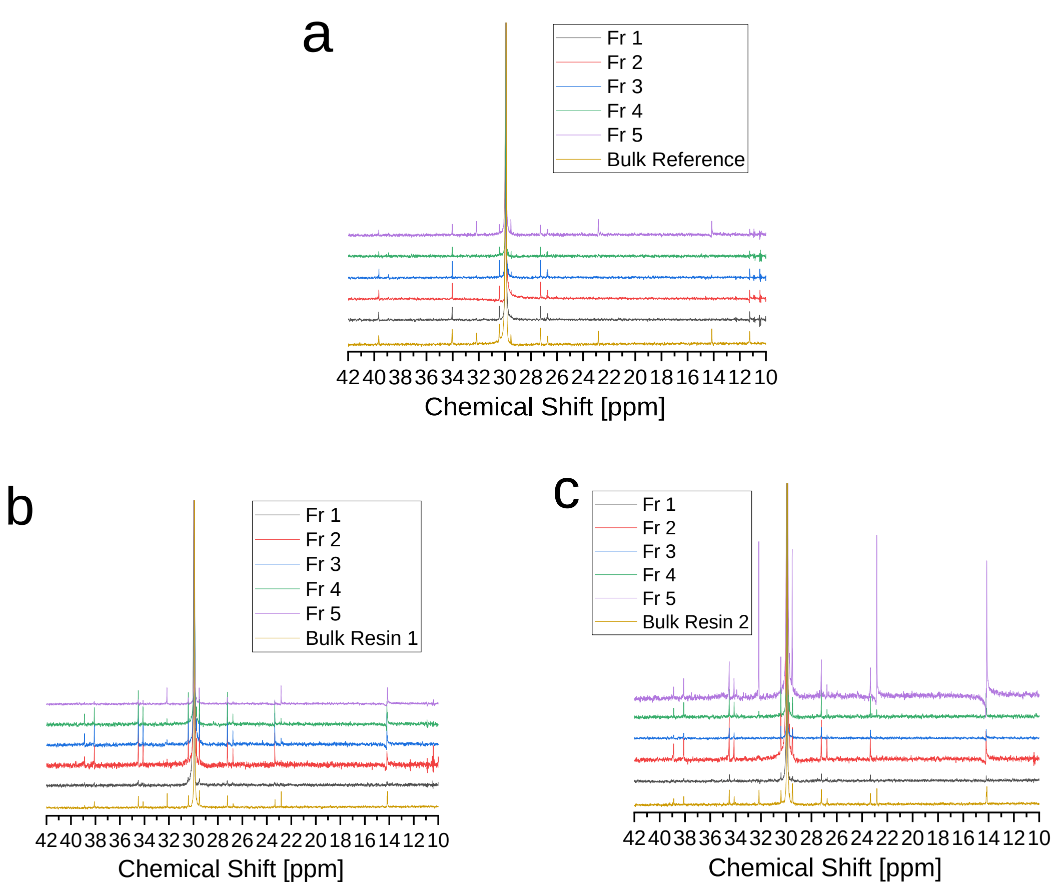

Figure 6.2 Solution ^{13}C NMR spectrum of bHDPE pMMF (a) Reference with 1-butene comonomer, (b) Resin 1 with 1-hexene and (c) Resin 2 with 1-hexene comonomer.

Calculated comonomer contents shown in Table 6.1 also confirm higher amounts of branching for Resin 2 at the earlier eluting Fraction 1 and Fraction 2. Unexpectedly, the dispersity of Resin 2 at these fractions are like those of Resin 1. This is to say, Resin 2 has more comonomer content incorporated in the high MM regions but, the distribution of the comonomer is narrow. Chemical composition ranges for the Reference, Resin 1 and Resin 2 are 0.34 – 0.77, 0.42 – 1.17 and 0.32 – 1.17 respectively. It has previously been concluded that rheological properties of a PE resin with bimodal molar mass is not determined by the amount of comonomer content but rather, how it is distributed through the polymer chain.[6,7]

6.3.2 Molar mass (MM) and molar mass distribution (MMD)

Table 6.2 Summary of molar mass data and comonomer content of preparative Molar Mass fractions as determined by HT-SEC and ^{13}C NMR spectroscopy.

Sample	NS/SR[c] [mL]	[C][a] mol%	Đ[b]	MM[b] (kg/mol)	M_n[b] (kg/mol)	M_p[b]
Fr 1	0.58	0.59	6.0	1823	303.1	527
Fr 2	0.04	0.63	5.2	1446	276	351
Fr 3	0.08	0.77	1.9	300	156	185
Fr 4	0.24	0.49	1.9	184	98.6	187
Fr 5	Soluble	0.34	3.5	52.6	14.9	34.2
Bulk Reference		0.55	44.9	974	21.6	57.7
Fr 1	0.58	0.51	5.2	1358	261.4	594
Fr 2	0.04	0.73	4.0	1013	256.1	381
Fr 3	0.08	1.17	1.9	292	155.9	182
Fr 4	0.24	0.86	2.1	199	93.1	98.1
Fr 5	Soluble	0.42	4.4	57.4	13.1	31.9
Bulk Resin 1		0.68	41.9	735.4	17.6	356
Fr 1	0.58	0.55	5.2	1368	262.6	500
Fr 2	0.04	1.10	4.1	1098	268.2	293
Fr 3	0.08	1.17	2.2	352	157.7	174
Fr 4	0.24	0.97	2.0	191	94.2	160
Fr 5	Soluble	0.32	3.3	38.1	11.6	28.4
Bulk Resin 2		0.77	54.9	1017	18.5	407

[a] Determined by Solution Carbon-thirteen NMR spectra, [b] Determined by HT-SEC, [c] denotes non-solvent/ solvent ratio.

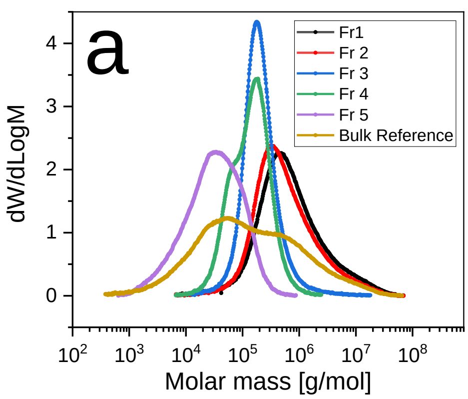

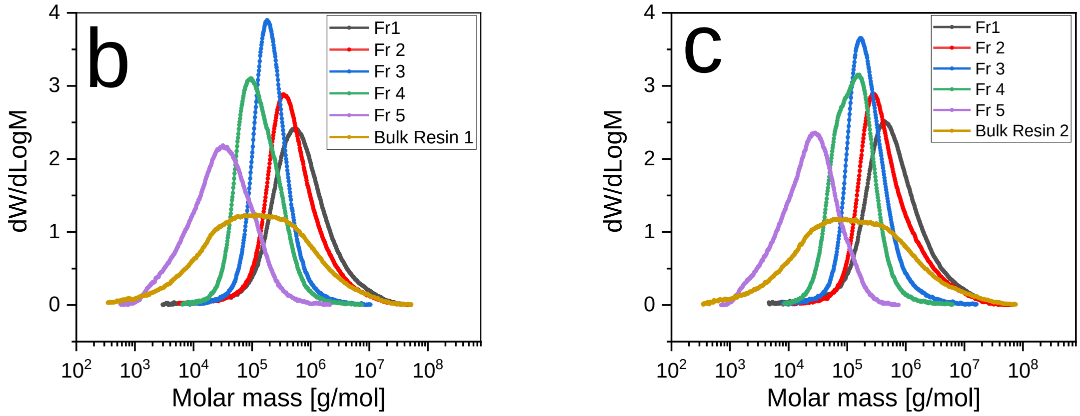

Figure 6.3 Molar mass distributions of bHDPE samples and their pMMF fractions.

Distribution curves in Figure 6.3 show that in comparison to the bulk, Fraction 1 and Fraction 2 relate to the high MM PE, Fraction 5 to the low MM PE and Fraction 3 and Fraction 4 to high MM copolymer segments. Also, all fractions appear unimodal with a reduction in the weight-average peak maximum (M_p) indicating that chain separation was according to molar mass. Furthermore, M_n is much lower for the bulk than it is for the fractions while the opposite is true for dispersity (Đ). This shows that molar mass fractionation succeeded in narrowing down the Đ of each fraction by increasing drastically the Mn.

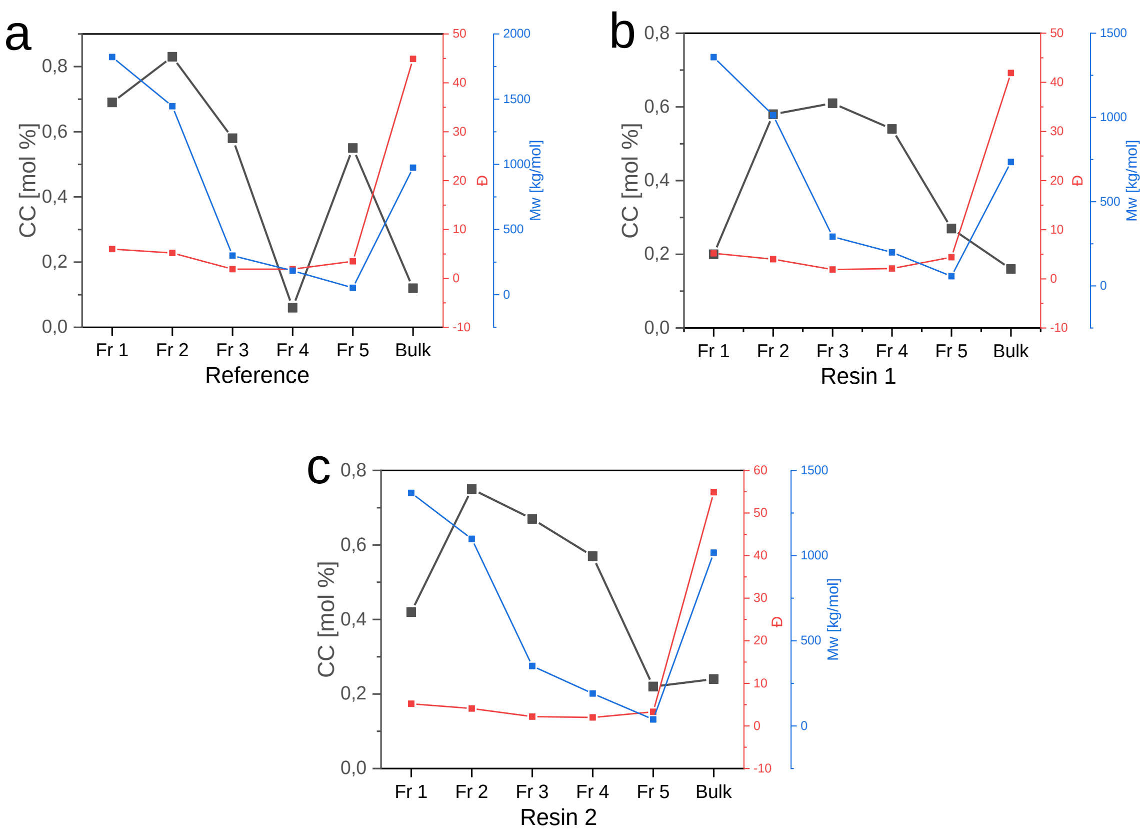

Figure 6.4 Plots of pMMF fractions showing the relationship between molar mass, dispersity and comonomer content.

It is however noticeable that at Fraction 4, both the Reference and Resin 2 have a neck in the lower MM regions indicating some heterogeneities in the molecular make-up. Additionally, a much broader chemical composition distribution is observed for the Reference at Fraction 5. These fractional differences are highlighted in overlays displayed in Figure 6.5. Despite the very low chemical compositions (<1 mol %) in the fractions, molar mass distributions are still high (>2.0) at the higher MM Fraction 1 and fraction 2 as well as the soluble Fraction 5. Again, these broad distributions are characteristic of bHDPE that display high melt strength during processing.[5,6]

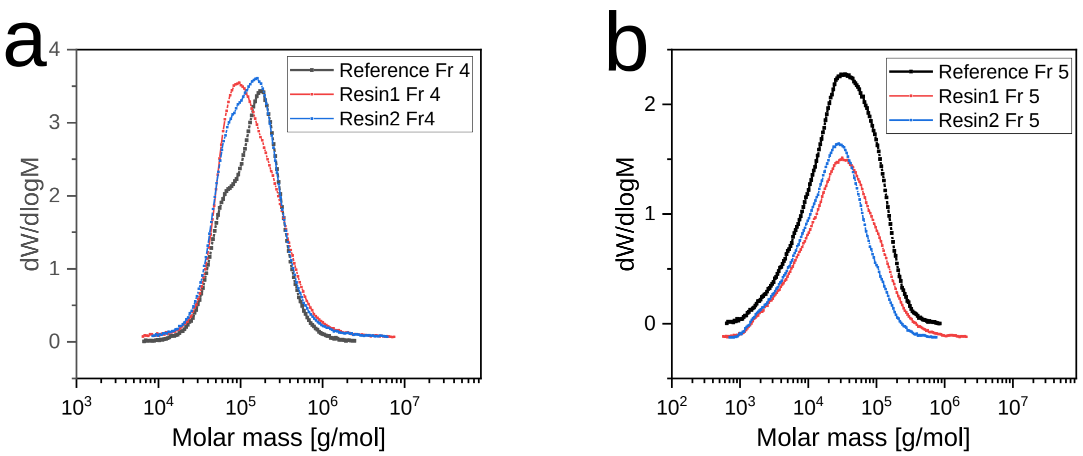

Figure 6.5 Plots showing differences in molar mass distributions of (a) Fraction 4 and (b) Fraction 5 of the pMMF fractions.

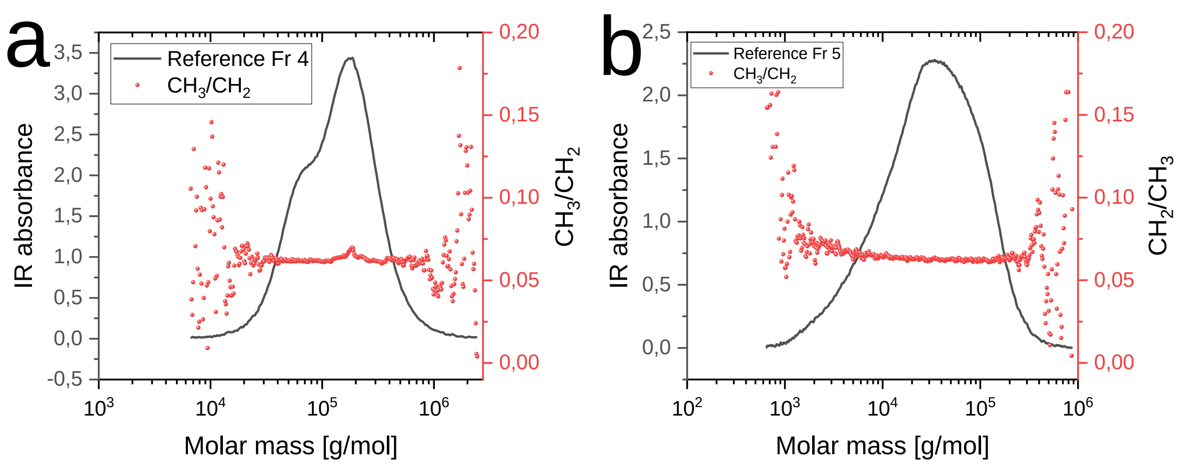

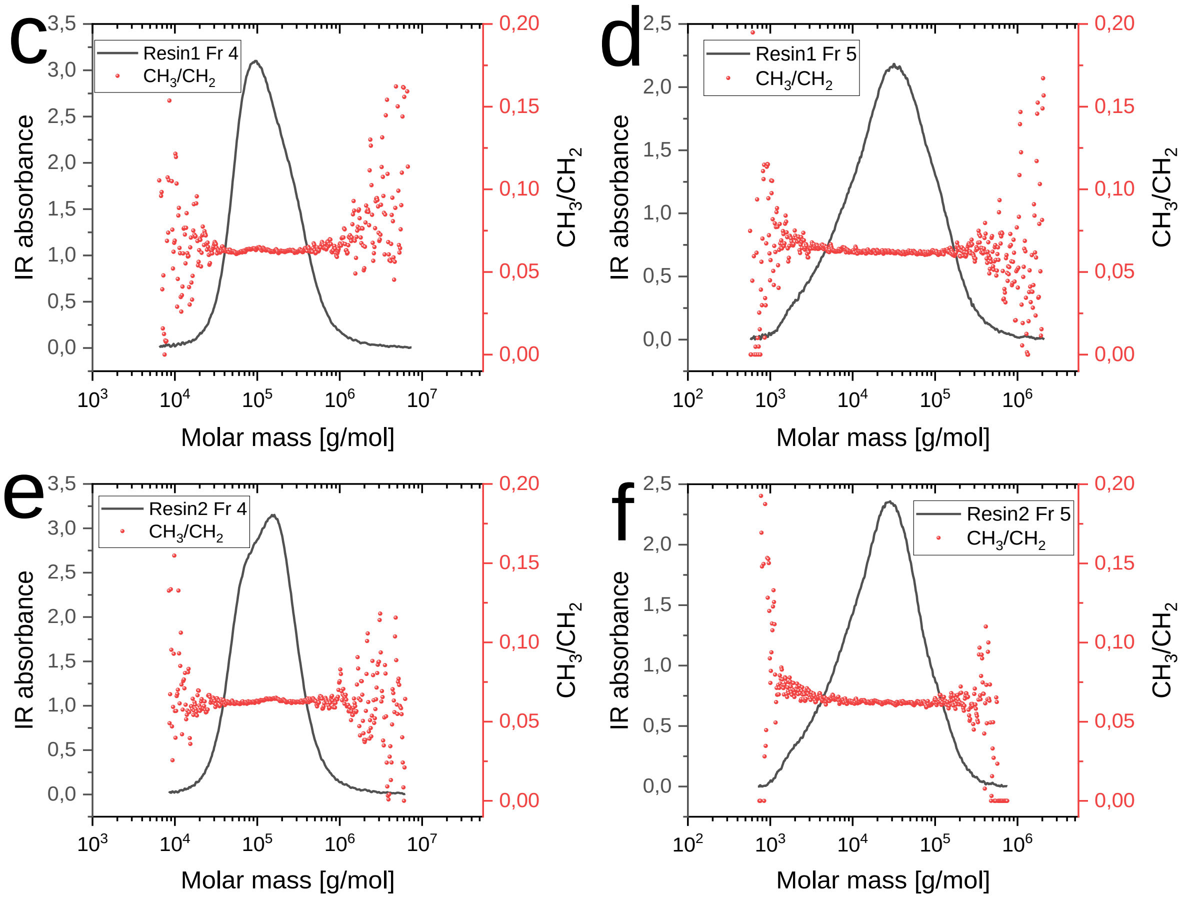

Figure 6.6 Molar mass distribution curves of the pMMF fractions at Fraction 4 and Fraction 5 showing comonomer content per ethylene backbone expressed as CH_3/CH_2.

Table 6.3 Summary of pMMF fractions' melting and crystallisation properties.

Sample	*Fractions*	*T_m (ºC)^a*	*T_c (ºC)^a*	*X_c (%)^{a,b}*
Reference	Fr 1	125.5	112.3	37.34
	Fr 2	126.7	111.8	39.67
	Fr 3	127.7	113.1	37.53
	Fr 4	129.0	113.4	55.31
	Fr 5	129.3	117.2	66.56
Resin 1	Fr 1	125.8	112.4	35.14
	Fr 2	126.3	111.0	37.71
	Fr 3	127.6	112.4	45.77
	Fr 4	129.9	114.2	54.42
	Fr 5	130.5	118.4	67.86
Resin 2	Fr 1	130.7	108.8, 118.2	96.57
	Fr 2	126.2	113.3	37.25
	Fr 3	128.0	112.4	42.36
	Fr 4	129.4	111.9	44.46
	Fr 5	130.5	118.5	81.53

^{a} Determined by DSC, ^{b} Xc = (ΔH_m / ΔH_m^e x 100%), ΔH_m^e = 293 J/g[8]

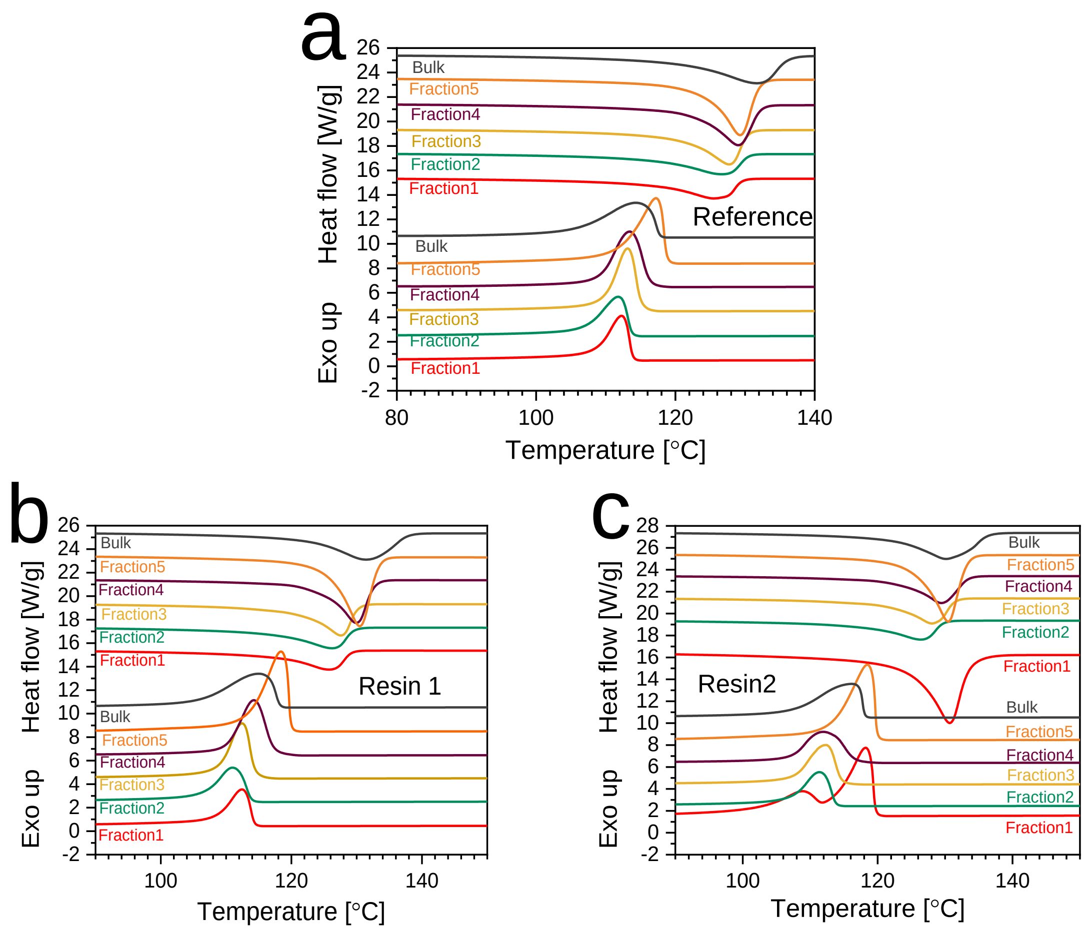

Figure 6.7 DSC second melting endotherms and first crystallisation exotherms of the pMMF fractions and their bulk samples.

Peak melting and crystallisation temperatures are summarised in Table 6.3 and plot overlays shown in Figure 6.7. Peaks show a trend of increase in peak melting and crystallisation temperatures with an increase in fraction number. The trend is more defined for the Reference and Resin 1 but, interrupted at Fraction 1 of Resin 2. Peak T_c of Resin 2 is bimodal with a smaller and broader peak appearing at lower peak temperatures of 108.0 ºC. The second peak T_c at 118.2 ºC is narrower, more intense, and has a higher peak temperature than expected according to the observed trend. Peak Tm is also higher for Resin 2 at Fraction 1. This observation on Fraction 1 of Resin 2 agrees with HT-SEC data that shows a narrow distribution of CC within the fraction. It is worth noting that the contribution of this fraction to the bulk is significant as it is the second largest fraction totalling 31.7 % as per elution data in Table 6.1.

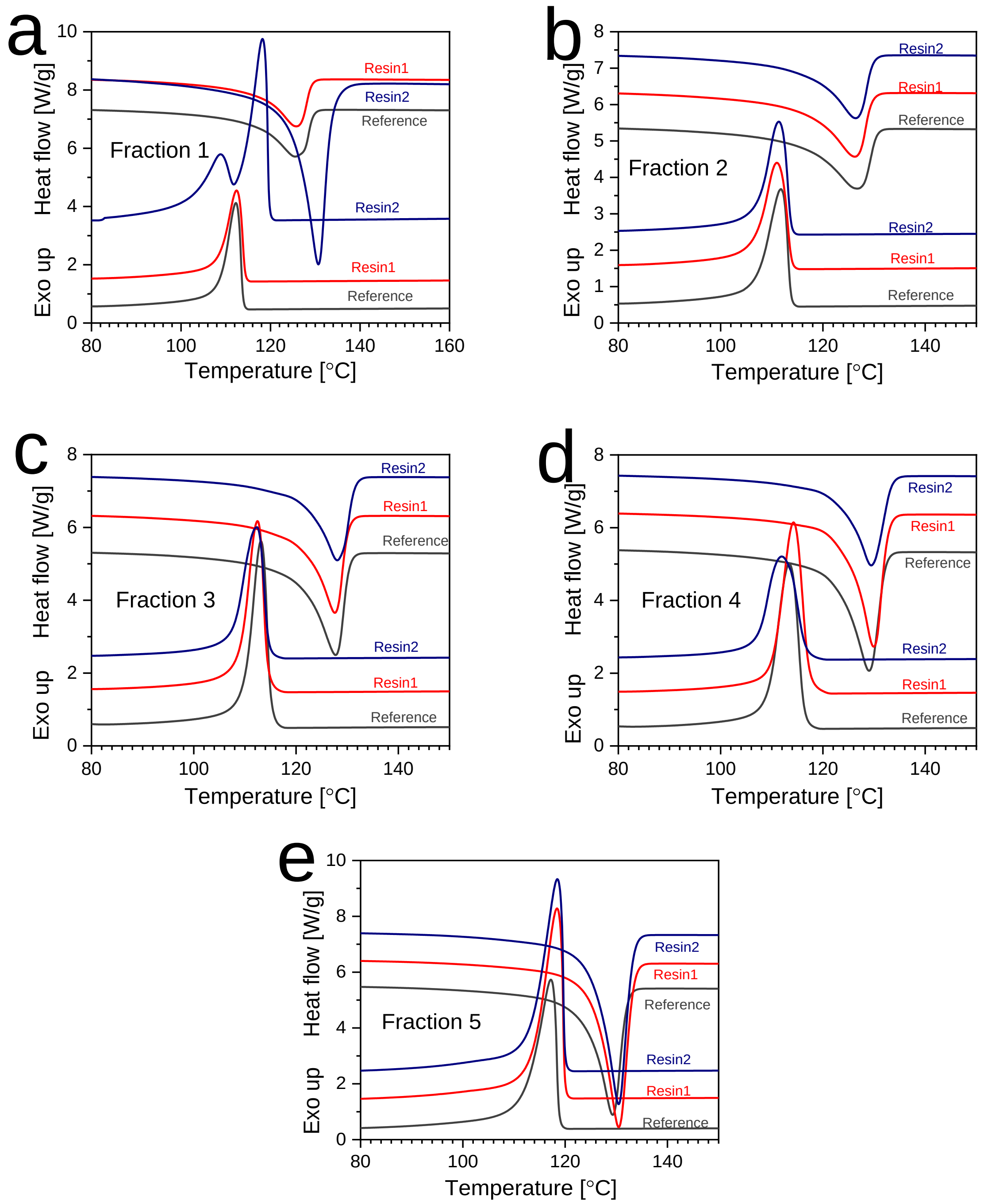

Figure 6.8 Comparison of the DSC second melting endotherms and first crystallisation exotherms for the pMMF fractions.

Overlays of the different fractions in Figure 6.8 show that Fraction 1 of the Reference has a broader peak T_m compared to Resin 1 and Resin 2. This indicates a broad CCD and agrees with HT-SEC data showing the highest MM and broadest dispersity for the fraction. Further agreement between HT-SEC and DSC is observed at Fraction 4 of Resin 2 that displays a broad peak T_m compared to the Reference and Resin 1. This indicates a slightly broader CC that was first observed with the broader MM distribution curve highlighted in Figure 6.5 (a).

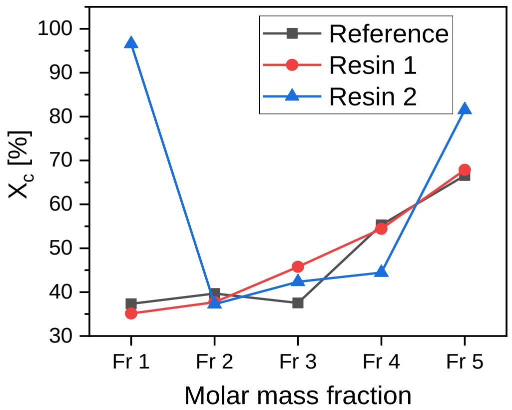

Figure 6.9 Plot showing differences in X_c of the molar mass fractions of the bHDPE resins.

6.4 Conclusions

The poorly processing Resin 2 contains more comonomer at the high MM chains Fraction 1 and Fraction 2. More importantly, the comonomer distribution is narrow. DSC also shows that Fraction 1 of Resin 2 is made up of two main components that crystallise at different temperatures. Peak T_m of this fraction is also higher than that of the similar Resin 1. This indicates that the fraction is made up of more of the high MM linear PE chains with high crystallinity. The high MM HDPE chains are known to make processing difficult, a challenge that was overcome with the addition of very low MM and branched chains in the design of bHDPE.

The soluble Fraction 5 is made up of very low MM PE and serves as a lubricant for the highly crystalline HDPE chains during processing.[9] This fraction is abundant in the benchmarking Reference sample which also displays lower X_c. Resin 2 however, at this fraction is more crystalline indicating a presence of more of the highly crystalline chains thus minimising the intended lubrication effect.

6.5 References

(1) Ginzburg, A.; Macko, T.; Dolle, V.; Brüll, R. *J. Appl. Polym. Sci.* **2013**, *129*, 1897–1906.

(2) Krumme, A.; Basiura, M.; Pijpers, T.; Vanden Poel, G.; Heinz, L. C.; Bruell, R.; BF Mathot, V. *Mater. Sci.* **2011**, *17*, 260–265.

(3) Fan, Y.; Xue, Y.; Nie, W.; Xiangling, J.; Bo, S. *Polym. J.* **2009**, *41*, 622–628.

(4) Ndiripo, A. *High temperature multidimensional chromatography of complex and functionalized polyolefins* PhD dissertation, Stellenbosch University: South Africa, **2018**.

(5) Hakim, S.; Moballegh, L.; *Macromol. Symp.*, **2011**, pp 191-197.

(6) Shan, C. L. P.; Soares, J. B.; Penlidis, A. *Polymer* **2003**, *44*, 177-185.

(7) Krishnaswamy, R. K.; Yang, Q.; Fernandez-Ballester, L.; Kornfield, J. A. *Macromolecules* **2008**, *41*, 1693–1704.

(8) Mirabella, F. M.; Bafna, A. *J. Polym. Sci., Part B: Polym. Phys.* **2002**, *40*, 1637–1643.

(9) Amos, J.; Chai, C. K.; Dheur, L. M. G.; *Bimodal polyethylene film*, **2011**, United States Patents, US7897710B2.

Chapter 7

Conclusions and recommendations

7.1 Summary

The aim of this work was to establish the cause of rheological differences in bimodal HDPE as seen during extrusion film blowing. The industrial benchmark resin "Reference" with the best processability is compared to developmental resins Resin 1 and Resin 2. Resin 1 and Resin 2 are of the same grade, produced by the same producer using the same technology but perform differently during processing. While Resin 1 behaves well during film blowing, Resin 2 has poor processability in the form of low melt strength and bubble instability. The differences on a molecular level were investigated to establish root cause of the rheological behaviour.

7.2 Conclusions

In the first part of this work, bulk bHDPE samples were studied using various analytical techniques. The various applied techniques did not reveal enough differences in the molecular make-up of the three resins as is to be expected for very low comonomer contents (<0.8 %). Solution Carbon-thirteen NMR did, however, show that the Reference was made up of a different comonomer to that of Resin 1 and Resin 2. Furthermore, it was shown that Resin 2 had a slightly higher comonomer content. For a thorough investigation into the molecular heterogeneities within the resins, preparative fraction methods were applied. These included pTREF and pMMF. Collected fractions from both fractionation techniques were further analysed using ^{13}C NMR spectroscopy, HT-SEC and DSC.

In the second part, pTREF fractionation successfully separated the bHDPE chains according to differences in chemical composition. The resultant fractions had a characteristic increase in MM with an increase in TREF elution temperature. Moreover, the fractions had very high dispersity indexes indicating that TREF is not sensitive to differences in MM and, co-elution effects. HT-SEC showed that Resin 2 had higher MM chains in the low TREF temperatures where it should be low MM. This interference inhibits the ease of processing that bHDPE benefits from its very low MM chains thus explaining the processing difficulties experienced with Resin 2. ^{13}C NMR showed a slightly higher comonomer content in the low TREF temperature fractions of Resin 2. This was confirmed by the lower X_c in these fractions as observed in DSC.

Lastly, the resins were fractionated according to molar mass using pMMF based on chain solubility in a solvent/non-solvent system. Fractions showed a characteristic decrease in MM with an increase in fraction number. Resin 2 had a more significant amount of its material elute in the highest MM Fraction 1 than those of the Reference and Resin 1. The most amount of material was eluted in the lowest MM (soluble) Fraction 5 for all samples with the Reference having the highest. This is presumably its advantage in the ease of processing over Resin 1 and Resin 2.

^{13}C NMR showed that the highest amount of comonomer was found in the high MM Fraction 2 for all samples. Although Resin 2 had more comonomer than Resin 1 in the high MM fractions, their dispersity indexes were the same. This showed that Resin 2 had an overall narrowly dispersed higher comonomer content in the high MM fractions than Resin 1. This further disadvantage the ease of processing for Resin 2 as good processability is dependent on an evenly distributed comonomer along the polymer backbone chain. HT-SEC confirmed that separation was due to MM. Fractions had low dispersity indexes and decreasing weight-average peak maxima with decreasing MM. DSC further showed that Resin 2 was more crystalline in the soluble material Fraction 5. Also, a much higher crystallinity was observed in the high MM Fraction 1 in agreement with the narrow distribution of comonomer observed in HT-SEC and ^{13}C NMR.

It is concluded that Resin 2 has a narrowly dispersed higher comonomer content in the low TREF temperature fractions where it should be linear and more crystalline. Moreover, it is a lot more crystalline in its high MM chains than the Reference and Resin 1. The benchmark Reference is the exact opposite at these fractions of interest.

7.3 Recommendations

1. Differences in the chemical structures of each fraction could be investigated using HT-SGIC to further establish any intermolecular heterogeneities.

2. Bulk resins and their fractions could be analysed for elongational rheology to mimic the elongation that occurs during the extrusion film blowing process. If differences are seen on a bulk level, this could serve as a useful quality control tool. At fractionation level, the suspected problematic fractions could be removed, and fractions recombined to understand the effect on the new material.

3. Different/ more batches of the “bad” processing resin could be subjected to a similar study to confirm the consistency of the observed differences.